5 Controlled nuclear fusion: general aspects

[E. Rebhan, D. Reiter, R. Weynants, U. Samm, W.J. Hogan, J. Raeder, T. Hamacher]

5.1 Fusion processes

[E. Rebhan]

5.1.1 Introduction

Nuclear fusion is the energy source for an infinity of processes in the universe, and, most importantly for mankind, it heats the center of the sun. This way it is, though sometimes rather indirectly, the origin of almost all energy resources which are currently used on earth. Already in 1919 the first nuclear fusion processes in a laboratory were achieved by E. Rutherford. In 1934 he succeeded together with M.L.E. Oliphant and P. Harteck to achieve the first fusion reactions between deuterons and deuterons or tritons. In 1926 A. Eddington postulated that the sun obtains its energy from fusion reactions. The way to a proof of this was paved by G. Gamow who explained the decay of heavy nuclei as well as the fusion of light elements by employing the quantum effect of tunneling. In 1929 this was applied to the processes in the interior of the sun by R. Atkinson and F. Houtermans. The specific fusion reactions yielding the energy for the nuclear fire of the sun and other stars were detected by H. Bethe and C.F. von Weizsäcker in 1938. Since almost sixty years physicists and engineers are working hard to utilize nuclear fusion as an energy source for the mankind. In 1951 the first man-made fusion reactions between deuterium and tritium on a larger scale were achieved on the Eniwetok atoll, and the first transportable H-bomb was fired by the US in 1954 on the Bikini atoll. In the context of fusion reactor research the first fusion reactions between deuterium and tritium, the fuel of a future fusion reactor, came about in inertial fusion devices during the seventies of the last century. In magnetically confined plasmas this fuel was used for the first time in the joint European fusion experiment JET and in the American tokamak TFTR (1992/1993) achieving until now a peak fusion power of 16.1 MW and under quasi-stationary conditions more than 4 MW [99Jaq].

5.1.2 Binding energy of nuclei

In the fusion of light nuclei there is a *mass defect*, the total rest mass of the fusion products being lower than that of the reactants. According to Einstein it corresponds to an energy $\Delta E = \Delta mc^2$ which is released as kinetic energy of the reaction products. It is usual to note this information in the reaction equation. With this the D-T fusion reaction foreseen for a fusion reactor reads

$$^{2}\mathrm{D} + {}^{3}\mathrm{T} \rightarrow {}^{4}\mathrm{He}\ (3.5\ \mathrm{MeV}) + {}^{1}\mathrm{n}\ (14.1\ \mathrm{MeV})\ . \tag{5.1}$$

Altogether 17.6 MeV of binding energy are released; 20 % of it go to the (heavier) alpha particles (^{4}He) and 80 % to the (lighter) neutrons, the distribution in the ratio 1:4 being due to momentum conservation.

Nuclei are composed of neutrons and protons, called *nucleons* collectively. The protons repel each other through Coulomb forces. The nuclei are nevertheless bound together by yet stronger nuclear forces acting attractively between all nucleons. Those are very short range forces having their origin in the quark composition of the nucleons. Roughly speaking they comprise that part of the binding forces between quarks that extends beyond the internal quark structure of the nucleons. Although the attractive forces between nuclei dominate the Coulomb forces at close distance, they decay so quickly that practically they act between immediate neighbors only. It is evident that a single nucleon is bound more strongly to the nucleus when it is not only acted on by the attractive forces of one or two but of many nucleons. Correspondingly, the binding energy per nucleon (= energy needed for the extraction of the nucleon from the nucleus) rises with growing numbers of nucleons at first. However, for all practical purposes this growth comes to and end as soon as the nucleons are surrounded so tightly by others that there is no place for an additional nucleon in their immediate neighborhood. In addition, the long range electric repulsion that acts on each proton increases with each additional proton. This counteracts the binding and causes the average binding energy to drop after a certain number of nucleons has been reached.

Since each nucleus possesses *negative* binding energy, its mass is always smaller than the sum of the masses of all neutrons and protons of which it consists. According to Einstein's formula, $E = mc^2$, from the mass-defect of a nucleus with A nucleons (Z protons and N neutrons) we obtain the binding energy

$$B(Z,N) = (Zm_p + Nm_n - m_A{}^+)\,c^2 = [Z(m_p + m_e) + Nm_n - (m_A{}^+ + Zm_e)]\,c^2, \tag{5.2}$$

where $m_A{}^+$ is the mass of the nucleus, and m_p , m_n and m_e are the masses of proton, neutron and electron. Figure 5.1 shows the average binding energy per nucleon derived from the empirical mass defects of the different nuclei. The binding energy of ^{4}He, ^{12}C and ^{16}O is markedly higher than that of the respective neighbors. In each of these nuclei both the protons and the neutrons are paired, and quantum theory predicts an especially strong binding between paired nucleons (see Table 5.1).

Table 5.1. Especially strong binding energies (in MeV) of nuclei (notation $^A_Z\mathrm{X}_N$) with paired protons and neutrons.

Nucleus	$^4_2\mathrm{He}_2$	$^6_3\mathrm{Li}_3$	$^7_3\mathrm{Li}_4$	$^8_4\mathrm{Be}_4$	$^9_4\mathrm{Be}_5$	$^{10}_5\mathrm{B}_5$	$^{11}_5\mathrm{B}_6$	$^{12}_6\mathrm{C}_6$
$-B$	28.3	32.0	39.2	56.2	58.2	64.8	76.2	92.2
$-B/A$	7.1	5.3	5.6	7.1	6.5	6.5	6.9	7.7

Since the binding energy of the nucleons must be expended for their separation from the nucleus, it is released in the reverse process, fusion. The maximum of B/A at $A = 56$ (iron) allows energy gain by fusion of light nuclei and fission of heavy nuclei. In the fission of ^{235}U induced by slow neutrons the initial attachment of a neutron creates an intermediate ^{236}U nucleus that decays into fragments. The average binding energy released in this process is about 195 MeV, and the energy gain per nucleon is 195 MeV/235 = 0.83 MeV. On the other hand, in the D-T fusion reaction the energy gain per nucleon of 3.5 MeV is more than four times as much.

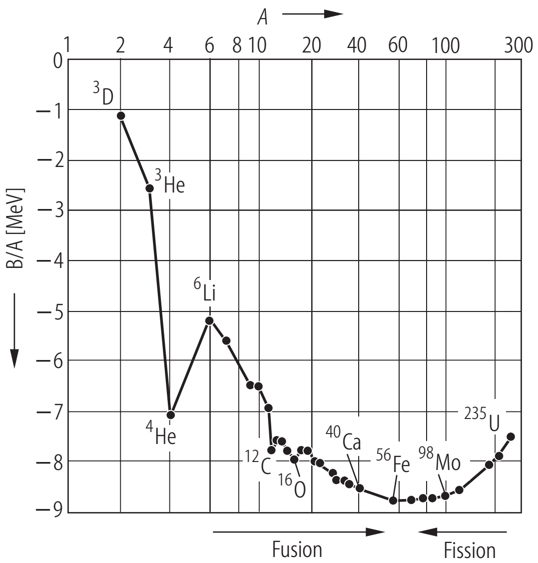

Fig. 5.1. Average binding energy per nucleon, B/A, versus nucleon number, A.

The repulsion between nuclei due to their electric charge provides a severe obstacle to the process of fusion. Down to a distance of 3.7×10^{-15} m repulsion dominates; only closer do the nuclear forces come into action and cause attraction. This means that, from a classical point of view, the D and T nuclei can only fuse when they come closer than 3.7×10^{-15} m. For that purpose they must overcome extreme repulsive forces. The energy needed to overcome the Coulomb-wall of mutual repulsion is about 0.4 MeV and corresponds to a temperature $T \approx 3 \times 10^9$ K if this is to be achieved by thermal motion. Fortunately the tunneling effect makes markedly lower temperatures possible. For a D-T reaction, the tunneling probability, called *Gamow factor* (see e.g. [88Kra]), is approximately given by

$$w \approx \exp\left(-34.4\sqrt{\mathrm{keV}/E_{\mathrm{kin}}}\right) . \tag{5.3}$$

Application of this to $E_{\mathrm{kin}} = 10$ keV and $E_{\mathrm{kin}} = 100$ keV results in a tunneling probability of $w \approx 1.9 \times 10^{-5}$ and $w \approx 3.2 \times 10^{-2}$ respectively. This indicates that markedly lower temperatures than the classically required 3 billion K can lead to fusion. However, the tunneling probability is not all that matters for fusion because after the penetration of the Coulomb-wall the two nuclei still have to fuse. For this purpose it is necessary that they get into a quantum state that is either the ground state or an excited state of the nucleus to be formed. This means that after tunneling the two nuclei must either have appropriate energies or must be able to radiate away excess energy rather quickly. These processes are very complicated to calculate, and in most cases theoretically unsolved so that one must be satisfied with experimental values or empirical formulae.

5.1.3 Fusion reactions

According to Fig. 5.1 the direct fusion of the ^{4}He nucleus out of its four nucleons would still be more energetic than the D-T reaction because a total binding energy of 28 MeV would be released in this process, 7.1 MeV per nucleon. However, a reaction of this kind would require the simultaneous collision of four nuclei. This process is so highly improbable that it does practically not occur. Indeed the fusion of two reaction partners is already a rather improbable process. Nevertheless, in a very subtle roundabout way the sun succeeds in fusing step by step four protons into a ^{4}He nucleus, each step fusing only two nuclei. This is achieved in the *proton-proton cycle* detected by Bethe in 1938 and the *carbon cycle* detected in the same year by Bethe and von Weizsäcker. In both cases the net reaction is

$$4\,{}^1\mathrm{H} \rightarrow {}^4\mathrm{He} + 2\mathrm{e}^+ + 2\nu + 2\gamma \ , \tag{5.4}$$

with an energy release of 26.7 MeV (due to the creation of some extra particles this is a little smaller than the binding energy of the ^{4}He nucleus.) Only about one percent of the sun's energy release is gained from the carbon cycle. In more massive stars than the sun, however, the proton-proton cycle does not release enough energy to maintain the internal pressure. Consequently these stars shrink, subsequently raising their temperature until the carbon cycle takes over. Therefore, in massive stars the latter is dominant.

Altogether more than 80 different fusion reactions are currently known [84Gro]. In fusion research the main interest lies in the D-T reaction, (5.1). It can be accompanied by several reaction branches:

$$^2\mathrm{D} + {}^3\mathrm{T} \rightarrow {}^4\mathrm{He}\ (3.5\ \mathrm{MeV}) + {}^1\mathrm{n}\ (14.1\ \mathrm{MeV})\ , \tag{5.1}$$

$$^2\mathrm{D} + {}^2\mathrm{D} \rightarrow {}^3\mathrm{He}\ (0.82\ \mathrm{MeV}) + {}^1\mathrm{n}\ (2.45\ \mathrm{MeV})\ , \tag{5.5}$$

$$^2\mathrm{D} + {}^2\mathrm{D} \rightarrow {}^3\mathrm{T}\ (1.01\ \mathrm{MeV}) + {}^1\mathrm{H}\ (3.02\ \mathrm{MeV})\ , \tag{5.6}$$

$$^2\mathrm{D} + {}^3\mathrm{He} \rightarrow {}^4\mathrm{He}\ (3.6\ \mathrm{MeV}) + {}^1\mathrm{H}\ (14.7\ \mathrm{MeV})\ , \tag{5.7}$$

$$^2\mathrm{D} + {}^4\mathrm{He} \rightarrow {}^6\mathrm{Li}\ (1.7\ \mathrm{MeV})\ , \tag{5.8}$$

$$^2\mathrm{D} + {}^6\mathrm{Li} \rightarrow {}^3\mathrm{He} + {}^4\mathrm{He} + {}^1\mathrm{n} + 2.56\ \mathrm{MeV}\ , \tag{5.9}$$

$$^3\mathrm{T} + {}^3\mathrm{T} \rightarrow {}^4\mathrm{He} + 2\,{}^1\mathrm{n} + 11.3\ \mathrm{MeV}\ , \tag{5.10}$$

$$^3\mathrm{T} + {}^3\mathrm{He} \rightarrow {}^4\mathrm{He} + {}^2\mathrm{D} + 14.3\ \mathrm{MeV}\ , \tag{5.11}$$

$$^3\mathrm{He} + {}^3\mathrm{He} \rightarrow {}^4\mathrm{He} + 2\,{}^1\mathrm{H} + 12.9\ \mathrm{MeV}\ , \tag{5.12}$$

$$^3\mathrm{He} + {}^4\mathrm{He} \rightarrow {}^7\mathrm{Be}\ (1.5\ \mathrm{MeV})\ . \tag{5.13}$$

It is seen that nuclei still more massive than ^{4}He are created, and in principle fusion reactions can also take place with them. These are, however, so rare that they do not need to be taken into account.

In the D-T reaction the main portion of the energy is released to the neutron. On the one hand the fast fusion neutrons created this way lead to secondary radioactivity in some materials surrounding the plasma (first wall, supports, etc.), on the other hand the neutrons help to exhaust the fusion power; being uncharged they are not held back by a confining magnetic field and they can also easily penetrate the confinement vessel. Outside of this their energy can be extracted by a moderator.

The D-^{3}He reaction, (5.7), still has a rather good reactivity and produces only charged particles as reaction products. In magnetic confinement schemes this would cause tremendous problems: Not only does it require much higher fusion temperatures than the D-T reaction but also no technically feasible solution is presently seen for how to extract the energy from the plasma vessel. In inertial confinement schemes this problem would not occur. Note, however, that ^{3}He is an extremely rare element on earth: In usual helium among 1 million ^{4}He atoms only one ^{3}He atom is found, and even ^{4}He is a rare and very expensive gas. Futuristic concepts foresee mining ^{3}He on the moon and bringing it to the earth. On the moon it is produced by the bombardment of the moon's surface by the solar wind and cosmic rays and is quite abundant though rather diluted.

The tritium needed for the D-T reaction is radioactive and decays according to

$$^3\mathrm{T} \rightarrow {}^3\mathrm{He} + \mathrm{e}^- \,, \tag{5.14}$$

with a half-life of 12.3 years. This is the reason why practically no tritium is found on earth. What one would find naturally is just the amount which is added as a supplement to the atmosphere and the oceans by nuclear transformation due to cosmic radiation, about 1 kg being a good guess for its total mass. In addition there exist about 100 kg that were produced artificially in fission reactors. The tritium needed for starting the first fusion reactor will have to be bought and will be extremely expensive. After that the tritium supply will be no problem since each fusion reactor can breed more than the tritium supply it needs.

The breeding of the tritium needed in a D-T fusion reactor is made rather easy by the neutron produced in the D-T reactions. By surrounding the reaction vessel with a blanket containing lithium, tritium is bred according to the reactions

$$^1\mathrm{n} + {}^6\mathrm{Li} \quad \rightarrow \quad {}^4\mathrm{He} + {}^3\mathrm{T} + 4.8\ \mathrm{MeV}\,, \tag{5.15}$$

$$^1\mathrm{n} + {}^7\mathrm{Li} \quad \rightarrow \quad {}^3\mathrm{He} + {}^3\mathrm{T} + {}^1\mathrm{n} - 2.5\ \mathrm{MeV}\,. \tag{5.16}$$

The blanket can be constructed in such a way that, acting as a moderator, it simultaneously extracts the energy from the neutrons and makes it accessible for use by standard technical methods.

5.1.4 Reaction cross-sections and reaction rates

A fusion reaction which releases a lot of energy but occurs very rarely is of little use. Thus the reaction cross-section and the reaction frequency is a crucial issue.

In a plasma the reaction cross-section can be decomposed in the form

$$\sigma = \sigma_{\mathrm{sc}} + \sigma_{\mathrm{fus}}\,, \tag{5.17}$$

where σ_{sc} accounts only for the scattering and σ_{fus} for the fusion collisions. The scattering collisions are due to long range Coulomb forces. Therefore one has to deal with two-particle collisions and with many particle interactions simultaneously. In the latter case a collision is considered to be a series of small-angle deflections leading to a 90° deflection. For the appropriately defined collision cross-section one obtains

$$\sigma_{90^\circ} = \frac{Z^4 e^2 \ln\Lambda}{25\pi\varepsilon_0{}^2 \left(kT\right)^2} \quad \text{with} \quad \Lambda = \frac{12}{\sqrt{n_\mathrm{e}}}\left(\frac{\varepsilon_0 kT}{e^2}\right)^{3/2}, \tag{5.18}$$

where ε_0 is the vacuum dielectric constant, e is the electron charge, and k the Boltzmann constant. In a 100 million degrees D-T fusion plasma having an electron density of $n_e = 0.5 \times 10^{20}$ m^{-3} one obtains $\sigma_{90°} \approx 10^{-24}$ m^2 for D-T collisions from this formula. For particle energies well below the tunneling barrier the total fusion cross-section is

$$\sigma_{\text{fus}} = \frac{S(E_\text{r})}{E_\text{r}} \mathrm{e}^{-G/\sqrt{E_\text{r}}} \quad \text{with} \quad E_\text{r} = \frac{\mu\left(\upsilon_i - \upsilon_j\right)^2}{2}, \quad G = \frac{Z_1 Z_2 e^2 \sqrt{2\mu}}{4\pi\varepsilon_0 \hbar}, \quad \mu = \frac{m_i m_j}{\left(m_i + m_j\right)}, \tag{5.19}$$

with E_r being the total energy of the fusion partners in their center-of-mass system, and m_i, m_j denoting the masses and υ_i, υ_j the velocities of the fusion partners. The Gamov factor, $\exp(-G/\sqrt{E_\text{r}})$, essentially represents the tunneling probability, and the front factor the probability for a fusion reaction to take place after the tunneling. $1/E_\text{r}$ accounts for the fact that with increasing energy E_r the time available for tunneling decreases. The factor $S(E_\text{r})$ describes the interaction of the nuclear forces after tunneling which can result in retardation or prevention of a fusion reaction. A good fit to experimental data is enabled by representing $S(E_\text{r})$ as a Padé polynomial,

$$S(E) = \frac{a_1 + E(a_2 + E(a_3 + E(a_4 + Ea_5)))}{1 + E(b_1 + E(b_2 + E(b_3 + Eb_4)))} \quad . \tag{5.20}$$

The theoretically calculated values of the fit factors a_i and b_i are rather inaccurate. However, through judicious choice of fit factors one can obtain a good fit to experimental data. Recent values for the D-T reaction are [92Bos]:

$$\begin{aligned} &G/\sqrt{\text{keV}} = 34.38\,, \\ &a_1 = 6.93 \times 10^4, \quad a_2 = 7.45 \times 10^8, \quad a_3 = 2.05 \times 10^6, \quad a_4 = 5.20 \times 10^4, \quad a_5 = 0.0, \\ &b_1 = 6.38 \times 10^1, \quad b_2 = -9.95 \times 10^{-1}, \quad b_3 = 6.98 \times 10^{-5}, \quad b_4 = 1.073 \times 10^{-4}. \end{aligned} \tag{5.21}$$

Figure 5.2 shows the dependence of the fusion cross-section on the energy E_r for these parameter values. The scattering cross-section of the D-ions, largely dominated by collisions with D- and T-ions, is larger than the D-T cross-section by at least one order of magnitude. Collisions with electrons play only a minor role since only a small momentum exchange is possible with them.

In a thermonuclear plasma the reaction rate for fusion reactions between nuclei of species i with density n_i and species j with density n_j is given by

$$R_{ij} = -\frac{n_i n_j}{1 + \delta_{ij}} \left\langle \sigma_{\text{fus}} \upsilon_\text{r} \right\rangle \,, \tag{5.22}$$

$$\text{with } \left\langle \sigma_{\text{fus}} \upsilon_\text{r} \right\rangle = \frac{4}{\sqrt{2\pi\mu(kT)^3}} \int_0^\infty \sigma_{\text{fus}}(E_\text{r}) E_\text{r} \mathrm{e}^{-E_\text{r}/kT} \mathrm{d}E_\text{r} \quad . \tag{5.23}$$

If in this equation the semi-empirical formula (5.19) is inserted with the values of S and G obtained from (5.20) and (5.21), one obtains the curves for the temperature dependence of the reactivities, $\left\langle \sigma_{\text{fus}} \upsilon_\text{r} \right\rangle$, shown in Fig. 5.3.

At the temperatures foreseen in a fusion reactor the main contribution to the reactivities comes from a small number of highly energetic particles in the high-energy tail of the corresponding Maxwell distribution. This tail is repopulated by scattering collisions that cause the plasma to approach a Maxwellian distribution. Thus while scattering collisions have the unpleasant side effect of causing diffusion and particle losses from the reaction vessel on the one hand, on the other hand they have the important task of replenishing highly energetic particles. This collisional process for the replacement of highly energetic particles lost by fusion is an essential characteristic of thermonuclear fusion. For the D-T reaction at a temperature of 10 keV and densities $n_\text{D} = n_\text{T} \approx 0.25 \times 10^{20}$ m^3 required in a fusion reactor, the average times of free flight before a fusion reaction and a 90° deflection are given by

$$\tau_{\text{fus}} = \frac{1}{n\langle\sigma_{\text{fus}}\, \upsilon\rangle} = 400\ \text{s}, \qquad \tau_{90^\circ} = \frac{1}{n\langle\sigma_{90^\circ}\, \upsilon\rangle} = 5\times10^{-2}\ \text{s}\,.$$

Thus on average for each fusion collision there are about 8000 scattering collisions. On the other hand a few scattering collisions will already be sufficient to provide a Maxwellian distribution. This way the replacement of highly energetic particles lost by fusion is guaranteed. Since the average ion velocity at 10 keV is about 1000 km/s, a waiting time of 400 s for a fusion reaction corresponds to a traveling distance of several 100000 km. However, the ions do not go that far before they escape confinement: The average confinement time of the ions in a fusion plasma is only about 10 s. This means that only about 2 to 3 percent of the ions participate in fusion reactions during confinement.

In the following it will be explained how the differences between the various fusion reactions in Fig. 5.3 arise. According to (5.22) the reactivity, $\langle\sigma_{\text{fus}}\upsilon_{\text{r}}\rangle = -R_{ij}(1+\delta_{ij})/(n_i n_j)$, is a measure of the yield of the reaction that is independent of the particle densities and can be interpreted as a reaction probability. Like the fusion cross-section it goes through a maximum as the temperature is increased more and more, owing to the same reason: At very high temperatures, while on the one hand sufficiently many particles have the energy for easy tunneling, the time available for this and for fusing after successful tunneling is much smaller on the other hand. The optimum temperatures of the D-^{3}He and the proton-boron reaction (p-^{11}B) lie above that of the D-T reaction. The reason is that ^{3}He is doubly charged and ^{11}B carries five charges, i.e. the repulsive electric forces between the nuclei are much stronger, and to be overcome they require larger velocities or temperatures. It may surprise that the maxima in the reactivities of reactions between other hydrogen isotopes occur at higher temperatures and are lower than that of the D-T reaction, although all hydrogen isotopes have the same charge. Already in 1934 M. Goldhaber found that the fusion of deuterium and tritium to ^{4}He proceeds through an intermediate step in which the meta-stable helium isotope ^{5}He is built. The transient formation of a single nucleus out of two reaction partners is a much more simple process than the transformation into more than one reaction product that occurs in the D-D and T-T reactions. Thus the probability for the D-T reaction is much larger than that for the D-D and the T-T reactions. However, the energies with which the two reaction partners meet each other must be tuned in a quasi-resonant manner to the binding energy of the transient state. Therefore the reactivity of the D-T reaction is not generally superior but has only a larger maximum value in the resonance regime of the reaction.

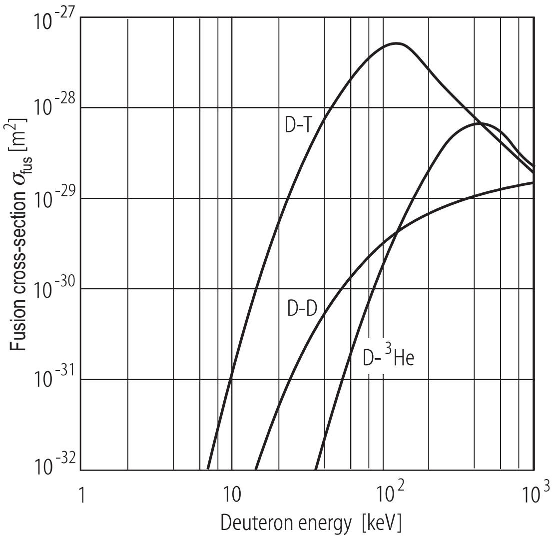

Fig. 5.2. E_{r} dependence of the fusion cross-sections for the D-D, D-T and D-^{3}He reaction with ln Λ = 18.

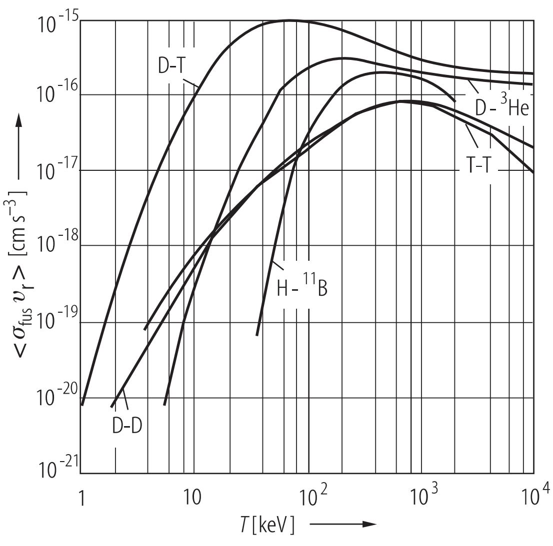

Fig. 5.3. Temperature dependence of the reactivity.

5.2 Operational conditions and balances

[D. Reiter]

5.2.1 Introduction

The basic concept rests on the fact that fusion of light atomic nuclei is accompanied by release of energy. If the interaction energy is provided mainly by the thermal motion of the fuel particles one speaks of thermonuclear fusion. The dominance of dissipative Coulomb interaction over fusion processes excludes beam-beam and beam-target concepts for a fusion reactor. Only a thermonuclear plasma, consisting of electrons and fuel ions has the potential to meet the criteria regarding energy balance and power density. The temperature of the fuel has to be in the range of (several) 100 million °C for a positive power balance. This is independent of whether the fusion process is initiated in a highly compressed solid (pellet) – ICF, or in a magnetically confined plasma – MCF.

Detailed operational conditions, energy balances (ICF) or power balances (MCF) of fusion reactors depend on spatial distributions of composition and temperature of the plasma, as well as on the temporal evolution in case of ICF. The resulting set of coupled differential equations [81Sta, 97Miy, 81Tel, 99Win, 92Kad] can only be studied with large computer simulations. Simpler "point-reactor models" as described here are obtained by averaging, and by introducing typical "loss-times" in order to eliminate derivatives [90Rei].

5.2.2 Fusion power density

The ultimate goal is often considered to be utilization of the D-D reaction because it will avoid, to a large extent, the technological difficulties associated with the breeding of and fueling with the radioactive isotope tritium. Present-day research is, however, oriented almost exclusively toward the D-T reaction. The reason for this is the anticipated fusion power density in the plasma. Other fusion reactions (D-D or D-^{3}He) require much higher temperatures and provide at the same pressure only 1 % of the D-T fusion power density.

Assuming equal electron- and fuel-densities (negligible impurity and Helium ash content in the flame), $n_e = n_i = n$, as well as the same temperature for all components of the plasma, $T_e = T_i = T$, the fusion power density for an optimal 50 %-50 % mixture of D and T ions is given as:

$$P_F = \frac{1}{4} n^2 \langle \sigma v \rangle E_F \quad = \frac{1}{16k^2} p^2 \frac{\langle \sigma v \rangle}{T^2} E_F, \quad \text{with } E_F = 17.6 \text{ MeV}. \tag{5.24}$$

Here the plasma pressure is $p = 2nkT$. The rate coefficients $<\sigma v>$ for fusion processes depend upon temperature (see Sect. 5.1). The fusion power density P_F has a maximum in the range $T = 10\ldots20$ keV, and in this range the ratio $<\sigma v>/T^2$ is approximately constant. For example for $p = 10$ bar, typical of magnetically confined plasmas, one has $P_F = 7.5$ MW/m^3. This is higher than in current coal-fired power stations and lower than in typical light water reactors.

5.2.3 The fusion energy gain factor *G* and the power gain factor *Q*

The two major concepts, magnetic confinement fusion (MCF) and inertial confinement fusion (ICF), differ from ordinary power plants in that not their fuel consumption is of any importance, but, instead, that significant power is required to run the plant. The goal is, therefore, to achieve a high energy gain *G*, defined as the ratio between output energy to input energy. Criteria for an economical fusion power operation then depend upon the duration of the plasma heating phase, efficiency of electric power conversion, plasma parameters and pulse length (duty cycle). Such conditions are particularly important for ICF, because this is an inherently pulsed concept and these pulses (micro-explosions) are short compared to the phase of generating and heating the thermonuclear plasma. The pulse length (pellet lifetime, τ_L) is about the same as the plasma fusion burn time, τ_b, and the latter is also a measure for the energy confinement time: $\tau_E \approx \tau_b$.

In MCF the plasma can be confined stationarily or, at least, for very long times (hours) compared to the other phases: $\tau_E << \tau_b$. It can, therefore, be operated like an oven, and the rather complex criteria for a positive energy balance involving all relevant efficiency factors can be replaced by a much simpler power balance consideration for the fusion flame alone; G can then be taken as stationary power gain factor (usually referred to as Q), which is now defined as the ratio of fusion power to heating power under stationary conditions.

5.2.4 Break-even, ignition

Producing an amount E_F of fusion energy is of interest only if it is, at least, larger then the (heating) energy E_H needed to make the reactions possible. Ignoring energy losses during the heating phase and also recovery of any internal energy stored in the plasma, this implies:

$$E_F = P_F \cdot \tau_b > E_H = (P_{init} \cdot \tau_{init}) / \eta_{init} + (P_{heating} \cdot \tau_b) / \eta_b \approx \frac{3nT}{\tau_E} \tau_b , \tag{5.25}$$

where P_{init} is the initial heating power required to heat both the electron and fuel ion plasma components to reach an initial internal energy density $u_e = u_i = 3/2nT$, such that fusion energy production is initiated at time τ_{init} and at a rate P_F. $P_{heating}$ is the external heating power which may be supplied to the plasma after the initial fusion conditions n, T have been reached. The power loss from the flame is written, globally, as $P_{loss} =: (u_e + u_i)/\tau_E$ .This defines the "energy confinement time", τ_E, which characterizes the quality of thermal insulation of the plasma confinement scheme and comprises transport (conduction and convection) and radiation losses. Some care is needed because sometimes radiation losses $P_{rad} = Cn^2g(T)$ (e.g. due to Bremsstrahlung or line radiation) are excluded from the definition of τ_E and are, instead, explicitly accounted for in the energy balance. The factors $1/\eta$ have been introduced to account for energy conversion efficiencies (fusion energy → electric energy → plasma heating).

As P_F and P_{rad} scale with n^2, and P_{loss} on the right-hand side scales with n/τ, energy or power balances for fusion reactors have the general form: $n\tau > f(T,\eta)$. In our case we find:

$$n\tau \geq \frac{12\,kT}{\eta\langle\sigma v\rangle E_F} \ . \tag{5.26}$$

In ICF the external heating during the pulse is negligible. Hence the relevant time τ here is, strictly, the burn time τ_b, which is also about the pellet lifetime τ_L, i.e. the duration of the micro-explosion. However: $\tau \approx \tau_E$. The relevant efficiency η is η_{init}, and $\eta_{init} \approx 10^{-4} << 1$. In MCF, by contrast, $\tau_b >> \tau_E$, the initial heating energy $3nT$ can be neglected. In this case, dividing (5.25) by τ_b, one recovers the stationary power balance for MCF. This is the same relation as (5.26), however with the relevant time τ now being τ_E , very distinct from the pulse length $\tau_L \approx \infty$, and the efficiency $\eta = \eta_b \approx 1$. The high efficiency value in this stationary mode results from the possibility to fuel the plasma by cold particles and to let these be heated by the fusion α-particles.

This so-called **"break-even"** criterion ($G \geq 1$ for $\eta = 1$) results in $n\tau_E \geq 0.7 \times 10^{20}$ m^{-3}s for typical fusion parameters $T = 10$ keV, $<\sigma v>_{D\text{-}T} \approx 10^{-22}$ m^3/s. By contrast, the **ignition** condition ("burn condition", $Q = \infty$) ensures that a confined plasma is kept at thermonuclear temperatures by self-heating through the confined (charged) particles generated in fusion reactions. For a stationary burning pure D-T plasma it is obtained when E_F is replaced by the α-particle energy, $E_\alpha = 3.5$ MeV, yielding: $n\tau_E > 3 \times 10^{20}$ m^{-3}s.

Instead of $n\tau$ often the so-called fusion triple product $n\tau T$ is used, in particular in MCF, which has to be around 6×10^{22} m^{-3}s mill. °C for an ignited reactor based on the D-T reaction. This triple product is a particularly useful measure if the plasma pressure is limited, e.g. by the magnetic field.

5.2.5 Power balances for magnetically confined plasmas

A plasma can be shaped and confined in a given volume inside a furnace chamber of reasonable size (several meters across) by applying external magnetic fields (several Tesla).

For magnetically confined plasmas a key parameter is β, defined as the ratio of plasma pressure to magnetic pressure. It is a measure of the cost effectiveness of the magnetic field system for confining the plasma. Inserting for the pressure $p = 1/2\ \mu_0\ \beta B^2$, the fusion power can be expressed as:

$$P_{\mathrm{F}} = \frac{1}{64k^2\mu_0^2}\beta^2 B^4 \frac{\langle\sigma v\rangle}{T^2} E_{\mathrm{F}}\ . \tag{5.27}$$

Typically $\beta << 1$, for reasons of magnetohydrodynamic stability. For kT of about 10 keV, and $B \approx 10$ T, hence: $n << 5 \times 10^{21}\ \mathrm{m}^{-3}$. In practice, the density n is typically chosen somewhat above $10^{20}\ \mathrm{m}^{-3}$. For a typical value, $\beta = 5$ %, a magnetic field of about 7 T can confine a plasma pressure of 10 bar, i.e. a D-T plasma with a fusion power density of 7.5 MW/m^3.

Magnetic plasma confinement is effective only perpendicular to the direction of the ***B***-field. Therefore the shape of a magnetically confined plasma must be a torus (or topologically equivalent) in order to avoid the end losses. Under the above-mentioned conditions and for densities of about $10^{20}\ \mathrm{m}^{-3}$, magnetic fields on the order of 10 T with field lines on nested toroidal surfaces have been estimated to be sufficient to isolate the hot plasma from the surrounding chamber. This results in a required confinement time τ_E of the order of magnitude of a second. From this the size of a MCF reactor can be estimated: for self-sustained burn the reaction volume must be larger than 1000 m^3 and the fusion power is then in the giga-watt range. The large torus radius R is of the order of 10 m, and the small radius is several (3…4) meters. For 2.5 to 3 GW thermal power (resulting in about 1 GW electric power), the 20 % carried by the ^{4}He particle constitutes the plasma heating power. Under stationary conditions, these 0.6 GW must be deposited on the walls, with a total area of about 500…1000 m^2. The average power load is then on the order of 1 MW/m^2.

Purity conditions affect the power balance strongly, through dilution (low-Z impurities) and radiation losses (high-Z impurities). This directly translates to a minimum helium ash-removal efficiency and, hence, to a certain minimum degree of plasma-surface contact in general. Therefore the operational window for a MCF reactor is, amongst others, also determined by a compromise between the maximum tolerable and minimum required plasma surface interaction [91May].In particular, the helium has to be removed actively from the flame within 10 energy confinement times to avoid choking of the flame by its own ash.

5.2.6 The Lawson criterion

The most famous and historically first of the $n\tau > f(T,\eta)$ conditions is the so-called "Lawson criterion", [57Law], specifically derived for pulsed confinement schemes. It is situated between the states of "break-even" and "ignition" mentioned above:

$$n\tau_{\mathrm{L}} > \frac{6}{E_{\mathrm{F}}} \cdot \frac{kT}{\langle\sigma v\rangle} \cdot \frac{1-\eta}{\eta}\ . \tag{5.28}$$

This criterion states that recovery of energy from fusion reactions (E_{F} [keV] per fusion reaction) with a thermal efficiency η sustains the plasma temperature, kT [keV], if the "fusion product" of fuel particle density, n, and plasma lifetime, τ_{L}, exceeds a critical value, which depends upon the temperature of the plasma. For the D-T reaction there is a minimum of about $n\tau_{\mathrm{L}} \approx 10^{20}\ \mathrm{m}^{-3}\mathrm{s}$ at a temperature of about 270 mill. °C, for the D-D reaction this minimum is shifted to about 500 mill. °C and to a value of $n\tau_{\mathrm{L}} \approx 5 \times 10^{21}\ \mathrm{m}^{-3}\mathrm{s}$.

5.2.7 Power balances for inertial confinement systems

If one relies on particle inertia, the plasma is certainly limited in time. Efficiencies of the various systems of the reactor will therefore play a crucial role [82Dud, 91May]. The achievable G values here are more relevant than the fusion triple product as such. One has: $\tau_E \approx \tau_P \approx \tau_L =: \tau$. In contrast to MCF, here the energy confinement time can easily be estimated, and eliminated from the operational conditions by expressing it in terms of other typical parameters of the fusion pellet.

This time τ is just given by $\tau \approx \Delta \cdot \overline{v}$, with Δ being the plasma-(= pellet-)diameter, and $\overline{v}$ the typical particle velocity, $\overline{v} \approx c_s = \sqrt{\gamma p / \rho}$, where γ is the adiabatic coefficient and ρ the mass density, i.e., $\overline{v} \approx 10^{10}$ m/s for $T = 10$ keV.

Hence, the confinement condition $n\tau > 10^{20}\ \mathrm{m^{-3}s}$ takes the form $n\Delta > 10^{26}\ \mathrm{m^2}$.

In order to keep the input and output energy within reasonable values, Δ has to be kept reasonably small. The heating energy E_{in} is given by

$$E_{\mathrm{in}} = 3nT \cdot \frac{4\pi}{3}\left(\frac{\Delta}{2}\right)^3 . \tag{5.29}$$

For the fusion gain factor, $G = E_F/E_{\mathrm{in}}$, one has: $G = \Delta/\Delta_{\mathrm{min}}$. Here Δ_{min} has to be such that the balance condition is fulfilled, and one finds:

$$E_{\mathrm{in}}\,[\mathrm{J}] \approx 2\times 10^{57}\, G^3 / n^2 . \tag{5.30}$$

Thus, for $G = 10$. with $E_{\mathrm{in}} \approx 10^6$ J, the plasma density must be above $10^{30}\ \mathrm{m^{-3}}$ (100 times the density of solid DT), the plasma size is of the order of millimeters, and the plasma lifetime in this case is $\tau \approx 10^{-9}$ s.

5.2.8 Burn-up fraction

Rather than the product $n\Delta$ it is more common in ICF to use the product ρR (mass density times pellet radius). The fusion energy E released in one cycle (i.e., from one ignited pellet) from a pellet of mass M is $E_{\mathrm{pellet}} = \varepsilon_{\mathrm{DT}} \Phi M_{\mathrm{pellet}}$. Here $\varepsilon_{\mathrm{DT}} \approx 3.4 \times 10^5$GJ/kg is the released fusion energy per unit mass and Φ is the fraction of the fuel that has been burned. Assuming that (a) the burning starts at a pellet radius R, (b) is maintained (through the heating by the helium fusion products) at a constant temperature T, and (c) the burning front expands with a (sound-) speed $c_s \propto (T/m)^{1/2}$, then the burn-up fraction is given as:

$$\Phi = \frac{(\rho R)}{(\rho R) + (\rho R)^*} = \frac{(\rho R)}{(\rho R) + \left(4c_s m_{\mathrm{DT}} / \langle \sigma v \rangle\right)} . \tag{5.31}$$

Here the burn-up parameter is $(\rho R)^* = 4c_s m_{\mathrm{DT}}/\langle\sigma v\rangle \approx 70\ \mathrm{kg\,m^{-2}}$ in the relevant temperature range. In order to achieve, at least, $\Phi = 30$ %, the condition for the ICF-product ρR in the temperature range around 10…20 keV then is: $(\rho R) \approx 30\ \mathrm{kg\,m^{-2}}$.

If one fixes the burn-up fraction Φ, and hence the product ρR, then the energy (and the mass M) of the pellet scales as $E_{\mathrm{pellet}} \propto M_{\mathrm{pellet}} \propto \rho R^3 = (\rho R)^3/\rho^2$, i.e., both scale with $1/\rho^2$. Reduction of the energy of one pellet explosion can only be achieved by increasing the density. Table 5.2 shows the energy of one pellet for $(\rho R) \approx 30\ \mathrm{kg\,m^{-2}}$.

At least 1000 times the density of liquid DT, i.e. $\rho_{\mathrm{DT}} = 2 \times 10^5\ \mathrm{kg/m^3}$, is required to reduce this energy to a level of several 100 MJ, corresponding to about 0.2 t TNT. An IC fusion reactor has to ignite about one such pellet per second in order to arrive at a thermal fusion power of the order of 1 GW.

Table 5.2. Values of the mass density, ρ_{DT}, and the corresponding pellet energy, E_{pellet}.

ρ_{DT} [kg m^{-3}]	E_{pellet} [GJ]	E_{pellet} [t TNT]
2×10^2	10^6	2×10^5
2×10^3	10^4	2×10^3
2×10^4	100	20
2×10^5	1	0.2

5.2.9 ICF reactor balance

Consider a reactor with a target energy gain factor G, an efficiency of the driver system η_D, a fraction f of electrical power, which is re-introduced into the system for the driver system, and a converter of thermal to electric power with an efficiency $\eta_{th} \approx 40\ldots45$ %. The balance equation then reads: $\eta_D\, G\, (\eta_{th} f) = 1$.

If we assume $f = 20$ % in an ICF reactor we find $\eta_D\, G > 10$: The ICF driver systems, by the time of writing this chapter, have efficiencies of about 5…10 % for lasers, and up to 25 % for heavy ion beam systems. That is, a required target energy gain factor G of 100…200 for laser-driven systems and of $G \approx 40$ for heavy ion beam systems results.

A "naive" energy gain can be estimated as the ratio of thermonuclear energy gain (per unit mass), $\varepsilon_{DT} \cdot \Phi\,[\mathrm{GJ/kg}] = 3.4\times10^5 \cdot \Phi$, to the energy cost for the internal energy of the plasma at ignition temperature T_{ig}, again per unit mass, $\varepsilon_{ig}\,[\mathrm{GJ/kg}] = 4(3/2)\ T_{ig}/m_{DT} = 115\ \ T_{ig}\,[\mathrm{keV}]$, and, hence,

$$
\begin{aligned}
G_{naive} &= \varepsilon_{DT} \cdot \Phi/\varepsilon_{ig} = 3\times10^3\, \Phi/T_{ig}\,[\mathrm{keV}] \\
&= 90 \quad \text{for} \quad \Phi = 0.3 \quad \text{and} \quad T_{ig} = 10\ \mathrm{keV}.
\end{aligned}
\tag{5.32}
$$

5.2.10 Spark ignition

Complications result from the fact that, typically, only a small fraction (≈ 5 %) of the input energy for compression of a pellet is transferred to the fuel. The achieved target energy gain factors are, therefore, only in the range of about $G \approx 5$ and, thus, significantly too low. One way to deal with this problem is the so-called concept of "spark ignition". The idea is based upon the concept of igniting only a small fraction of the fuel in the center of the pellet. From this ignited center, which has to be heated up to ignition temperature, a thermonuclear ignition front spreads out (faster than thermal expansion) and ignites the outer layers of the pellet, which have to be highly compressed, yielding many times the driver input energy, i.e., ≈ 1 GJ.

The **central part** of the pellet can be regarded as an ideal hydrogenic plasma with a pressure $p_s = 2\rho_s T_s/m_{DT}$, with $m_{DT} = 4.2 \times 10^{-27}$ kg. Multiplying with the radius R_s of the central "spark region" yields: $p_s R_s = 2(\rho R)_s\, T_s/m_{DT} \approx 15\,\mathrm{T\,bar\,\mu m}$. In this important relation the parameters $(\rho R)_s = 4\ \mathrm{kg\,m^{-2}}$ and $T_s = 5$ keV have been used. These latter parameters result from detailed ignition and burn calculations. The internal energy per mass unit is then $\varepsilon_s \approx 600$ GJ/kg.

The value of $(\rho R)_s = 4\ \mathrm{kg\,m^{-2}}$ is just sufficient to guarantee that the 3.5 MeV α-particles from the D-T fusion in the spark are stopped in the hot spot and raise its temperature to about 20…40 keV. The alphas and thermal conduction then result in a thermonuclear burn propagating into the outer region and hence can heat the fuel to ignition there. The 14 MeV fusion neutrons still escape from the flame. They might, however, be moderated somewhat already inside the fuel. For $\rho R = 3$, e.g., the fuel is about 1/2 mean free path thick.

The **outer layer** of the pellet consists of rather cold, highly compressed fuel. In this region the electron gas is degenerated, with a pressure $p_c = 2/5\,\alpha n_e \varepsilon_F$ and internal energy $u_c = 3/5\,\alpha\varepsilon_F\, M_C/m_{DT}$. The factor α (with $\alpha \geq 1$) in these expressions is introduced to account for deviation from complete degeneracy. Here, again, $(\rho R)_c \approx 30\ \mathrm{kg\,m^{-2}}$, and for $\rho_c = 2 \times 10^5\ \mathrm{kg\,m^{-3}}$ and for $\alpha = 1$ one finds: $\varepsilon_F \approx 500$ eV and $\varepsilon_c = u_c/M_c \approx 12$ GJ/kg. The pellet mass is then $M_c = (4\pi/3)(\rho R)_c^{\,3}/\rho_c^{\,2} \approx 3$ mg.

If the "spark" contains 2 % of the fuel, and if the efficiency of the compression is 5 %, the "gain" is

$$G = \frac{\left(E_{\mathrm{DT}}\Phi\right)\cdot 5\times 10^{-2}}{0.02\varepsilon_{\mathrm{s}} + \varepsilon_{\mathrm{c}}} \approx 200\,. \tag{5.33}$$

In this case lasers with a few MJ of energy should be sufficient to achieve ignition of the spark region and to spread the ignition front through the outer layers of fuel (thermonuclear burn). This clearly shows the huge advantage of the spark ignition concept as compared to a direct ignition of the entire fuel of the pellet.

As a result from the global considerations one can conclude that for MCF the key problem is to obtain sufficient heat-insulation by the magnetic field (i.e., sufficiently large energy confinement times) with only moderately large reactor units. Stationary, self-heated burn, with fueling by cold D and T is a natural option. Helium particles are needed in the flame sufficiently long for self heating, (their thermalization time is of the order of 1 s) , but must then be removed from the flame with a typical particle confinement time not larger than 10 times τ_E, i.e. typically within 10 s.

For ICF the key problems are to limit the initial heating energy, to increase efficiencies for the driver systems, and to keep the fusion energy in a single explosion at a manageable level. Self heating by the helium ash is an attractive option here too, although in a highly dynamic state.

5.3 Main principles of a fusion reactor

[R. Weynants]

5.3.1 Introduction

Any energetically economical fusion power plant must generate an amount of output energy that largely exceeds the energy needed to keep the plant running. In Sect. 5.2, it was shown for each of the two main lines of pursuit, inertial confinement fusion (ICF) and magnetic confinement fusion (MCF), that a minimum quantity of fuel, represented by the fuel density n, must be maintained together for a minimum time span τ at a sufficiently high temperature T in order to assure adequate energy economy.

For a stationary MCF reactor, a given value of Q, the ratio of generated to consumed power, demands the realization of a minimum value of the triple product $n\tau T$, given by

$$n\tau T = 60\, kT^2 \,/\, (<\sigma\upsilon>\, E_{\mathrm{fus}}\, (1+5/Q)), \tag{5.34}$$

where $Q \geq 50$ is thought to be reactor grade, E_{fus} is the energy released per fusion reaction,$<\sigma\upsilon>$ is the fusion reaction-rate constant averaged over particles of all possible velocities and k is the Boltzmann constant. The temperature dependence of the triple product required, for a D-T fuel with equal concentrations of D and T, shows a minimum at about $T = 15$ keV. For the inherently pulsed ICF reactor the necessary target gain values $G \geq 50$ also require a minimum $n\tau T$ [95Lin], this time given by

$$n\tau T = T \,/\, <\sigma\upsilon>, \tag{5.35}$$

with a minimum at about $T = 30$ keV.

A first challenge for the fusion reactor is the achievement and sustainment of these extreme temperatures, requiring the development of adequate heating methods, which will be discussed in Sect. 5.4. The time τ obviously plays a crucial role and should be understood properly. It is the characteristic time with which the reactor would lose its energy content if the fusion reactions were to stop. One therefore calls it the energy replacement time or more generally the *energy confinement time*. Energy can be lost from the reactor in different ways: by diffusion of particles (carrying their energy along), by conduction and by several forms of radiation (bremsstrahlung, synchrotron radiation, line radiation, recombination radiation). How well diffusion and conduction losses can be curtailed, and thereby τ increased, depends very strongly on the *confinement scheme* considered. Both MCF and ICF have achieved considerable advances in recent years and in both instances the prospect for successful reactor application has been strengthened. In the next section the basic principles of the confinement for each of these lines are given.

5.3.2 Magnetic confinement fusion (MCF)

5.3.2.1 Principles of confinement by magnetic fields

When a plasma is immersed in a magnetic field, the Lorentz force constrains its charged particles to move in helical orbits about the magnetic field lines. In a uniform field and in the absence of Coulomb collisions and plasma turbulence, the particles (better: their guiding centers) remain tied to the field lines but are free to move along them. The distance between the actual particle orbit and the magnetic field line is the Larmor radius, or gyroradius, r_L. The larger the magnetic field, the smaller r_L. A magnetic field is thus, in first approximation, capable of impeding the particle motion perpendicular to the magnetic field but does not prevent particles from moving along the magnetic field. This effect serves as the basis for all magnetic confinement schemes [56Spi, 76Miy, 84Che], while at the same time pointing to the absolute necessity to cope with the particle losses, or end losses, along the magnetic field.

The perturbative effect of collisions and turbulence on the transport of particles and energy across the magnetic field can be understood in terms of a simple statistical diffusion process applied here to a cylindrical plasma. Let us first consider Coulomb collisions. The particles suffer collisions with a characteristic collision time τ_c. A collision allows the particle to step across B with a step length equal to r_L. This gives a diffusion coefficient $D \approx r_L^2/\tau_c$. The effect of (electrostatic) turbulence on the other hand can be estimated in a similar fashion. A simple model pictures the particles to be dragged along by the turbulent waves. The step length is now of the order of the wavelength perpendicular to the magnetic field, $k_\perp^{-1}$, and the effective "collision time" is that of the correlation time of the turbulence, τ_{corr}, yielding $D \approx 1/k_\perp^2 \tau_{corr}$ [65Kad]. In both cases, the confinement time is linked to D by means of the simple relation

$$\tau \approx \frac{a^2}{D}, \tag{5.36}$$

where a is the radius of the plasma, such that in any case high τ requires a large plasma cross-section.

In its motion around a magnetic field line, a gyrating particle constitutes a small current loop of magnetic moment μ that generates a magnetic field opposing the imposed magnetic field by an amount that is proportional to the kinetic energy contained in the perpendicular particle motion. As a result, the actual magnetic field in a plasma, made up of many gyrating particles, will be lower than the applied one: plasmas in magnetic fields are therefore naturally diamagnetic. The larger the sum of the kinetic energies of all the plasma particles, the lower will be the field. This obviously means that there is a limit to the total energy content ($3nT$) that a given magnetic field can confine. The same conclusion is reached by an alternative approach, in which the action of the magnetic field on the confined plasma can be viewed as a balance between the magnetic pressure, $B^2/2\mu_0$, and the plasma pressure, p, according to the relation $p + B^2/2\mu_0 = \text{const}$. The maximum pressure that can possibly be confined at a given B, is thus $B^2/2\mu_0$. Stability constraints prevent, however, the attainment of this maximum, and the pressure thus reaches at most a fraction β (beta) of its theoretical limit [63Sha, 89Whi]. A large value of B is therefore the key to achieve large values of nT.

From what we have just seen, it is to be expected that the fusion triple product in devices without end losses will increase with plasma cross section and magnetic field pressure. Such a dependence is substantiated in Fig. 5.4 which shows the $n\tau T$ values experimentally achieved over 30 years of research in a large number of toroidal magnetic fusion devices as a function of $E_{mag} = B^2/2\mu_0 V$, the total magnetic energy stored in the plasma volume V. The scatter in the data is caused by differences in configuration and in secondary engineering parameters. This data predicts that magnetic fusion will achieve reactor-grade $n\tau T$ values in the projected ITER-FEAT device.

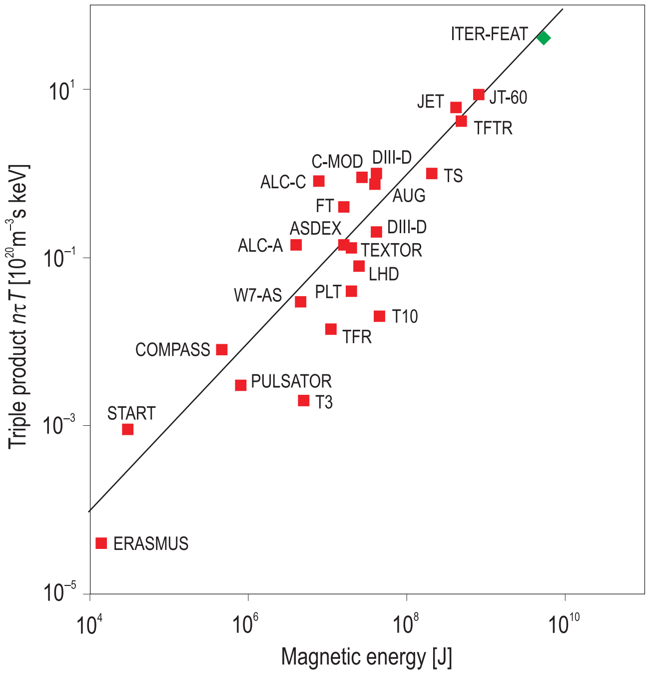

Fig. 5.4. Values of $n\tau T$ reached by MCF devices versus the magnetic energy stored in their plasma volume.

5.3.2.2 Main magnetic confinement configurations

By juxtaposition of magnetic field coils, distinct magnetic configurations can be generated. The simplest approach would be the use of a long straight solenoid of length L. Unfortunately, the rapid, unhampered transport along the field lines leads to unsustainable losses through the ends ("end losses") of the configuration. Defining an effective energy confinement time, $\tau = L/V_{\mathrm{thi}}$, where $V_{\mathrm{thi}} = (kT/m_{\mathrm{i}})\exp 1/2$ is the thermal velocity of ions having a temperature T, one easily finds from (5.34) that ignition requires $n > 2 \times 10^{23}\ \mathrm{m}^{-3}$ at $T = 15$ keV if L attains one kilometer. The required confining field B reaches then the huge value of 50 T even at $\beta = 1$. It is therefore clear that the end losses have to be curtailed in a fusion reactor.

One way to achieve this is through an increase of the magnetic field strength at each end of the solenoid. The gyrating particles will then be repulsed from these areas with higher field strength, which thus effectively act as "*magnetic mirrors*". Although the end losses can be significantly reduced in such a mirror [87Pos], the confinement of such a device proved to be too low and mirror machines have almost completely disappeared from the fusion scene.

If the solenoid is however bent into a torus (major radius R, minor radius $0 < r < a$) the problem of end losses disappears, giving rise to the class of *toroidal configurations*. When aligning the field-producing coils along a circumference of radius R, a toroidal magnetic field will be created, having a gradient in the direction of R. The particles then sample a different field strength over the inner and outer part of their Larmor orbits around the field lines. As a result, they experience an upward or downward drift motion (called toroidal drift), depending on the sign of their charges. A charge separation is thus set up between the top and bottom part of the configuration, giving rise to the creation of a vertical electric field E and arresting the toroidal drift motion. However, under the combined action of the toroidal B-field and the vertical E-field, electrons and ions together experience a radially outward drift motion of magnitude $\boldsymbol{E} \times \boldsymbol{B}/B^2$ and leave the magnetic configuration, thus shattering the hope of getting rid of the end losses and creating the ideal confinement system.

The catastrophic effect of the toroidal drift can however be avoided by twisting the magnetic field lines helicoidally [58Sak, 76Miy]. In this way, one connects the regions of opposite charge polarity and effectively short-circuits the vertical E-field. One uses the term *rotational transform* to characterize the twisting, which results itself in the generation of a poloidal magnetic field component B_θ. The amount of rotational transform is measured by the ratio B_θ / B_ϕ, or by the rotational transform angle, $\iota = 2\pi/q$, where q, the *safety factor*, is defined as

$$q = \frac{rB_\phi}{RB_\theta} . \tag{5.37}$$

If one follows a given field line many times around the torus, a closed flux tube is mapped, a so-called magnetic surface. Surfaces pertaining to different field lines form a set of nested surfaces around the torus axis. It should be noted that the rotational transform angle is in general different from surface to surface: the configuration therefore possesses *magnetic shear*, a property that is quite effective against large-scale plasma instabilities.

By considering the motion of a single particle in this twisted field configuration, it is found that the projection of the guiding center trajectory onto a plane perpendicular to the toroidal axis can be either circular or can resemble the form of a banana. In both cases the particle will deviate from its magnetic field line by a distance which is at least q times the Larmor radius. While a toroidal system with rotational transform can indeed confine particles, the price that must be paid to get rid of the end losses is then a substantially increased step length for collisional transport across the magnetic field. Note that the maximally allowed amount of twist is imposed by stability considerations [63Sha, 89Whi] and that q values of about 3 or more are usually safe from this point of view.

The most advanced protagonists among the toroidal configurations are the *tokamak* [92Kad, 97Wes] and the *stellarator* [98Wag]. In the tokamak, the poloidal magnetic field is created by a toroidal current I_p flowing through the plasma. Figure 5.5 gives a schematic diagram of a tokamak. The toroidal current is induced by means of a transformer. The plasma itself forms the secondary winding of the transformer, the primary being wound on an iron core and constituting the poloidal field coils. In addition to providing rotational transform, the plasma current will also heat the plasma by ohmic heating. Because of its reliance on magnetic induction, the tokamak is not a steady state device, unless the current can be maintained by an alternative current drive mechanism.

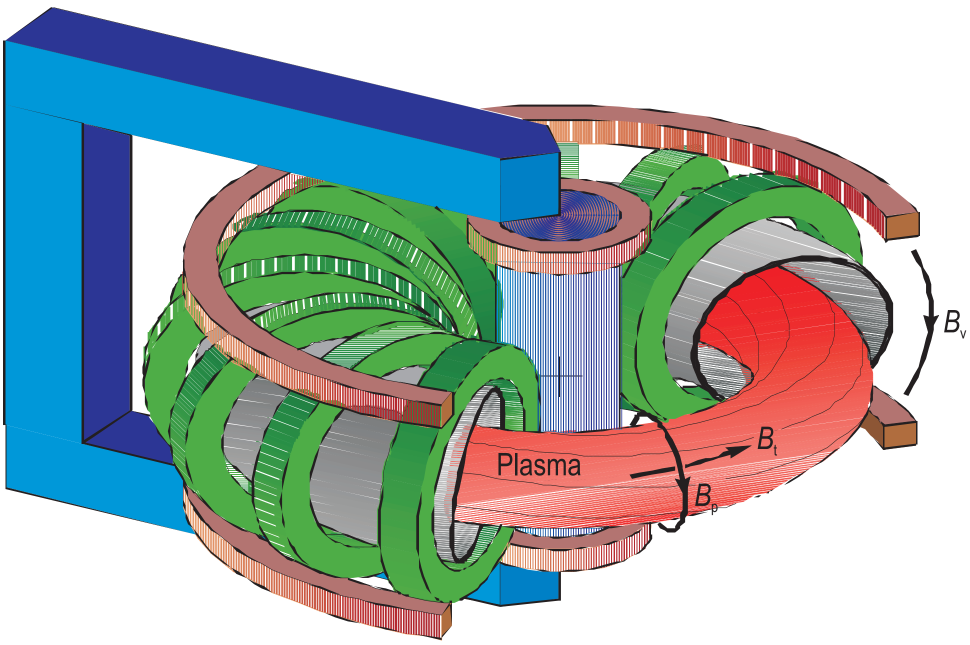

Fig. 5.5. Schematic diagram of a tokamak.

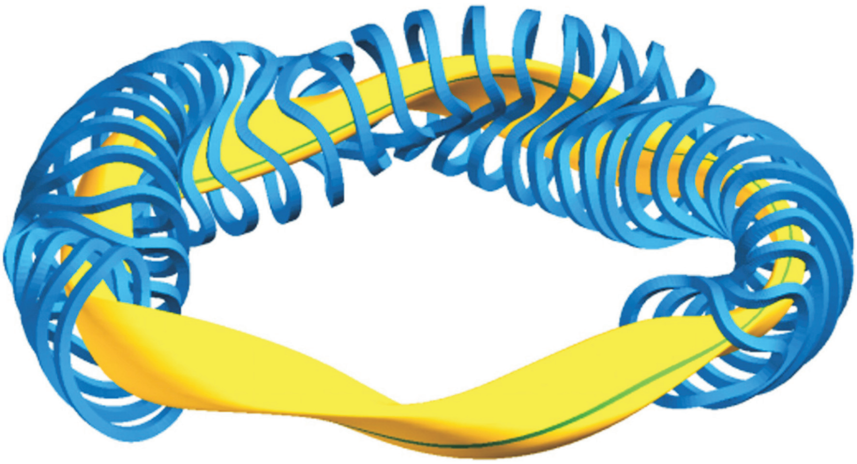

Fig. 5.6. Schematic view of the plasma and part of the magnetic coils of the W7-X stellarator.

In the stellarator, the rotational transform is achieved by means of currents flowing in external windings. Modern stellarators possess in fact only one set of modular coils that are non-planar and toroidally arranged as shown in Fig. 5.6. The currents flowing in these coils have poloidal and toroidal components that generate the required B_ϕ and B_θ fields. The magnetic topology is quite different from that of a tokamak as the cross section of a magnetic surface is quite deformed and is characterized by a certain number of toroidal periods. A stellarator has no need for a plasma current and is intrinsically steady state. Notwithstanding their significant configurational differences, the confinement properties of equal-size stellarators and tokamaks are quite similar. The confinement time for these configurations still lacks a quantitative first-principle derivation on account of the fact that turbulence, associated with small scale plasma instabilities, dwarfs the effect of Coulomb collisions. Important progress could however be achieved through an empirical approach, akin to wind-tunneling and destined to find the most important engineering parameters affecting confinement [75Kad].

Alternative MCF concepts on a more exploratory level include the Reversed Field Pinch [90Bod], the Spheromak [94Jar] and the Field Reversed Configuration [88Tus]. Whereas the first two are toroidal configurations, the latter is a linear device.

5.3.2.3 Outline of an MF reactor

Figure 5.7 shows a schematic of a magnetic fusion power plant. Starting from the plasma core, one can distinguish the following components:

– *The plasma*: The burning mixture of deuterium and tritium produces helium and neutrons. Up to one fifth of the fusion power (the part stored in the α-particles) can leave the plasma as a convective or conductive flux towards the so-called first wall (see below). It has been found to be essential that this power be exhausted by diverting it to a part of the first wall, called the divertor plates, that is especially equipped with heat resistant materials, adequate cooling and ample pump capacity in its immediate neighborhood. Preventing material that would possibly be released from these surfaces from reaching the plasma, is of utmost importance in order to avoid excessive fuel dilution. For the same reason, prompt exhaust of helium from the plasma is essential and should be assured by the divertor operation.
– *The deuterium and tritium feed system*: Deuterium and tritium can be supplied either by gas injection or by injection of pellets of deuterium or tritium ice. Tritium has a half-life of 12.3 years and is virtually non-existent in nature: it must be bred in the blanket.
– *The first wall:* Providing the needed vacuum enclosure, it is probably the most critical reactor component, as it is the target of very intense radiation from the plasma (14 MeV neutrons, energetic neutral particles produced by charge exchange, photons of various energies). Its mechanical strength will be

weakened by lattice damage and swelling, by wall erosion through sputtering and by temperature excursions. In addition, neutron-induced transmutation reactions can render the wall radioactive. Based on these extreme operational conditions, it is presently estimated that the time integrated neutron flux through the first wall will have to be lower than about 18 MWa per m^2 [97Naj]. Upon reaching this limit, the first wall will have to be replaced.

– *The blanket:* The neutrons that escape from the plasma are thermalized in a blanket, the main constitutive element of which is lithium. The latter element is not only a good moderator, but it also allows to breed the tritium that is needed to fuel the reactor, using the neutron-induced fission reactions:

$$^6\text{Li} + \text{n} \rightarrow \text{T} + {}^4\text{He} + 4.8\ \text{MeV},$$
$$^7\text{Li} + \text{n} \rightarrow \text{T} + {}^4\text{He} + \text{n} - 2.5\ \text{MeV}.$$

The natural abundances of lithium are 7.4 % ^{6}Li and 92.6 % ^{7}Li. Because of the corrosivity of pure lithium, only lithium alloys can be used, at the cost of parasitic absorption of neutrons. Appropriate tritium extraction methods must be developed.

– *The magnetic coils:* To reduce the Joule losses, the coils that produce the various magnetic fields will have to be superconducting. To protect them from neutrons that might escape from the blanket and from the eddy-currents induced by the poloidal field coils, appropriate shielding from the plasma must be provided.
– *The biological shield:* Protects the personnel and the environment from X-ray and neutron emission.
– *The heat-to-electricity conversion:* The fusion energy is stored as heat in the blanket, from where it is extracted using conventional heat exchangers. A classical cycle of steam generators, turbines and electric generators then completes the plant lay-out.

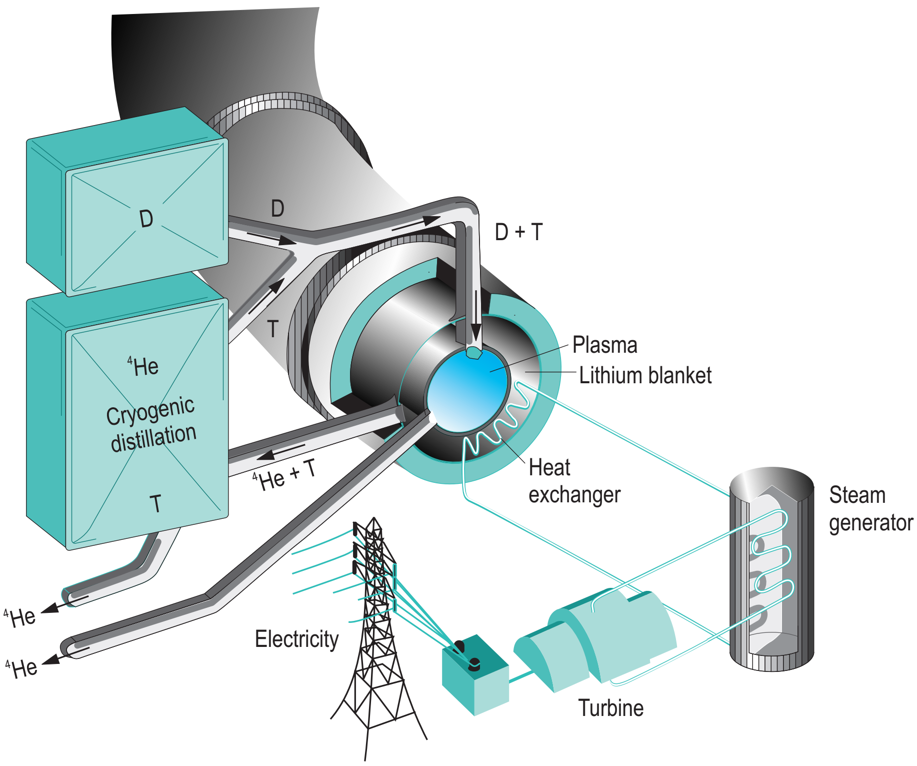

Fig. 5.7. Schematic view of an MCF power plant.

The size and power output of a magnetic fusion reactor is strongly linked to its expected first wall lifetime. Assuming a replacement every four years, the allowed reactor power flux f (= P/S) is then limited to about 5.5 MW/m^2. This in turn automatically limits the power density p_f (= P/V), in first approximation, to $p_f = 2f/a$. A reactor with $a = 1.5$ m and $R = 4.5$ m would then have a power density of some 7.5 MW/m^3 and produce a total fusion power P of 1500 MW. The total volume within the contour of the magnetic coils would then attain about 10000 m^3 [97Naj].

5.3.3 Inertial confinement fusion (ICF)

5.3.3.1 Main inertial confinement principles

Inertial confinement fusion (ICF) uses an energy source called a driver (laser, particle beam or z-pinch) to heat frozen D-T pellets (of radius R), either directly or indirectly via conversion into X-rays, to the necessary fusion temperatures [92Hog, 95Hog]. In contrast to magnetic confinement, no magnetic field contains the fuel. The heating pulses are typically 1 to 10 ns long and the heated plasma is free to expand. A reactor based on this concept is inherently pulsed and, hence, the basic reactor requirement should be to produce a substantial target gain, $G = Y/E_D$, defined as the energy yield, Y, of the fusion reactions divided by the energy of the driver, E_D. The efficiencies in the external systems of the power plant and the typical driver efficiencies ask for reactor target gains of about 100. The yield is determined by the number of fusion reactions that can occur in the time before the fuel disassembles, or, in the manner of speech of the previous section, during the time the fuel is confined. As explained in Sect. 5.2, an energetically economical system appears feasible only if the pellet *burn-up fraction* Φ is of order unity. The condition that expresses this requirement is the yardstick by which progress in inertial confinement is measured, and in this respect it plays the same role as (5.34) for magnetic fusion. It is known as the *high-gain-* or *ρR-criterion*.

A critical element for the derivation of the high-gain-criterion is the confinement time of the pellet, which is termed inertial, as the inertial mass holds the fuel together. At first glance, a good approximation for τ would be the time it takes for an ion to move over the distance R, at its thermal speed (taken as the sound speed of the fuel), $C_s = (kT/m)^{1/2}$, i.e. $\tau = R/C_s$. A more sophisticated calculation involves the hydrodynamic concept that in an assembled fuel, surrounded by a vacuum, the interior will know that there is a vacuum into which it is free to expand, only after a signaling rarefaction wave has arrived from the boundary. Given the fact that such a wave propagates at the speed of sound, but that most of the mass is located at the outer part of the radius, the previous expression for τ is reduced by a factor of 4. Using this value, the necessary condition [99Ros] to reach a burn fraction Φ of 1/3 can be cast in the form

$$\rho R = 4\,(mKT)^{1/2} <\sigma\upsilon>^{-1}, \tag{5.38}$$

where $\rho = mn$. This critical ρR has a minimum value of about 30 kg/m^2 at $T = 50$ keV. Since DT-ice has a mass density $\rho = 200$ kg/m^3, satisfying the ρR-criterion asks for massive targets, requiring for their heating unattainable amounts of driver energies. An escape from this apparent impasse is however possible. By compression of the pellet, ρ could be increased significantly. An increase by, for instance, a factor of 1000 lowers the energy demand by 10^9, thus bringing it in the range of what is technically achievable. In addition, it is not necessary to provide the total amount of heat, which is needed to bring the fuel to fusion temperatures, by the driver. It is sufficient to ignite a fraction of the pellet and let the fusion energy, thus liberated, heat the rest. The reader is referred to Sects. 5.2 and 5.4 for more details on pellet compression and hot-spot creation (or spark ignition).

Experiments show that satisfying (5.38) might be sufficient to achieve the high values of G needed. Figure 5.8 shows the calculated target gain as a function of direct drive energy [92Lin, 95Lin]. Based on the experimental progress and on the steady advances in system efficiency, it is predicted that ignition should be possible with a driver energy of about 1 MJ, whereas high-gain reactor operation becomes feasible with a 5…10 MJ of driver energy. The projected operation point of the US National Ignition

Facility (NIF), which is presently under construction [01Htt] and in which ignition is predicted, is also shown in the figure.

While comparing MCF and ICF, it is interesting to observe that the ρR-criterion can also be rewritten in terms of density and confinement time, as $n\tau = <\sigma\upsilon>^{-1}$. The minimum triple product that results puts the reactor requirement for ICF typically 15 times higher than what is asked for in MCF, a consequence of the inherent inefficiency in assembling the fuel. Please also note that in ICF the term ignition does not have the same meaning as in MCF, as it refers to the condition of efficient α-particle capture, a ρR value of at least 3 kg/m^2 being required to slow the α-particles down in the pellet [95Lin].

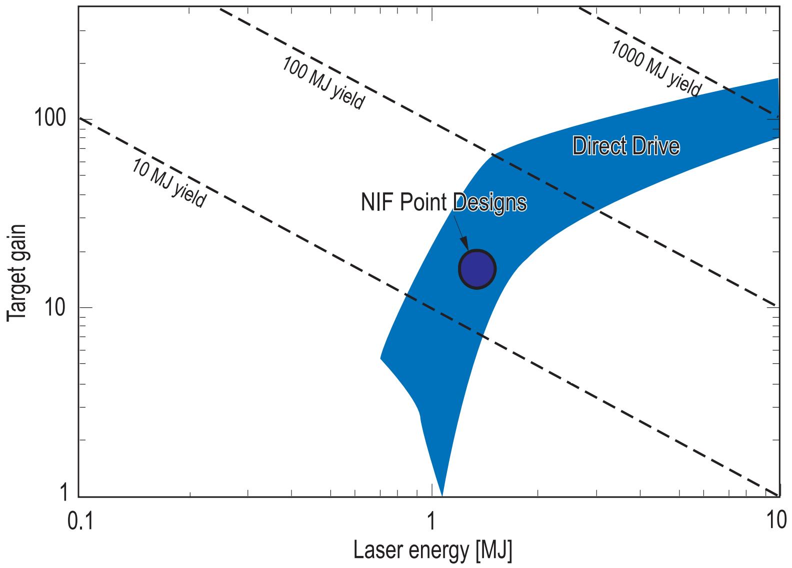

Fig. 5.8. Expected path of ICF towards achieving ignition and high gain.

5.3.3.2 Main inertial confinement configurations

At the heart of an inertial fusion explosion is a target that has to be compressed and heated to fusion conditions by the absorption of energy carried by a driver. For the so-called direct drive, the target consists of a spherical capsule that contains the DT fuel (Fig. 5.9b). For indirect drive, the capsule is contained within a cylindrical or spherical metal container or "hohlraum" whose function is to absorb the incident driver energy and reradiates it as X-rays that drive the capsule implosion (Fig. 5.9a). The drivers can be a laser, a heavy ion beam or a z-pinch accelerator. The latter consists of a huge array of separate pulsed power devices timed to fire, all to within ten billionths of a second, a current of tens of millions of amperes into two spool-of-thread-sized arrays of 100 to 400 wires, symmetrically positioned with respect to the hohlraum (only one such array is shown in Fig. 5.9c). The currents vaporize the wires, thus creating a plasma, and produce powerful magnetic fields pinching this plasma to densities and temperatures sufficient to generate an intense source of X-rays.

The primary advantages of direct drive are the simplicity of the target and the excellent coupling efficiency of the driver energy. The required spherical illumination symmetry is however so extreme that presently only multiple laser beams are considered for direct drive.

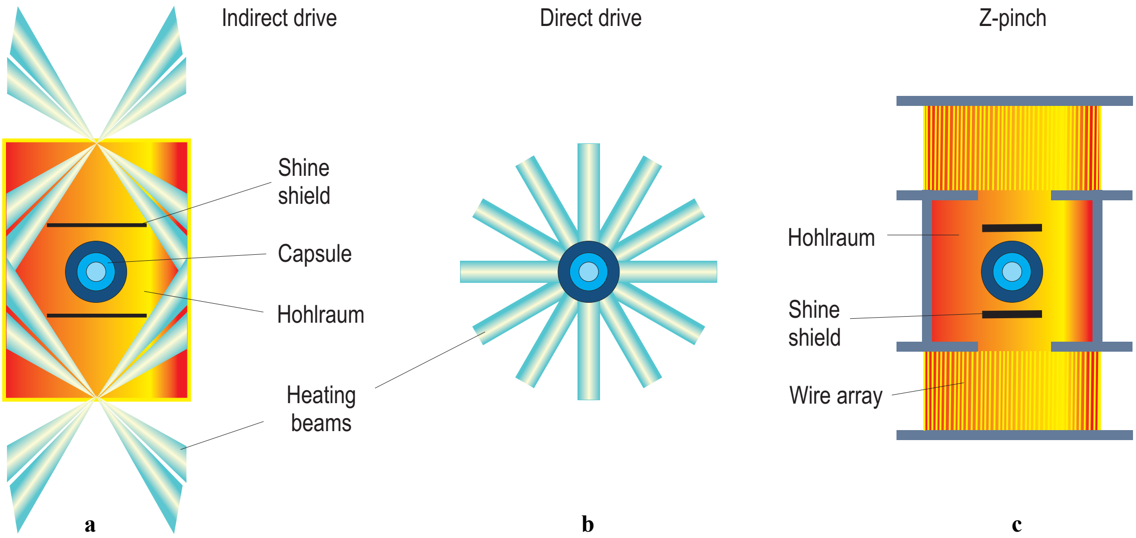

Fig. 5.9. Geometrical arrangements used to implode ICF capsules: **(a)** heating beams in cone arrays , **(b)** heating beams from all directions, and **(c)** heating by high-power electrical pulses through wire array.

5.3.3.3 Outline of an inertial confinement reactor

An ICF reactor plant (Fig. 5.10) comprises four major, separate but interconnected components:

– *The target factory* must produce about $1\ldots2 \times 10^8$ targets each year, fill them with fuel, layer the fuel into a symmetric and smooth shell inside the capsule, and deliver the complete target with extreme precision and without damage to the target chamber at a rate of about 5 Hz for laser or particle beams. To be economical, the manufacturing cost must be brought down by four orders of magnitude with respect to current ICF target fabrication experience.
– *The driver* mainly consists of many laser or ion beams that must be focused on the target through a number of focusing elements. The final focusing optics (magnetic coils in the case of ion beams, lenses for the lasers) are high-precision and costly components that need to be protected from the target implosion. This is achieved by providing adequate “standoff” between the capsule and the final optics and raises a number of issues that have to be tackled together with the target chamber design. For a z-pinch drive, this type of problems reduces to that of replacing the feeding transmission line every 10 seconds.
– *The fusion target chamber* is the most critical component as it provides the interface between the target, the driver and the blanket. Inside the chamber, a number of systems must be foreseen to (1) protect the chamber structures and the final optics against micro-explosions (of a few hundred MJ every 0.2 s for lasers and heavy ion beams, or a few GJ every 10 s for z-pinches) for many years or allow easy replacement, (2) extract fusion energy in a high-temperature coolant and produce tritium, (3) regenerate chamber conditions for target injection, driver beam propagation at sufficiently high rates, (4) reduce the volume of radioactive waste.
Whereas about two third of the thermonuclear energy is carried away by the neutrons, the rest is in the form of X-rays, target debris ions and fast ions. For a laser direct-drive target, the first wall (if unprotected) would receive about $0.5\ldots5$ J/cm^2 X-ray fluence per shot, ablating 0.1 to 1 μm per shot (depending on the material) off a solid wall at a nominal 5 m radius (tolerable would be << 1 nm per shot). To avoid this ablation, the chamber diameter could be filled with Kr or Xe gas at about 0.5 Torr. Whereas a laser beam penetrates this gas, the X-rays are absorbed by it and their energy reradiated on a longer time scale. This approach is known as the dry-wall concept.
Heavy ion beam drivers and z-pinches perform best when the standoff length is minimized. In this case the wetted-wall or the thick-liquid-wall concept can be used to protect the wall from ablation. In

the thick-liquid wall case, liquid jets of the eutectic mixture Flibe (2/3 LiF, 1/3 BeF_2) are located within tens of centimeters from the target to protect the walls from both neutrons and X-rays, while at the same time playing the role of blanket. Beam propagation at the residual gas pressure of Flibe (typically 10^{-3}) is under study.

– *The balance of plant (BOP)*, where many processes are performed: Tritium is extracted from the recirculating blanket gases and sent to the target factory, heat in the blanket is converted into electricity, waste materials are extracted and shipped off site.

Today, three mainline drive approaches are pursued – heavy ions, lasers and z-pinches. The heavy ion scenario uses an induction linac heavy-ion driver, an indirect-drive target and a liquid-wall or wetted-wall chamber. The laser scenario uses a krypton fluoride or a diode-pumped solid state laser, a direct-drive target, and a dry chamber. The z-pinch scenario uses a pulsed power driven z-pinch, an indirect-drive target and a thick-liquid wall chamber. For all three mainline drivers, a target option is the Fast Igniter concept in which the driver compresses the fuel and the Fast Igniter initiates burn in a small spot [94Tab]. Somewhere between MCF and ICF is the Magnetized Target Fusion approach [95Kir].

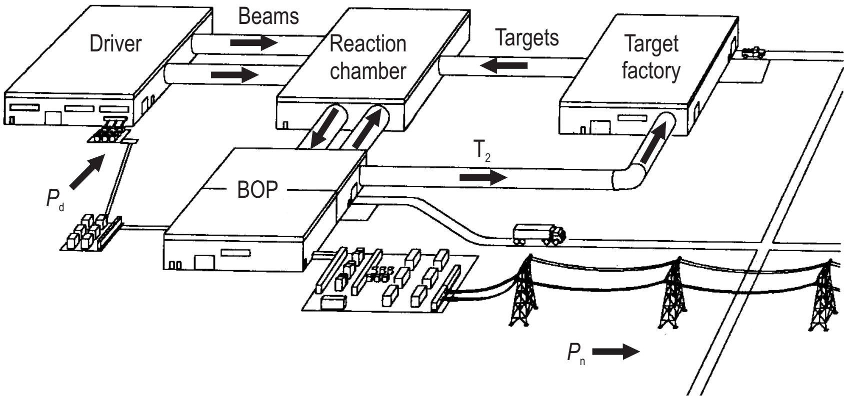

Fig. 5.10. Schematic diagram of a possible ICF power plant with a heavy ion driver and a liquid-wall target chamber. (Derived from Fig. 1.1 of "Energy from Inertial Fusion", IAEA, Vienna, Austria, p. 2, 1995).

5.4 Reactor technology for magnetic confinement

[U. Samm]

The ITER design includes all the technology needed to demonstrate a burning fusion plasma with a burn time of about 8 minutes and 500 MW fusion power [98Tec]. The key technology elements are: *high heat flux components*, *neutron shielding*, a *closed fuel cycle*, *heating methods*, *magnet systems* and *remote handling techniques*. Moreover, breeder blanket modules will be introduced which can produce a fraction of the tritium needed.

It is expected that after ITER also the missing technology elements will be available which then allow to build a first of a kind fusion power plant (often called DEMO) with a steady-state burning fusion plasma, sufficient lifetime, high availability and a minimum of radioactive waste. R&D on these issues can be performed to a large extent in the ITER experiment, e.g. optimization of plasma facing materials, breeder blanket technology or heating and current drive. Other issues have to be addressed outside of ITER. In particular the development and characterization of low activation ferritic-martensitic steels under heavy neutron irradiation is an outstanding issue, for which special neutron irradiation facilities are needed [00Moe].

5.4.1 First wall and high heat flux components

The first wall and the high heat flux components constitute the so-called Plasma Facing Components (PFCs) as shown in Fig. 5.11. They have to withstand different loads [01Jan, 01Fed]: (a) surface heat flux caused by plasma flow and radiation, (b) erosion and deposition of wall materials, (c) mechanical stress due to eddy currents during off-normal events, and (d) volumetric loads by neutrons changing their thermo-mechanical properties.

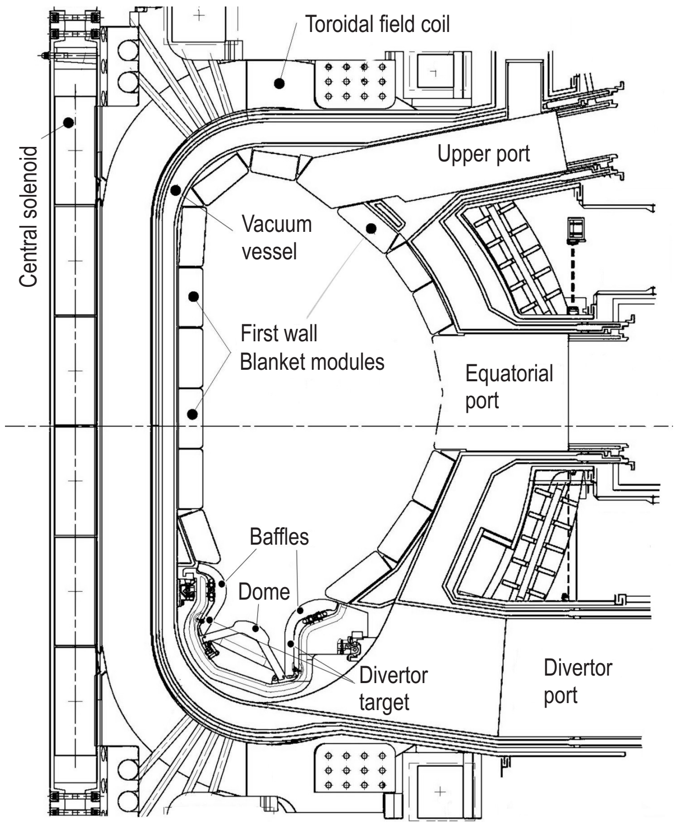

Fig. 5.11. Plasma-facing components of the ITER machine.

The *first wall* of the main chamber has the largest area. The heat flux density provided mainly by radiation (photons and neutral particles) is rather low. A high heat flux component is the so-called *port limiter*. During plasma start-up and shutdown the port limiter is in direct contact with the plasma protecting the first wall and the antennas. The *baffle* at the divertor entrance and the *dome* between the two divertor legs help to reduce the back diffusion of neutrals from the divertor region. Both are high heat flux components.

The *peak heat load* occurs in the *divertor* where the magnetic field lines intercept the vertical target plates (VT) at the so-called strike point. The plasma ions enter the divertor region and impinge on the target plates where they are neutralized. This gas is exhausted through the gas box liner located beneath the dome, then radially outwards beneath the outer VT and through a pumping slot in the cassette body and finally through the divertor port. The peak heat load is concentrated within a rather thin scrape-off layer having a thickness of only about 1 cm. This generates a heat flux density of up to 10 MW/m^2 at the strike point of the VT along a thin line winding around the torus. The thermal gradients linked to this well localized heat load cause thermal stresses in the target plates. In addition to the average heat flow, the standard plasma scenario foreseen for ITER (H-mode) comprises also the occurrence of regular short heat pulses to the strike point: the so-called Edge Localized Modes (ELM) [98Con]. These ELMs are instabilities which partly expel the edge plasma energy content within less than 1 ms. The frequency at which these ELMs appear (1…30 Hz) and their magnitude (1 %…8 % of the plasma energy content) vary. Ongoing R&D is aiming at optimizing the plasma scenarios such that the magnitude of these ELMs is small enough to avoid overloading (melting, erosion at the strike point). This will also influence the choice of wall materials.

Erosion of wall materials by sputtering, chemistry, melting or evaporation may be the decisive processes which determine the lifetime of PFCs [97Pac]. On the one hand the thickness of the PFC can be progressively reduced. On the other hand, since a tokamak is nearly a closed system, eroded particles are also re-deposited on the PFCs and may generate thick layers. Both occurs simultaneously at the same location. The balance between erosion and deposition rates determines whether we have areas of net-erosion or net-deposition. The lifetime of the PFC is affected by both processes. Moreover, the co-deposition of tritium, in particular with graphite, needs special attention, since large amounts of tritium can be trapped in these layers.

The choice of materials is also influenced by the impact the eroded particles have on the plasma. Radiation from plasma impurities leads to additional energy losses, and an accumulation of impurity ions in the plasma center reduces the fusion power by diluting the fuel (deuterium and tritium). Low-Z materials (e.g. carbon, beryllium) are rather quickly fully ionized such that they only radiate significantly at the plasma boundary. This is a major advantage, because radiation from the plasma edge can distribute large fractions of the power exhaust on the large area of the first wall thereby reducing the peak load on the divertor strike point. For this purpose also the special injection of radiating impurities (e.g. neon, argon) is foreseen in ITER. On the other hand low-Z materials have the disadvantage of rather high erosion rates in contrast to high-Z materials (e.g. tungsten or molybdenum), with very low erosion rates.

Major plasma instabilities induce eddy currents inside the PFCs which interact with the toroidal magnetic field resulting in high forces which may generate *mechanical stresses* up to a few hundred MPa. However, stress limits due to earthquakes – a design element also to be taken into account – are much higher. The crucial question is how frequent these events are, since mechanical fatigue due to varying stress is the limiting factor. In a power plant reactor major instabilities (e.g. plasma disruptions) should be limited to less than one per year.

The *neutron flux* crossing the boundary and penetrating into the first wall is referred to as *wall loading* and measured in MW/m^2. The two main effects of the neutron flux are the volumetric heat deposition and the neutron damage. The volumetric heat deposition has a typical maximum value of a few W/cm^3 in the first wall structures which is not of particular concern. The damage to the wall materials by the neutrons will be the main lifetime-limiting issue for fusion power plants. It is measured in "displacements per atom" (dpa): the number of times an atom is displaced from its position in the lattice due to neutron collisions. The dpa is proportional to the neutron fluence. As an example, 1 MW a/m^2 causes about 3 dpa in beryllium and 10 dpa in copper or steel (Table 5.3). Typical effects of this damage are embrittlement, swelling, transmutation (He-production) and a change of thermal conductivity. These damages may partly recover when the wall material reaches elevated temperatures.

Table 5.3. Steady-state surface heat loads and neutron damage over the lifetime of the device in the PFCs of ITER and of a power plant reactor, respectively.

Component	ITER		Power plant reactor (indicative values)	
	Surface heat load [MW/m^2]	Neutron damage [dpa]	Surface heat load [MW/m^2]	Neutron damage [dpa]
First wall	0.3…1.0	1.6	0.6…1.0	120
Divertor vertical target	10…20	0.7	15…30	40
Dome	3	0.5	3	30
Liner	0.02…0.5	0.5	0.03…0.8	30
Port limiter at start-up/shutdown	8…10	≈ 2	10…15	≈ 40
Baffle	2	1.0	2…3	70

A PFC is generally a structure that consists of different materials joined together and is actively cooled (Fig. 5.12). The plasma-facing layer is usually referred to as *armor*. Immediately below the armor, there is the *heat sink*. Its main function is to route the heat flux from the armor to the cooling tube. A high thermal conductivity is the main requirement and a typical material for this part is copper alloy. The cooling tube, normally from austenitic stainless steel, has to be from copper alloy for the high heat flux components.

Design solutions for ITER [98Tec]

The First Wall consists of a series of panels that are separable from the blanket modules thus reducing the fabrication cost and the volume of radioactive waste. In ITER the panels are covered with 10-mm thick beryllium armor. For the lower part of the VT where the highest heat flux is expected a carbon fiber reinforced carbon (CFC) armor is envisaged. CFC is the preferred material choice due to its high thermal conductivity, its excellent resistance to thermal shocks and its sublimation temperature higher than 3500 °C. For the upper part of the VT tungsten or molybdenum is preferred to minimize the erosion rate and the tritium inventory. Extensive R&D effort led to the design of the cooling system for the VT based on a highly subcooled, high-velocity water flow with a turbulence promoter (twisted tape). Figure 5.13 shows a VT prototype manufactured by the European industry. The component endured 1000 cycles at 15 MW/m^2 and 2000 cycles at 20 MW/m^2 on the tungsten and CFC armored region, respectively [99Raf].

As armor material for the port limiter, both beryllium and CFC (8…10 % silicon doped) are being considered [98Car]. Beryllium does not trap tritium like carbon, but due to its rather low thermal conductivity the minimum thickness would be limited to 4 mm. On the other hand, a CFC armor can have a thickness of 15 mm and a corresponding lifetime of about one order of magnitude higher than beryllium. The silicon doping in the CFC material is required to reduce the chemical erosion.

Current R&D work is aiming at finding the optimum combination of wall materials which ensure the maximum lifetime and a high availability of a fusion reactor [00Wu].

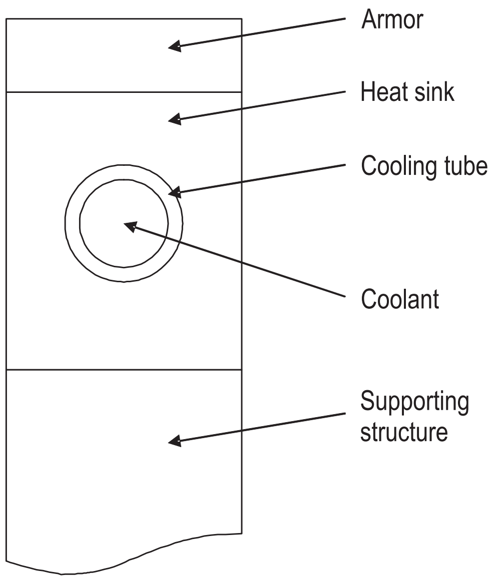

Fig. 5.12. Typical structure of a PFC.

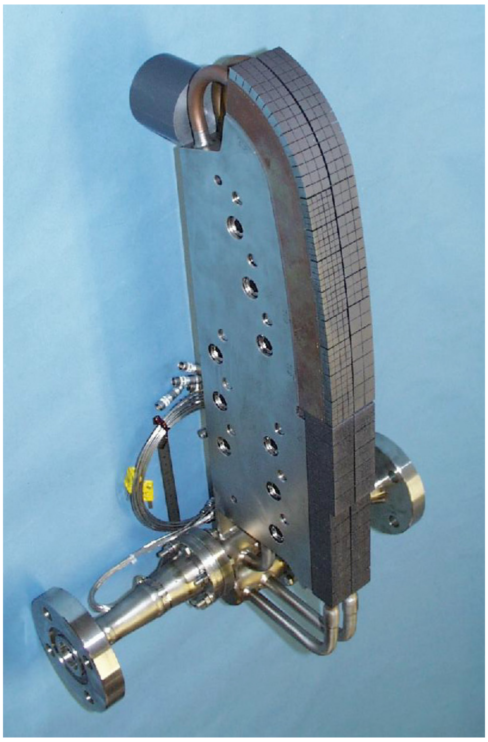

Fig. 5.13. VT prototype with a tungsten and CFC armor manufactured by the European industry.

5.4.2 Systems for heating, current drive, profile control and refueling

Auxiliary heating systems are needed to reach the starting conditions for a burning fusion plasma. Since the energy transfer to the plasma particles can be such that also toroidal momentum is transferred to the charged particles, the heating systems can also be used for plasma current drive. Means for on- and off-axis current drive will be important elements for optimization of plasma scenarios [99Rob]. Techniques for fueling the plasma by injection of particles are required for density and burn control.

Heating and current drive

Auxiliary heating is needed because in the resistive heating (ohmic heating) by the toroidal electric current flowing in the tokamak plasma is insufficient and in a stellarator plasma even not existing. The development of auxiliary heating methods during the past decades was the key element towards the success of present day fusion devices with magnetic confinement. The achievement of plasma temperatures much above those required for fusion is no longer a problem (e.g. up to 400 mill. °C in JET [99Wes]). R&D in this field is now concentrating on additional requirements arising from larger devices, like e.g. deeper penetration into the plasma bulk or steady state issues. Two fundamentally different heating methods are in use: neutral beam injection (NBI) and radio frequency (RF).

NBI

With NBI high-energy neutral atoms (e.g. 80 keV deuterium in JET) are injected into the plasma, where they are ionized. They are then trapped by the magnetic field and transfer their energy to the plasma via Coulomb collisions. The injected particles must be neutral to allow them to pass through the magnetic field surrounding the plasma. The main components of an NBI system (Fig. 5.14) are: the plasma source for ions, the ion extraction and acceleration system, the neutralizer and the injection port. The remaining ions after neutralization are removed from the beam by a magnetic or electrostatic deflection system towards a beam dump. The vacuum pumps distributed along the beam line remove most of the gas emerging from the neutralizer and the ion-beam dump. In present-day experiments the technology for using positive ion beams (e.g. D^+) in NBI are well developed [99Spe].

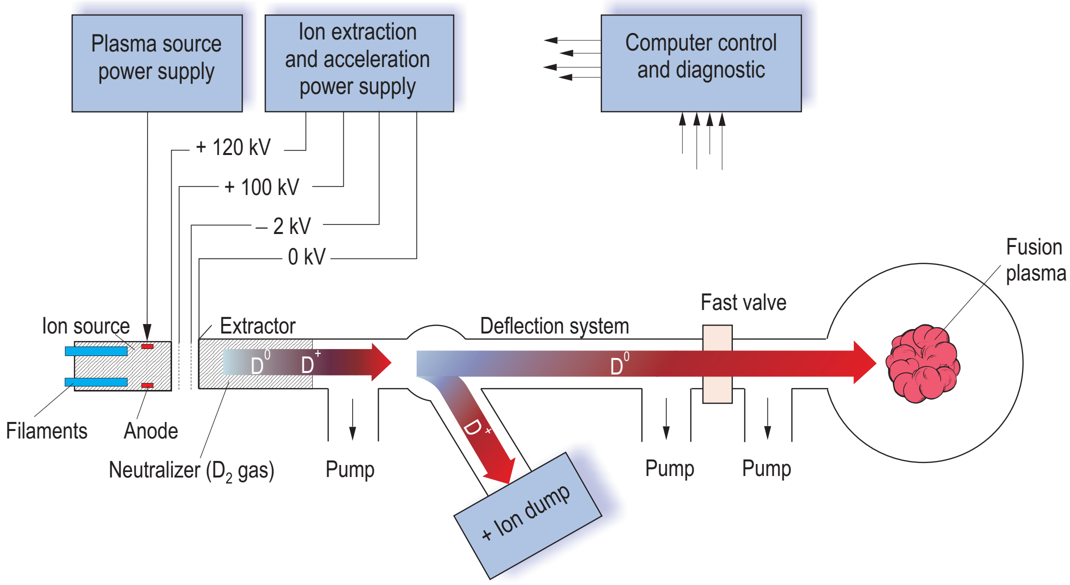

Fig. 5.14. Schematic diagram of a beam line for a neutral-beam injection system [01Fed].

In future devices with much larger plasma dimensions the limited penetration of 80 keV projectiles would not be sufficient to heat the plasma center efficiently. Higher energies are needed, which leads to the difficulty that the efficiency of the neutralizer chamber decreases rapidly because the relevant charge-exchange cross section diminishes strongly with increasing ion energy [00Kur]. This is not the case with negative ion beams which have a much higher and nearly energy-independent neutralization efficiency. For injection energies above 150 keV negative ions have to be used. Thus, all current R&D concentrates on negative ion systems. For ITER two 1 MeV D^0 beams with a total power of 33 MW are foreseen. The injection will be through separate quasi-tangential equatorial ports, so that the beams will generate a current density of 0.2×10^{20} A/(Wm^2). The development of ion sources capable of providing 40 A of D^- (20 mA/cm^2) at a source operating pressure of < 0.3 Pa (to avoid excessive stripping of the negative ion beam within the accelerator) is required. A caesiated volume ion source, coupled to a multi-stage multi-aperture accelerator (of 0.6 m × 1.65 m extraction area) produces the required negative ion beam. The neutralization is achieved in a gas target cell or via photo detachment in a laser-generated plasma. The present status of R&D is that all the required system parameters, except current and injected power, have been achieved individually and the key outstanding development issue remains the demonstration that all the injector requirements can be met simultaneously [99Rob, 00Kur].

RF

In RF heating a high-power wave at an appropriate frequency propagates through the plasma until it reaches the resonance location, where the wave frequency is in resonance with the plasma frequency (gyration of ions or electrons in the magnetic field) and transfers energy to the charged particles. There are different types of RF methods available (Table 5.4) making use of the coupling to the ion gyration (ICH), electron gyration (ECH) or the parallel velocity of the electrons (LH).

Table 5.4. Characteristics of RF heating and current drive (H&CD) systems.

H&CD method	f [GHz]	Power source	Transmission system	Antenna	Coupling medium
Electron cyclotron	28…170	Gyrotron	Oversized circular waveguides or mirror lines	Oversized waveguides and reflectors (100 MW/m^2)	Vacuum
Lower hybrid	1…8	Klystron/ Gyrotron	Standard rectangular waveguides	Waveguide grill (25 MW/m^2)	Low-density plasma [a])
Ion cyclotron	0.02…0.4	Tetrode/ Klystron	Coaxial lines	Loop antenna struct. with Faraday shield (10 MW/m^2)	Low-density plasma [a])

[a]) Antenna guard limiter is required.

The advantages of RF systems compared to NBI are that (a) dielectric windows serve as tritium barriers, and (b) there is no particle fueling. The tetrode power sources that exist today are adequate, with minor upgrading, for fusion power plant applications in the case of ICH. However, the klystrons and gyrotrons that will be required for reactor application of LHCD and ECH represent a major technological development. Gyrotrons are microwave oscillators based on the Electron Cyclotron Maser (ECM) instability. In contrast to klystrons the interaction circuit is a high order mode cavity allowing higher power at higher frequencies. The transmission technologies needed for future RF applications on fusion power plants essentially exist today. The overall transmission efficiencies are around 85 %.

Effective ICH has been demonstrated on many tokamaks. In plasmas with relatively modest core thermal ion temperatures, ICH power is damped predominantly on a minority ion species (usually on a few percent H or ^{3}He ions). An energetic minority ion tail is formed which subsequently heats the background plasma. In plasmas with large central ion temperatures, the RF power can also be damped on a bulk (e.g. D or T) ion species at the 2nd harmonic of its cyclotron frequency, thus heating the fuel species directly. A fraction of the ICH power also heats thermal electrons directly which may allow substantial non-inductive fast wave current drive (FWCD). Disadvantages with ICH are the low antenna power density and the sensitive coupling to the plasma.

Tetrodes which can produce 1 MW for long periods over the whole frequency range have been used in ICH systems for many years. The 2 MW units (35…60 MHz) needed for the 20 MW ITER ICH system [98Tec] could use two of these tubes. On-axis current drive in ITER can be performed at $f_{CD} \approx 56$ MHz, with an expected CD efficiency of approximately 0.2×10^{20} A/(Wm^2).

In addition to effective plasma heating, ECH has the potential to provide significant current drive, both in the core and off-axis, for plasma optimization and instability control. The flexible high-frequency power modulation capability [95Thu] has been exploited for phase feedback control of plasma instabilities and for transport studies. Furthermore, ECH-assisted start-up is an established and robust technique which has been demonstrated in a large number of tokamaks and is employed routinely in stellarators. Also the effectiveness of ECH discharge wall cleaning during the inter-pulse and machine conditioning phases has been demonstrated in a number of devices. The millimeter-wave beam at the launching antenna must be well collimated (low divergence and low side lobes) and should have a controllable polarization depending on the launching direction. A major advantage is that no launching structure close to the plasma is needed. The port size per unit power can be kept comparatively small because of the high power density of the RF beam. However, density limits exist for penetration of the millimeter waves into the plasma; e.g., the O-mode cutoff density at the fundamental resonance is given by n_c [m^{-3}] = 0.0124 (f [Hz])^2. The location of the power deposition in toroidal devices can be controlled by adjustment of the toroidal field or by poloidal and/or toroidal steering of the beam. The expected CD efficiency for ITER is approximately 0.1×10^{20} A/(Wm^2).

Good progress has been made in the development of sources [98Thu]. The reference source proposed for ITER is a 170 GHz, 1 MW, CW gyrotron equipped with a single-stage depressed collector to achieve an efficiency of 50 %. High-power CW operation remains a key issue since low levels of stray radiation inside the tube could, in principle, lead to overheating on a relatively long timescale. A unit power of ≈ 1.5 MW is likely to be the upper limit for a conventional cavity gyrotron. The transmission system can handle powers much greater than 1 MW, and 2 MW diamond windows now appear feasible.

Lower hybrid current drive (LHCD) is considered as the most efficient non-inductive CD scheme. LHCD has been used to sustain non-inductive plasmas for two minutes in TORE SUPRA and hours in TRIAM-1 M. However, because of the strong damping, the waves cannot penetrate to the core of a burning plasma and, furthermore, there may only be limited means to control the current drive location.

ITER operates at 5 GHz, which is selected mainly to avoid absorption by alpha particles. The power deposition on electrons is mostly off-axis, for $n_e T_e < 1.5 \times 10^{21}$ keV m^{-3}. The current drive efficiency above 0.3×10^{20} A/(Wm^2) has already been demonstrated in JT-60U where a non-inductive plasma current of 3.6 MA has been driven by 5 MW LHCD at 2 GHz.

The required waveguide power densities are routinely achieved in present experiments at 3.7 GHz, but the 5 GHz, 1 MW, CW klystron amplifier as proposed for the 20 MW LHCD system for ITER is still a development issue.

Refueling

To compensate for the loss of particles from the plasma pumped away from the divertor and the consumption of fuel by fusion reactions, the plasma must be refueled by injecting deuterium and tritium. More efficient than simple gas puffing is the method of high velocity injection of frozen pellets made from D or T. The velocity must be in the order of several km/s to allow the pellet to penetrate into the plasma center. The injection frequency of pellets must correspond to several times $1/\tau$ (where τ is the particle confinement time) in order to allow for a significant change of the plasma density profile. A combined average fueling rate of up to 200 Pa m^{3}s^{-1} is required for ITER. There are two competing methods for acceleration of the pellets: the centrifuge and the pneumatic gas gun launchers [98Vin, 98Rez]. The pellet fueling rate in ITER will be up to 100 Pa m^{3}s^{-1} for all gases except T_2, which will be limited to 50 Pa m^{3}s^{-1}. Injection rates for impurities, e.g. for the purpose of radiation cooling, will be limited to 10 Pa m^{3}s^{-1}. A combination of pellet size and injection frequency will be used to limit density perturbations to < 10 %. To satisfy the fueling requirement, pellet sizes in the range of 3…6 mm will be available with injection frequencies up to 50 Hz provided for the smaller pellet size.

5.4.3 Blanket, shield, and energy conversion system

The plasma in a fusion power plant is surrounded by blankets which have to meet the following objectives: (a) breeding all the tritium necessary as "fuel" for the fusion reaction, (b) converting the energy from the fusion reaction into heat usable for electricity production, and (c) contributing to the shielding of the superconducting magnets from neutron radiation damages.

Tritium breeding blankets

Tritium is bred in lithium containing materials mainly by the reaction $^6Li + n \rightarrow {}^4He + T + 4.78$ MeV. In most breeder designs an additional neutron multiplier is required to compensate for unavoidable neutron losses. Suitable materials for neutron multiplication by a (n,2n) reaction are mainly lead and beryllium. The breeding blankets are characterized by the *breeding material*, the *structural material*, the *neutron multiplier*, and the *coolant* (Table 5.5). In addition, there is in some cases a need for special materials (mostly coatings) serving as tritium permeation barrier, electrical insulator or corrosion barrier.

Table 5.5. Primary candidate materials considered for first-wall/breeding blankets.

Structure materials	Breeding materials	Neutron multipliers	Coolants	Special materials
Ferritic-martensitic steels	Lithium-ceramics	Beryllium	H_2O	Al_2O_3
Oxide dispersion strengthened (ODS) ferrite steels	Lithium	Lead	He	AlN
	Lead-lithium alloy		Liquid metals	CaO
Vanadium alloys	FLiBe		FLiBe	SiC
SiC/SiC-composits				
Mo, Ta, W				

We have to distinguish different types of breeding blanket concepts [00Gia]:

- The Helium Cooled Pebble Bed (HCPB) blanket [00Boc] under development in the framework of the European Union Blanket Development Programme [97Gia] may serve as a typical example of the *solid breeder blanket concept* with ternary lithium-ceramics as breeder material, beryllium as neutron multiplier, and the low activation ferritic-martensitic steel EUROFER as structural material. Breeder material and multiplier are arranged as pebble beds between flat cooling plates and cooled with helium at 8 MPa pressure. The achievable coolant outlet temperatures are around 500 °C.
  The main advantage of solid breeder blankets is the good compatibility between breeder, structural material, and coolant. They have in general also good safety features due to the low chemical reactivity with air or water in case of an accident. The main disadvantages are the limited power density due to the relatively low thermal conductivity of the ceramic breeder and the limits on blanket lifetime caused by irradiation damages in the breeder material. For neutronics reasons, the lithium contained in this material must be enriched to 30…60 % ^{6}Li (natural content 7.5 %), therefore, re-processing of the lithium after a blanket replacement is mandatory.
- The water cooled lead lithium blanket (WCLL) [98Gia] (Fig. 5.15) may serve as a typical example for the *liquid breeder blanket concept*. It employs a quasi stagnant pool of the eutectic lead lithium alloy Pb-17Li cooled by pressurized water. The liquid metal is circulated slowly to a tritium extraction system outside the plasma chamber. This low velocity avoids problems caused by the impact of the magnetic field on the liquid metal. Structural material is EUROFER. Cooling tubes made of this metal are coated with a thin layer of Al_2O_3 which serves as a tritium permeation barrier in order to minimize tritium permeation losses to the coolant. The water conditions (pressure, temperatures) are identical to those in a pressurized-water fission reactor with coolant outlet temperatures of about 325 °C.
  Liquid metals are attractive breeder materials due to their high tritium breeding capability, their relatively large thermal conductivity, and their immunity to irradiation damage [95Mal]. They can lead to

tritium self-sufficiency without employing additional neutron multipliers and offer unlimited lifetime of the breeder material due to the possibility to replenish on-line the ^{6}Li burn-up. This implies that the liquid breeder can even be re-used in new power stations after a power station comes to the end of its operating time. Liquid breeders have the potential for high power density. A major drawback is the high chemical reactivity of the breeder with air and water (especially in case of lithium) which is a safety concern.

– Most challenging is the *dual coolant blanket concept* which is characterized by a helium-cooled first wall and a self-cooled lead-lithium breeding zone. There are flow channel inserts made of SiC or a SiC/SiC-composite arranged in the large liquid metal ducts serving as electrical insulator and, at the same time, as thermal insulator between the helium-cooled steel walls and the flowing Pb-17Li [99Nor]. This concept could allow for a liquid metal exit temperature of up to 700 °C.

A final selection between the candidate breeder concepts will depend on their long-time behavior.

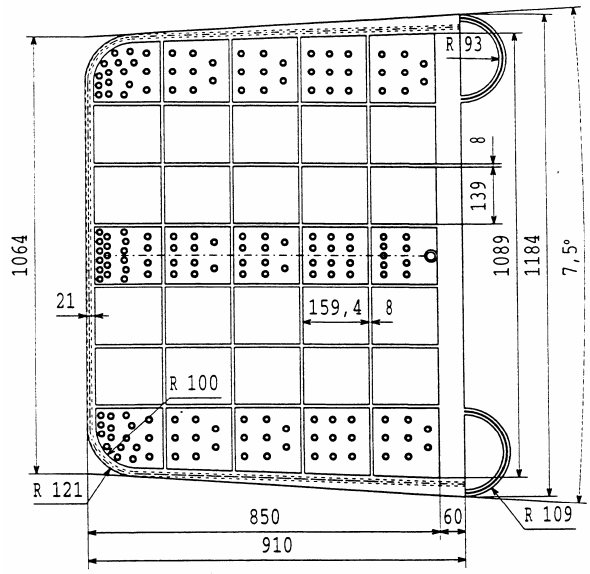

Fig. 5.15. EU WCLL blanket design, vertical cross section of outboard segment.

Shielding

An important function of the breeding blankets is shielding of the superconducting magnets which are very sensitive to irradiation damage by the neutrons and to heat generation by gamma-radiation. A desired lifetime of the magnets of 40 years requires a reduction of the neutron flux density from roughly 10^{15} cm^{-2}s^{-1} at the first wall to 10^9 cm^{-2}s^{-1} inside the magnets. In most cases a shield of about 50 cm thickness made of borated steel with a water volume fraction inside the breeder of about 50 % provides enough shielding for both the vacuum vessel and the magnets. If helium has to be used for cooling, either a considerably thicker shield or the insertion of rods filled with ZrH_2 inside the shield has to be considered.

Power conversion system

Inside the blanket the energy of the fusion reaction is converted from the neutron kinetic energy into heat which is transported by the blanket coolant to an external heat exchanger. From here, the heat is transported in a secondary loop to a system where it is converted into electricity. The power conversion system of choice for all blankets cooled with water, and all helium or liquid metal cooled blankets with coolant outlet temperatures lower than 650 °C is the classical steam turbine cycle with thermal efficiencies between 34 % and 45 % [02Wit]. If blanket outlet temperatures of at least 650 °C can be achieved, closed cycle gas turbine power conversion systems become attractive. In combination with SiC-blankets they offer thermal efficiencies higher than 50 %. The cost of electricity will of course depend on this efficiency. However, it is important to note that the dominating factor for the cost of electricity is the cost of the entire plant rather than the fuel cost. Thus, a cost increase due to a more complex breeder has to be balanced with the possible gain in power conversion efficiency.

5.4.4 Fuel cycle

Since the exhausted gas from a fusion reactor still contains significant fractions of unburned fuel (D, T), efficient systems for processing this gas are required in order to produce impurity-free and isotopically adjusted streams for recycle into the fueling system. The major subsystems constituting the inner fuel cycle are: (a) *tokamak exhaust processing*, (b) *isotope separation*, (c) *water detritiation*, and (d) *storage and delivery* [03Glu]. In addition, analytical facilities and several atmosphere detritiation systems are essential not only during operation, but also during maintenance of the machine.

The *tokamak exhaust processing* system involves three consecutive process steps. First, the unburned molecular DT fuel is separated from helium and from impurities produced by plasma wall interactions via so-called front-end permeators, essentially consisting of a bundle of palladium/silver tubes that are exclusively permeable to hydrogen isotopes. D and T chemically bound in impurities such as hydrocarbons or water are recovered in a second step by heterogeneously catalyzed cracking reactions and the water gas shift reaction combined with permeation of hydrogen isotopes through palladium/silver. Final decontamination of the residual gas is achieved in a countercurrent isotopic swamping stage, again by a combination of catalytic reactions and hydrogen isotope permeation. This process concept has already been experimentally validated and very high decontamination factors of 10^8 have been measured [03Bor].

The *isotope separation system* for ITER is based on cryogenic distillation and comprises a cascade of four distillation columns. It receives the pure hydrogen isotope mixtures recovered by the tokamak exhaust processing system and a hydrogen stream contaminated with tritium from the water detritiation system. Pure D_2 and T_2 (90 % T and 10 % D) is transferred to the storage and delivery system.

The *water detritiation system* is based on electrolysis combined with liquid-phase catalytic exchange reactions. The operation of the water detritiation system and the isotope separation system is strongly interlinked.

The fuel s*torage and delivery system* receives deuterium and tritium from the isotope separation system and supplies the D, T fuel to the tokamak. Metal hydride storage beds with a capacity of 100 g tritium each are employed for safe tritium handling. The storage beds have a double containment: The inner primary zone contains the metal getter, while an outer containment constitutes a vacuum insulation and at the same time serves for the recovery of tritium permeated through the hot walls of the inner vessel. Helium gas pumped through a separate pipe work wound around the metal hydride bed picks up the decay heat and allows for in-bed tritium inventory determinations by calorimetry [02Lae].

5.4.5 Magnet systems

The plasma is confined and shaped by a combination of magnetic fields from three origins: toroidal field (TF) coils, poloidal field (PF) coils and plasma currents. For steady-state operation all the coils must be superconducting. Copper coils would require too large an electric power to be acceptable. With superconducting magnets only the cooling power for compensating heat losses is required, which represents in a reactor typically a few percent of the electric output power. The design process has to be a multi-parameter optimization from the technical and the economic point of view and has up to now achieved a high state of the art. A considerable progress was the successful development of forced flow cooled magnets which are more suitable for this optimization process (see Fig. 5.16). In the R&D for ITER conductors, TF and PF coils were designed, fabricated and successfully tested in the ITER model coils: Central Solenoid Model Coil (CSMC) and Toroidal Field Model Coil (TFMC) [00Wu, 95Thu, 97Gia].

The parameters foreseen for ITER which are given below [98Tec] are already rather close to power plant conditions, where mainly the stored magnetic energy would be larger (up to 100 GJ) because of larger coil dimensions:

– *TF coils*: The toroidal magnetic field value on the plasma axis is about 5.3 T, which leads to a maximum field on the conductor of ≤ 12 T. Because of this high field value, Nb_3Sn is used as superconducting material, cooled at 4.5 K by a flow of supercritical helium at ≈ 0.6 MPa. The total magnetic energy in the toroidal field is around 40 GJ, and leads to very large forces on each coil which are restrained by a thick steel case to resist circumferential tension (≈ 100 MN) and by constructing a vault with the inboard legs of all 18 coils (the large centripetal forces are due to the $1/R$ variation of the toroidal field). The compressive stress levels inside this vault are large, and therefore the side surfaces of each coil should match one another as perfectly as possible.
– *PF coils*: The plasma shape is controlled by the currents distributed inside the modules of the central solenoid (CS) and the large coils placed outside the TF coils. All these axisymmetric coils use superconductors cooled by a flow of supercritical helium at 4.5 K and 0.6 MPa. Nb_3Sn is used in the CS modules, NbTi in the PF coils, where the maximum field value is lower than 6 T.

The magnetic configuration provided by these currents with its elongated shape is vertically unstable. Stabilization of the plasma vertical position can be achieved by two means: (1) passive stabilization by eddy currents in the vacuum vessel and (2) using a feedback position control system employing the four large poloidal field coils. During the inductive phase, the plasma current is generated by the magnetic flux change inside the toroidal plasma annulus. This flux swing is largely realized by the CS coil, which will see a complete inversion of field from +13.5 T to −12 T in the central modules. After the plasma current is set up inductively, a non-inductive scenario can follow, in which the plasma current is driven by other means.

Fig. 5.16. Magnet system elevation.

Superconducting coil protection and cryogenic cooling

The superconductor of all coils should be protected against local overheating, should the coil current continue to flow after a local transition from superconducting to normal conducting state. In this case an external resistor is switched in, rapidly dumping a large part of the coil magnetic energy. There is a large pulsed heat load on the coils from two origins: the neutron flux produced by the fusion reaction and attenuated by the blanket and vessel shields, and eddy currents induced by any field change in the coil superconductor and steel cases. The extra energy dumped into the coils at 4.5 K during a nominal pulse amounts to 19 MJ; and a plasma disruption can add a further 14 MJ. Owing to the assumed duty cycle, the time average load on the cryogenic plant (all users) amounts to 41 kW.

5.4.6 Remote handling

The high-energy neutrons in a fusion reactor activate the surrounding structure and preclude human interventions inside the main vacuum vessel. Already in JET the Deuterium-Tritium campaign carried out in 1997 (DTE1) resulted in an activity level in the torus of 7…8 mSv/h [98Pat], which precluded personnel access in the vessel for anything but the most brief task for around one year. Thus, in a fusion reactor all in-vessel inspection and maintenance operations must be carried out remotely. Outside the vessel, because of the neutron shielding, the activation of the structure may allow some hands-on assistance. Nevertheless, most maintenance and inspection operations inside the cryostat ("ex-vessel" operations) will also have to be carried out remotely. Human access with limited restrictions will only be possible outside the biological shield. The so-called "low activation" structural materials will not help in this respect since they are optimized to reduce the radioactive inventory on a time scale relevant to waste management rather than on the shorter time scale relevant to maintenance.

The Remote Handling Technology has already reached a high state of the art. Already the JET design was based on "maintenance-friendly" concepts such as the toroidal modular segmentation, allowing the individual removal of any individual octant. For the remote handling techniques, JET elected to rely on force reflecting servo-manipulators (MASCOT model IV) to be positioned inside or outside the vessel by transporters, under the direct control of human operators. The transport of heavy components to be installed inside the vessel is carried by the articulated boom [85Jon] equipped with one of several ad-hoc grippers (Fig. 5.17). Components located outside the vessel are carried by specialized transporters. The articulated boom in its "long" version with 5 arms can cover the complete vessel from one entry duct, and the load capacity out of the equatorial plane is 350 kg at 13.5 m distance from the support. This system was successfully used for extensive modifications (e.g. the divertor) and repair work.

In ITER it is expected to require the replacement of the complete divertor assembly approximately every 3 calendar years. To ensure an adequate machine availability, this operation must be carried out in less than 6 months. A dedicated transporter, called Toroidal Mover, travels on a pair of rails located on the bottom of the vessel [98Kak]. Once it reaches a divertor cassette, special tools are used to unlock the cassette. Then the cassette (weight between 12 and 25 t) is transported along the rails in front of a radial duct dedicated to maintenance. The cassette is then grasped by a Radial Mover, withdrawn in a transfer cask and transported to the hot cell. The In-Vessel-Transporter concept [99Dam] adopted by ITER for module handling is an alternative to the articulated boom and the preferred case when a complete blanket change-over is required. A major technical challenge for in-vessel handling and inspection systems is the nuclear environment. In a next-step machine the dose rate to be considered is between 1 and 10 kGy/h. Considerable R&D effort is required to qualify radiation-hardened components [94Dec, 96Sha].

Efficient remote handling techniques will be crucial in providing a sufficient availability of the of fusion power plant [98Mal]. The divertor lifetime is assumed to be 2 full power years (FPY) and that of the blanket 5 FPY. The blanket change-over can be realized in one single operation but it will probably be more convenient, from the availability standpoint, to replace it in fractions to take advantage of its non- uniform nuclear loading (strongest at mid-plane, approximately half at upper and lower regions). Since the outage time is practically proportional to the number of components to be replaced, it is possible to identify the maximum number of in-vessel components compatible with a given reactor availability from the assumed replacement time for each component. Thus, remote handling requirements become important design drivers.

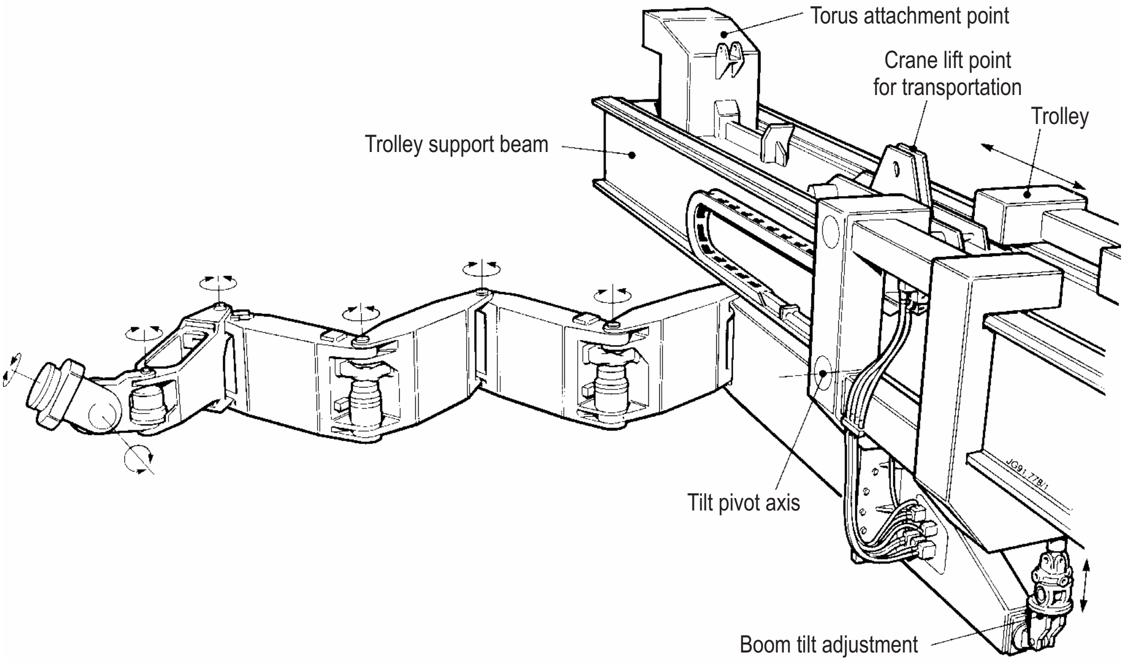

Fig. 5.17. Layout of the JET articulated boom ("long" configuration).

Acknowledgements

The author would like to thank M. Glugla, D. Maissonier, S. Malang, M. Merola, R.D. Penzhorn, M. Thumm and A. Ulbricht for essential input.

5.5 Reactor technology for inertial confinement

[W.J. Hogan]

5.5.1 Introduction

As described in Sect. 5.3.3.3, an inertial confinement energy (IFE) power plant consists of four major, separate but interconnected systems: the driver, the target factory, the reaction chamber, and the balance of plant (BOP). In an IFE power plant there are two major cycles to consider: the target materials cycle and the power cycle. These determine many of the technological requirements for the above four systems.

In the target materials cycle, complete targets disintegrate in the reactor and a portion of the DT fuel is burned. Target debris is deposited in the chamber gas and/or in the blanket material. Tritium is produced in the blanket through nuclear interactions between the fast neutrons and lithium (see Sect. 5.1.). The tritium and other target materials are extracted, conditioned and returned to the target factory for use in future targets. For IFE power plants there are other target materials that will also likely be recycled (see Sect. 5.5.6).

In the power cycle several energy conversion steps produce the power cycle gain. Electrical power supplied to the driver, P_d, is converted to driver beam power (note that the average beam power is just the pulse energy times the pulse repetition rate) with a characteristic efficiency η. The beam energy is used in the target to produce thermonuclear energy with an energy gain G (this is also the power gain, of course, when multiplied by the repetition rate). The thermonuclear power (fast moving neutrons, X-rays, and debris) is converted to heat energy in the blanket (with a small loss) and increased due to neutron reactions in the blanket. The net gain in the blanket is expressed as M. The heat in the blanket is converted to electricity in the BOP with an efficiency ε. Thus the gross power produced, P_g, is just the driver power, P_d, multiplied by the power cycle gain, $\eta GM\varepsilon$. Finally, a fraction of the gross power is sold, P_n, while some is cycled back into the auxiliary systems, P_a, and to the driver, P_d, completing the power cycle.

The power balance equation describes this power cycle:

$$P_n = P_g - P_a - P_d = P_g\left(1 - f_a - \frac{1}{\eta GM\varepsilon}\right), \tag{5.39}$$

where f_a is the fraction of the gross power used for auxiliary equipment and it is noted that the recirculating power fraction for the driver is just the inverse of the power cycle gain. Studies of power plant economics [85Mei] note that the cost of electricity rises rapidly if the recirculating power fraction grows larger than about 25 %. This is because there is less electricity to sell to amortize the large driver cost. A typical value of f_a is 5 %, M is 1.05 to 1.25, and ε is 0.3 to 0.4. Therefore, ηG should be larger than about 10 to keep the recirculating power fraction reasonable. Different drivers have different efficiencies and, therefore, require different target gains in order to be economically attractive. Drivers with efficiencies of 10 % or less (e.g. lasers) will require gains of 100 or more while those with efficiencies of up to 35 % (e.g. heavy ion beams) may be profitable at target gains of only 30. The economic studies also conclude that increasing ηG much above 20 produces rapidly diminishing economic returns and, therefore, effort should shift to decreasing driver cost when an ηG above 10 has been achieved.

5.5.2 Targets

The energy from a driver pulse is used to compress and heat a small capsule of fusion fuel until it ignites and burns. A few milligrams of DT fuel are compressed by the driver energy to densities of several hundred g/cm^3 and a few percent of the fuel are rapidly heated to 5…10 keV (the hot spot). If the areal density of the compressed hot spot is large enough (≥ 0.3 g/cm^2) the alpha particles created in the fusion reactions will stop within the fuel and, therefore, provide additional heating. The target is said to have ignited when the alpha heating is greater than the compression heating. A thermonuclear burn front forms and propagates radially outward through the cold dense fuel much as a flame moves down a matchstick. Good burn efficiency (e.g. ≥ 30 %) requires a fuel ρR (as distinct from the hot spot ρR) of ≥ 3.0 g/cm^2. At the normal liquid DT fuel density of 0.21 g/cm^3 an impractically large mass of fuel would have to be burned for good burn efficiency. The fuel mass in a compressed sphere is:

$$M = \frac{4\pi}{3}\frac{(\rho R)^3}{\rho^2}. \tag{5.40}$$

A value of $\rho R = 3$ g/cm^3 and normal density results in a mass of over 2.5 kg. Burning 1/3 of this would result in a yield of about 70 kt, hardly practical for a power plant. On the other hand compression by a factor of 1000 to densities of a few hundred g/cm^3 in a spherical shell results in a ρR of 3 g/cm^3 with a mass of a few mg. This density has already been achieved in experiments on the Gekko XII laser at Osaka University [91Aze]. Burning a few mg of DT results in a yield of a few hundred MJ, which, at a few Hz repetition rate, would support a 1 GW (el) power plant.

At these large compressed fuel densities the thermonuclear burn front moves through the fuel within a few tens of picoseconds. During this time the expanding fuel cannot move very far (typical compression and expansion times for this mass of fuel are a few nanoseconds) and, thus, it is said that the fuel is held together by its own inertia. It is also true that during this short burn time photons will travel only a few centimeters. Therefore, once ignited, target burn cannot be influenced by material interactions beyond the immediate vicinity of the target. It is said that the target performance is decoupled from the reaction chamber walls. This gives considerable latitude to design of the reaction chamber and other systems outside it.

As discussed in Sect. 5.3.3, there are two principal types of IFE targets: direct drive and indirect drive. Figure 5.18 shows the principles of operation of these targets.

In direct drive targets the driver energy is placed directly on the fuel capsule. The driver beams ablate the outer capsule material (called the ablator) causing the fuel layer inside to be compressed. When the compression stagnates, a few percent of the fuel at the center are heated to ignition conditions and a thermonuclear burn front propagates outward. During the compression, hydrodynamic instabilities grow in the imploding layers any time there is an acceleration of a denser material by a less dense material. If these instabilities grow too large, the imploding shell can mix with the fuel or even break up and the center will never reach the required ignition conditions. The possible seeds for instability growth (e.g. roughness on the capsule surface and/or non-uniformity in the driver energy on the surface) must be carefully controlled to make it possible to converge successfully and ignite the hot spot in the center. The larger the convergence (generally defined as the ratio of the initial outer radius of the ablator to the final compressed radius of the hot spot) sought, the longer the time instabilities will grow. The change in fuel radius need only be a factor of ten to achieve the desired increase in fuel density of a factor of 1000. However, the need to form a hot spot within the center few percent of the fuel places greater demands on convergence and symmetry, and that is why the necessary convergence ratio as defined above is about 30. This places exacting requirements on target surface finish and on illumination uniformity.

In indirect drive targets, a case of high atomic number material, called the hohlraum, surrounds the fuel capsule and the driver beams are aimed at the inside surface (in the case of laser drivers) of this hohlraum. The driver beams are absorbed in material inside the hohlraum heating it to such high temperatures that it emits X-rays. The interior of the hohlraum reaches radiation temperatures of a few hundred eV. At this radiation temperature the surface of the fuel capsule is ablated and in reaction the fuel layers inside are compressed and the center heated to ignition as in the direct drive target. Figure 5.18 shows that the processes in the fuel capsule during and after compression are the same for both direct and indirect drive targets. Furthermore, in indirect drive targets the fuel capsule does not really “know” where the X-rays come from. Therefore any means of producing intense X-rays near the capsule can, in principle, be made to work. Either laser beams or heavy ion beams can be made to generate the necessary source of X-rays. Pulse power machines do not use beams of any kind. Z-pinch machines generate an intense source of X-rays by using the self-compression of a very high current flowing in a plasma. These X-rays then flow into a hohlraum containing a fuel capsule where the processes proceed as above (see Fig. 5.9c) for beam-generated X-rays.

Because of the extra energy conversion step in converting beam energy (or z-pinch energy) into X-rays, the indirect drive process is less efficient than the direct drive process. However, the X-rays inside the hohlraum form a uniform temperature “bath” for the fuel capsule, and, therefore, growth of hydrodynamic instabilities is easier to control. Therefore, both target types are being pursued in main-line ICF research.

Ideally one would like to ignite as small a target as possible since the smaller the amount of fuel burned, the easier it is to contain the effects of the micro-explosion and extract and use the energy produced. However, the smaller the target initially, the higher is the convergence necessary to obtain the required ρR to stop the alpha particles. As discussed above, the larger is the required convergence, the more difficult it is to control the growth of hydrodynamic instabilities. Therefore, for the central-hot-spot ignition scheme there are minimum driver sizes determined by the largest convergence believed achievable. Practical limits to the convergence ratio are judged to be 30…40. This puts a lower limit on the driver size needed to ignite a central-hot-spot target at about a megajoule.

In either direct or indirect drive it is the ablation of the surface of the fuel capsule that causes the compression of the fuel inside. Near the end of the compression, the fuel reaches very high densities (few hundred g/cm^2) and a hot, low-density core is formed, as shown in Fig. 5.19a. The formation of this hot, low-density core simultaneously with the cold, high-density surrounding fuel is critical to the ignition and efficient burn of these targets. Figure 5.19b shows a diagram of temperature versus ρR of the compressed capsule. In most regions of this diagram the losses dominate the gains in DT fuel and the capsule will not ignite. However if the compression is just right, a hole in the so-called “Wheeler” diagram is created and the target will ignite. This is shown in the figure in the NIF spot compared to the Nova spot. NIF targets will be large enough that, when compressed, the cold dense fuel will stop the alpha particles emitted in the burning hot spot. This will launch a thermonuclear “flame” front that will burn radially outward. Extremely good symmetry of the implosion is required in order to form the hot spot in the center. This requirement sets the extremely tight driver symmetry requirements.

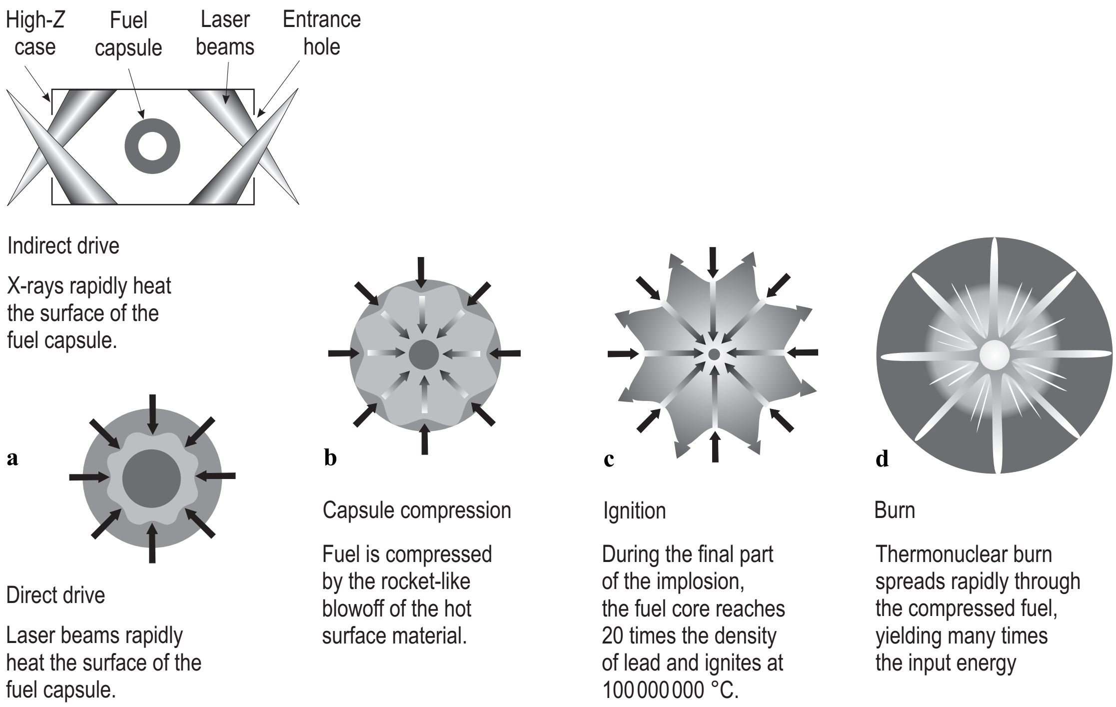

Fig. 5.18. The operation of a central ignition ICF target consists of four steps: **(a)** deposition of the driver energy in the target, **(b)** implosion of the fuel capsule, **(c)** formation and ignition of the central hot spot, and **(d)** propagation of a thermonuclear burn front outward through the cold, compressed fuel. The physical processes in steps b-d are the same for both direct and indirect drive targets.

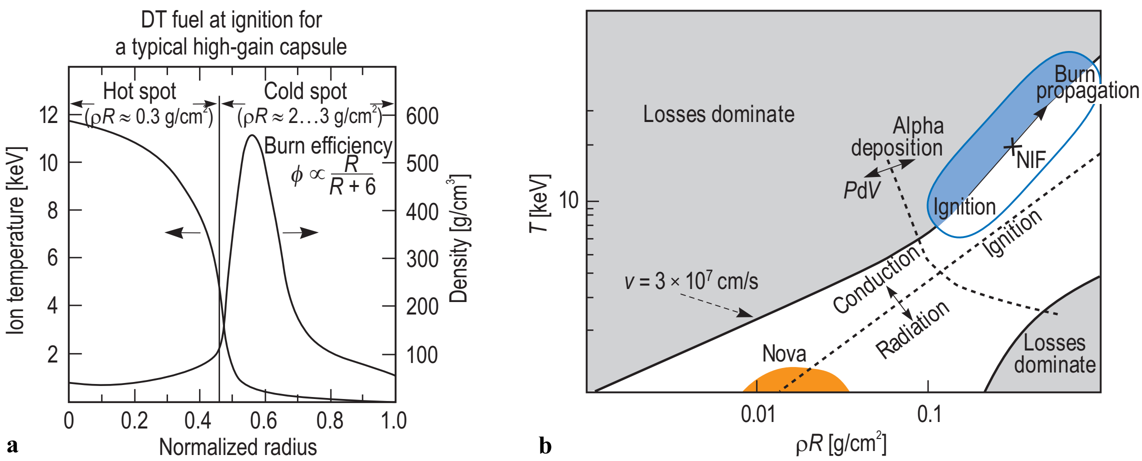

Fig. 5.19. **(a)** Ion temperature and density as a function of the normalized capsule radius at peak compression; **(b)** the "Wheeler" diagram (named after Princeton physicist John Wheeler).

An alternative to the central-hot-spot ignition targets above has recently gained considerable attention: the fast ignition (FI) target. Fig. 5.20 shows the principles of operation of this new type of target. The fuel capsule is compressed but there is no attempt to form a low-density, high-temperature central hot spot. Instead after the fuel is compressed to peak density, a separate driver injects enough energy into a spot on the side of the compressed fuel to ignite that spot. The ignited spot then creates the propagation thermonuclear burn front as in the conventional targets. The ignitor driver must deliver its energy to the spot in a time short compared to the energy diffusion time in the compressed target. For typical inertial fusion targets this delivery time must be measured in picoseconds, not nanoseconds like the compression driver. This has been made possible by the invention of extremely short pulse lasers by chirped pulse amplification that will be described in Sect. 8.4. The compression phase of this type of target can be accomplished by any driver and the symmetry requirements are not as stringent as for central ignition targets.

The expected gain performance of each type of target is shown in Fig. 8.9 in Chap. 8. Since the cost of the driver is a substantial portion of the total cost of an IFE power plant, the FI target concept is receiving much interest in the international community at present. However, it is a relatively new concept and there are many physics questions to answer before it can be considered viable. For example, after compression, the high-density fuel core is surrounded by a hot plasma. It is not known with what efficiency the short pulse igniter beam(s) can penetrate this plasma or if they can penetrate it at all. Therefore, at present, the FI scheme is considered a high-risk but potentially high-payoff alternative to central ignition. Gains of 30 to more than 100 are required, depending upon the driver efficiency. Thus Fig. 8.9 shows that driver energies of several MJ are required for central ignition targets, while drivers of a few hundred kJ may be adequate for fast ignition targets.

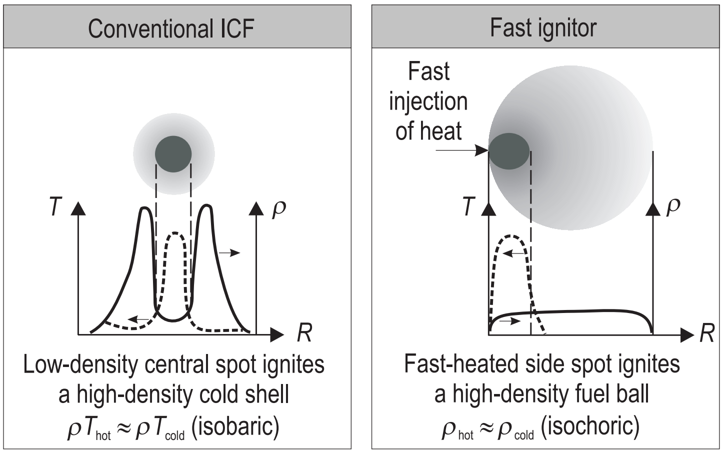

Fig. 5.20. Principles of operation of fast ignition targets compared to conventional central ignition targets. The dashed lines are the temperature profiles, and the solid ones are the density profiles.

5.5.3 Drivers

The major power plant drivers under development today are solid state lasers, KrF lasers, heavy ion accelerators, and z-pinches. These drivers will have characteristics somewhat different from the research facility drivers in use today. The great majority of target research has been done with flashlamp-pumped solid state lasers, though target experiments with z-pinches are beginning to produce substantial target physics data. While quite adequate for their designed purpose, drivers for target physics research facilities generally have low repetition rates (a few per day) and low efficiency (the Nova laser had an efficiency of 0.1 %; the NIF will be the most efficient large flashlamp-pumped solid state lasers ever built and it is still only about 1 % efficient) compared to what will be needed for a power plant. Therefore, power plant driver development programs are focusing on how to change certain characteristics of the research drivers to make them satisfy the requirements for a power plant driver.

Any IFE power plant driver must satisfy a set of requirements determined by two types of boundary conditions: (1) what it takes for that driver to make a target ignite and produce adequate gain and (2) engineering and economic factors that make a power plant competitive with other energy sources. A set of eleven requirements has been developed [95Hog] to illustrate the factors driving development. However, it must be noted that the specific numerical requirements for a given driver depend upon the exact combination of driver, target type, reaction chamber system chosen.

(1) *Intensity and focusability*: To compress the fuel intensities of $10^{13}\ldots10^{15}$ W/cm^2 are required for a few nanoseconds in a spot less than the target size (< 1 cm). Fast ignition drivers must reach $10^{18}\ldots10^{19}$ W/cm^2 in less than one picosecond on spots of a few hundred µm.
(2) *Energy*: A drive energy of 1…5 MJ is needed for the central ignition targets while the FI targets may suffice with a drive energy of 0.5…1 MJ.
(3) *Temporal control (pulse shape)*: Target compression is most efficiently achieved when the driving pulse consists of a gradually increasing intensity. This is desirable to keep the fuel being compressed in close to a Fermi degenerate state. If this is not possible, tailored hydrodynamic response internal to the target is necessary.
(4) *Spatial control*: The spatial variation of the intensity over the surface of a central ignition target must be less than 1…2 %. This results in specific beam uniformity requirements for direct and indirect drive targets.
(5) *Laser wavelength or particle beam range*: Good target coupling requires a laser wavelength ≤ 0.5 µm. Particle beam ranges of 0.02…0.2 g/cm^2 are being examined to produce sufficient temperature in hohlraum targets.
(6) *Efficiency*: Gains for central ignition targets are estimated at no more than about 100…150. Therefore, drivers of 7…10 % are required to keep the recirculating power reasonable. Drivers with higher efficiency (up to 30 % or more for heavy ion accelerators) can use target gains of only about 30.
(7) *Repetition rate*: The optimum pulse rate for a given power level will depend upon the shape of the target gain curve, the cost dependencies of the various power plant subsystems, the maximum pulse rate achievable in a given reaction chamber type, and whether multiple chambers can be driven with the given driver. For a target yield of a few hundred MJ, a repetition rate of a few Hz is typical.
(8) *Cost*: To be competitive with a 1000 MW (el) coal or fission plant, the driver of a similar-sized IFE plant should have a capital cost of less than about 630 mill. $ (in 2001 US $) less the cost of the target factory (estimated at about 125 mill. $).
(9) *Lifetime*: About 10^{10} pulses for a 40-year lifetime. The driver is costly enough that it should not have to be replaced during the plant lifetime.
(10) *Operation and maintenance costs*: To keep O&M costs reasonable, a driver should be able to be maintained by a smaller and less skilled crew than currently maintain research drivers.
(11) *Reliability and/or redundancy*: The reliability and redundancy of all subsystems directly affect the availability of the power plant and, therefore, the cost of electricity. Each driver type approaches this tradeoff in a different fashion.

Later sections will discuss the development of four specific driver technologies in more detail – diode-pumped solid state lasers, KrF lasers, heavy ion drivers and z-pinches. Suffice it in this introductory section to note that to increase efficiency, solid state laser developers are examining diode pumping since diodes can be selected to efficiently emit at just the frequency that the lasing ions resonantly absorb, resulting in much less wasted energy and greater efficiency. The other drivers are more inherently efficient and their issues will be centered on other issues in the above list. Each section will discuss how that driver will address the above general requirements.

5.5.4 Target fabrication and positioning systems

Regardless of which driver is used, all IFE power plants will have a target factory in which targets are mass-produced from new and recycled material. In this factory about 10^8 targets per year must be manufactured reliably and inexpensively. The required dimensional precision of tiny components and the fact that radioactive fuel must be handled at cryogenic temperatures pose major challenges for development of the target factory. Many target concepts are still under consideration and, in principle, each of these can be paired with any driver. Here the general issues associated with all target types and the major unique issues of each will be discussed.

The fuel capsule in IFE targets usually consists of a hollow spherical shell of plastic (polystyrene or polyimide) or Be. The plastic or Be acts both as a fuel container and an ablator that compresses the fuel upon illumination by the driver beams or the X-rays produced by them. The spherical fuel container must be fabricated with great precision – of order 100 nm surface roughness on few hundred micron thick shells a few millimeters in diameter. The DT fuel must be inserted into the shell and then formed into a frozen spherical shell of fuel on the inside surface of the ablator/container. Furthermore the filling must be done in such a manner as to leave no imperfections on the surface.

To fabricate the plastic shells with the required precision two basic methods have been studied [95Hog] – drop tower generation and controlled mass microencapsulation. In the former a drop generator ejects a known mass of liquid into a drop tower whose vertical temperature profile is carefully controlled. As the drops fall through the hot column, the solvent inside them evaporates and leaves a shell of solute material. In the microencapsulation technique, mixtures of water, solvent and solutions of polystyrene in a solvent are physically shaken to form minute drops in a complex emulsion (similar to salad dressing). This produces very round shells of uniform thickness but the shaking process makes shells of a large range of diameters. To control the size, the controlled mass technique makes drops of water of uniform mass with a uniform layer of an appropriate polymer by means of a multiple concentric orifice drop generator. This combines the advantages of the tower and microencapsulation techniques.

Once the shells are formed, they are often coated with thin layers of material that improve the retention of hydrogen isotopes, increase the thickness of the ablator, reflect thermal radiation to reduce losses during injection, and/or help reduce the “imprinting” caused by variations in laser intensity on the surface.

To fill the fuel capsules, DT gas can be diffused through the thin capsule shells under pressure. Then the temperature is reduced to freeze the DT inside. Of course, the DT pools to one side. However, the local heating caused by beta decay heats the thickest parts of the frozen DT faster than the thinner areas so that DT sublimates from the thick region to the cold side of the capsule. After a few hours, the DT has formed itself into an almost perfect spherical shell. The process can be sped up considerably through RF or plasma heating [99Bes]. Direct injection of DT through a tiny orifice has also been considered though it is difficult and uncertain because of the tight surface finish requirements. After filling the fill tube must be removed and the hole filled so that there is no local perturbation. Only experiments with igniting capsules will determine if this method of filling will prove to be acceptable.

The tritium inventory in the IFE power plant is very dependent upon the filling and layering method chosen. Room temperature diffusion filling and layering (i.e. forming the spherical shell of DT) through dependence solely upon beta heating led to very long times (e.g. days) for the process. A 1000 MW (el) power plant cycles about 2.5 kg of tritium through the reaction chamber each day. If several days of targets have to be in the filling or layering process, then tritium inventories in the target factory could exceed 10 kg of tritium. This could pose serious safety issues that would lead to increased costs through partitioning of the inventory to prevent release. Studies find that if the tritium inventory is less than about 1 kg, the safety issues can be easily handled. This has led to concentrating on developments to speed the target manufacture process.

One direct drive target concept does not use a plastic or Be ablator/container at all. Rather it depends upon making a spherical shell of open cell plastic foam and then wicking up the DT into the foam shell. After the shell is formed, additional DT can be diffused in and a pure DT layer formed on the inside surface as above. The outer DT in the foam shell acts as the ablator. This fill and layering process can be very fast, leading to process times of about 2 hours and, therefore, tritium inventories much less than 1 kg. However, such targets are very vulnerable to heating from the thermal radiation from the reaction chamber walls during injection or even from convective heating while passing through the residual gas in the chamber. To address this problem some suggest surrounding the target with a sabot that would be removed when the target is near the center of the chamber. In indirect drive targets the fuel capsule is surrounded by the hohlraum wall. Therefore, it is protected from the thermal radiation during injection.

Many technically elegant solutions have been proposed for the target injection process but the best seems to be the simplest – a gas gun, essentially equivalent to a BB gun but at cryogenic temperatures. The major issue to consider in this process is how much acceleration can the target withstand without breaking or distorting to the point that it will not work. Calculations and some experimental work [98Pet] have concluded that the gas gun parameters are reasonable and that the target can be placed and tracked with sufficient accuracy that minor corrections in the beam pointing will allow accurate enough beam target illumination for the targets to work. Ultimately experiments with igniting targets will be necessary to determine how much the positioning, tracking and pointing precision can be relaxed.

5.5.5 Reaction chamber systems

The reaction chamber is the heart of any IFE power plant. In it, the targets are ignited by the driver beams, the thermonuclear energy is released and processed, tritium is bred for future targets, the outside world is protected from the series of mini-thermonuclear explosions, and the chamber environment is restored so that the next target can be injected. Like a large cylinder of an internal combustion engine, the walls will be subject to pulsed stresses.

Economic studies (see, for example, Chap. 7 of [95Hog]) have shown that minimizing the cost of electricity will require that the plant operate at the "knee" of the target gain curves (see Fig. 8.9). At any given power plant size, this will minimize the combination of the recirculating power and the cost of handling larger thermal loads. These analyses lead to target yields of 100…1000 MJ and pulse rates of 2…20 Hz. At these values a chamber about 10 m in diameter will "feel" stresses that are about the same as those in a diesel engine and the total number of such pulses in a 30-year lifetime is about the same as for a typical diesel engine. Thus, except for the fact that the "cylinder" is 10 m in diameter, the design of the reaction chamber to survive the cyclic stresses should not be a major issue. Furthermore, since the target performance is not affected at all by what materials are in the "first wall" or the other structural elements, there is a great deal of design flexibility for the reaction chamber.

The reaction chamber and its subsystems must perform several functions:

- accommodate whatever illumination geometry required by the driver/target combination,
- convert the thermonuclear energy released by the target into heat,
- breed tritium for future targets,
- contain the effects of the thermonuclear mini-explosions,
- restore the chamber environment to that necessary to allow the driver to deliver its energy to the target in the proper form for ignition and high gain.

In designing chamber subsystems to perform these functions it is desirable to:

- minimize negative impacts on the health, safety and environment of the workers and public,
- maximize the lifetime of structural components,
- accommodate wide power variations in a plant of a given size,
- be economically competitive at power plant sizes smaller than 1000 MW (el),
- minimize the amount of remote maintenance required.

In most DT-fueled fusion power plants (whether inertial or magnetic confinement) a system called the blanket is used to capture the thermonuclear energy from the target and to breed tritium. Often the blanket material is a liquid such as Li, LiPb, or Flibe (a combination of fluorine, lithium and beryllium). The target emits X-rays, neutrons, charged particles, and plasma debris (leftover material from the vaporized target). The exact proportions and energies of these materials depend upon the target type and specific design. In general, however, it should be noted that the fraction of energy in the neutrons is not as large as for magnetic fusion because the IFE targets are thick enough that there is significant neutron moderation in the target itself. The blanket must be thick enough to absorb all these forms of energy and the 14 MeV neutrons that do leave the target are the most difficult to stop. In general it will take up to a meter of material to capture all the neutron energy and to cause most neutron nuclear reactions to take place within the blanket (desirable to maximize the tritium production and minimize the incidental production of radioactive waste).

In IFE reaction chambers, the blanket may be inside or outside the first structural wall because the vacuum requirements for driver beam propagation are tolerant of a small amount of residual gas inside the chamber and the target performance is not affected by the presence of this gas. The required driver illumination geometry for a given target type is the strongest factor determining whether the blanket can be inside the structural wall. Because of the design flexibility noted above, more than 40 different power plant concepts have been proposed and studied to a varying extent (see Table 3.4.1 [95Hog] for a list of the studies as of 1995).

Two examples that illustrate many of the reaction chamber system design requirements are shown in Figs. 5.21 and 5.22. The first is Sombrero, a dry wall design particularly amenable to the direct drive illumination geometry. The second is HYLIFE-II, a chamber with a thick, renewable liquid curtain inside the structural wall.

In Fig. 5.21 the dry wall Sombrero design is shown [92Svi]. In this reaction chamber the blanket consists of Li_2O granules that are entrained in a flowing gas through the graphite chamber walls. The chamber is filled with Xe gas at about 100 Pa in order to protect the graphite walls from the X-rays emitted by the target. If not stopped in the gas, the target x-rays (in a few tens of picoseconds pulse) can create a high enough energy density in graphite that a few microns would be vaporized with each pulse. The debris and neutrons however spread in time so that by the time they reach a wall 7 m away, their power density is low enough that wall material is not vaporized. In this concept the chamber is pumped to restore the chamber environment to the initial conditions necessary for propagation of driver beams and the concept can handle almost any illumination geometry. The one shown is for a direct drive target with a laser driver. As shown in Fig. 5.18, the beams must come from all directions and uniformly illuminate the direct drive target. In Fig. 5.21 the laser entry holes through the target chamber walls are clearly visible.

In Fig. 5.22 the thick-liquid walled HYLIFE-II design is shown. In this concept a thick blanket of Flibe surrounds the exploding target inside the structural walls. All target emissions are stopped in this blanket before reaching the structural walls. This results in the desirable features that the structure can be made of steel and still will last the lifetime of the plant (without succumbing to radiation damage) and the waste produced by neutron interactions is minimized. Creating this thick, self-renewing liquid wall between each target injection is done with oscillating jets that form the Flibe into a falling pocket. At the appropriate time, the target is injected into this pocket and ignited.

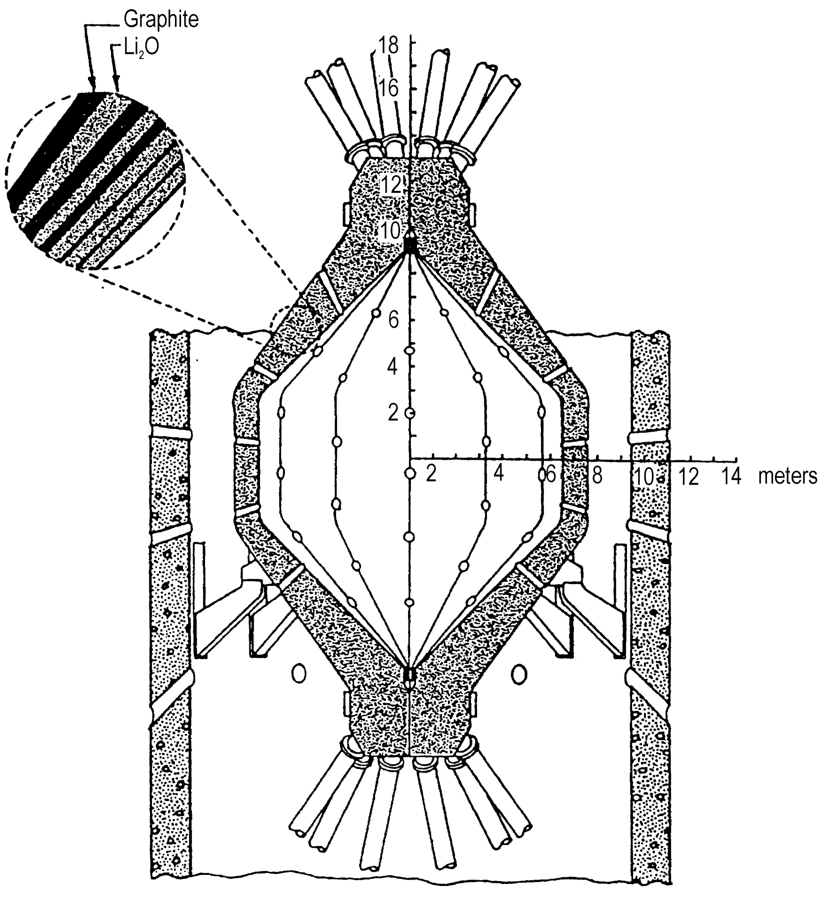

Fig. 5.21. Cross section of the Sombrero dry wall reaction chamber concept [92Svi].

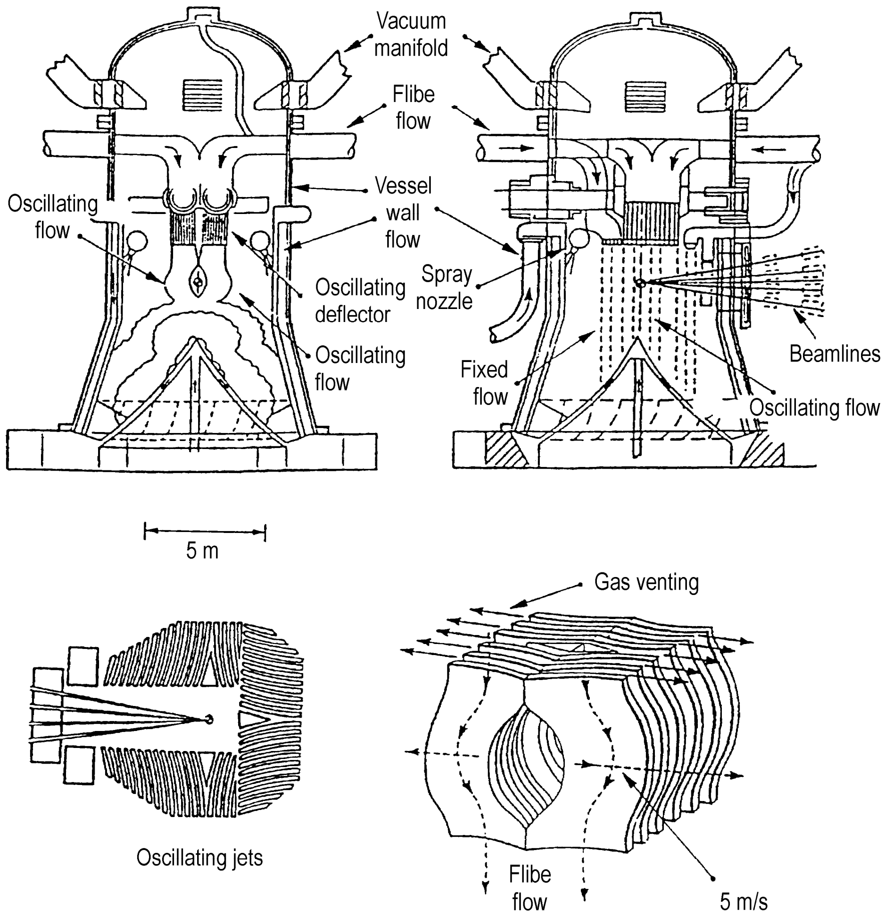

Fig. 5.22. Cross section of the HYLIFE-II reaction chamber concept [94Moi].

The HYLIFE-II concept (and many like it) is most useful for indirect drive target geometries and perhaps the fast ignition target also. Driver beams for indirect and fast ignition targets can be clustered into two cones coming from opposite directions. For heavy ion drivers the angle of the illumination cone may be even smaller than for a laser driver because the ion energy deposition range in the target is much longer than that for lasers. It may also be possible that all beams can come from one direction as shown in Fig. 5.22.

Thick-liquid wall reaction chambers have the potential advantage that the flowing blanket stops all X-rays, neutrons, charged particles and debris before it interacts with the structural walls. This makes thermal conversion and tritium breeding more efficient and the structural walls and components are protected from radiation damage. Finally, less radioactive waste will be produced through induced activity. Walls can be moved closer to the fusion explosion and still survive.

A major reaction chamber issue in any fusion power plant is the neutron damage to the structural walls. It is well known that materials bombarded with large fluences of high energy neutrons for long periods of times will see degradation of material properties. The energetic neutrons displace atoms and produce He through nuclear reactions. Both processes can limit the lifetime of structural components.

Radiation damage of material properties in fusion reaction chambers has been studied for many years and the processes that result in degradation of properties are fairly well identified for many materials. However, it was noted in the early 1980s [82Gho] that IFE reaction chambers could see extremely large neutron fluxes and, consequently, very large rates of producing displacements (DPA/s). The concern was that the measured material survival levels may not apply to pulsed reaction chambers like IFE (or possibly even some magnetic concepts that are inherently pulsed). Recent work with molecular dynamics and Monte Carlo models of the neutron damage processes (see Chap. 4.1 of [95Hog]) indicates however that there is almost no difference between pulsed and continuous irradiation for the same integrated dose. The time between pulses is the governing parameter.

The effect of having a thick-liquid wall inside the structural chamber wall can be seen in Fig. 5.23. The lifetime of a steel structural wall outside of a lithium blanket is shown as a function of the thickness of that blanket. As shown, a 70…80 cm blanket would make the structural wall last the lifetime of the plant.

Analogous analyses of IFE reaction chambers in which the structural wall is protected by a 70 cm thick inner liquid blanket of LiPb reveal that the induced activity can be reduced by three orders of magnitude [85Bad]. Thus a thick inner blanket reduces the amount of radioactive waste that must be handled significantly.

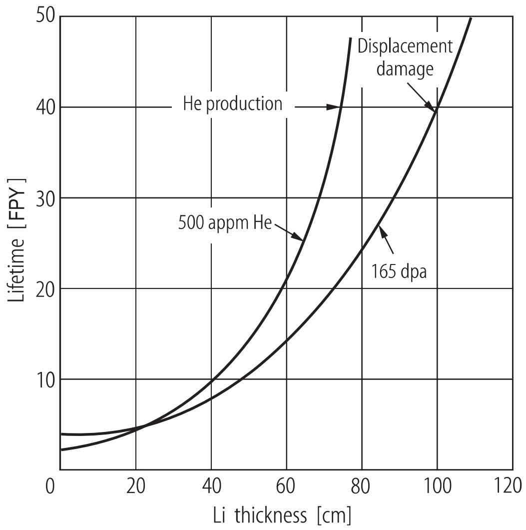

Fig. 5.23. Lifetime (in full power years, FPY) of a 5 m radius structural wall, made from 2.25Cr1Mo ferritic steel, behind a Li curtain at 2 m inner radius in a 2700 MW (th) IFE power plant.

5.5.6 Balance-of-plant systems

One characteristic of IFE power plants that is unique and is often thought to pose either very difficult challenges or great opportunities is the fact that the energy is produced in a series of tiny thermonuclear explosions each of very short duration (of order tens of picoseconds). Systems in the reaction chamber and balance of plant (BOP) must convert the pulsed fusion output into a continuous stream of electricity.

For thermal based power conversion systems this is not really a difficult proposition. Just as the internal combustion engine converts a series of tiny chemical explosions into the smooth, continuous motion of an automobile, the IFE reaction chamber blanket can be designed to absorb all the pulsed thermonuclear energy into a continuous flowing material at an elevated temperature. In IFE the thermonuclear energy released is very high "quality", i.e. the energy resides in a very small mass, producing very high local temperatures. It is also well "ordered", i.e. all forms of the thermonuclear energy are moving radially outward from the point of the micro-explosion. Because the designer can choose the interaction properties and flow rate of the blanket material to a certain extent, he can choose the temperature at which he will convert the thermal energy to electricity. This can produce high conversion efficiencies. One design, Cascade [83Pit], used a blanket of $LiAlO_2$ granules inside the reaction chamber. The ceramic blanket was raised to a temperature of 1100…1700 K (the inner layer, of course, achieves the higher temperature) and, using a He Brayton cycle, a generation efficiency of 55 % was achieved in calculations. A few studies have also examined whether the high "quality" of the thermonuclear pulses could lead to direct energy conversion. Most IFE power plant concepts, however, envision using the conventional steam cycle.

In an IFE BOP a portion of the electricity produced must be recirculated to run the driver. The type of conditioning that must be done depends upon the driver characteristics. For example in lasers the type of power conditioning depends on the storage ability of the lasing medium. In KrF lasers the short energy decay time (≈ 3 ns) and the time required for efficient extraction of light (a few hundred nanoseconds) dictates the characteristics of the power system required. On the other hand, solid state lasers fluorescence lifetimes of 0.35…10 ms are possible. Therefore the lasing medium can be pumped for these longer times and the requirements on the power conditioning system are relaxed.

The BOP must also have systems for extracting tritium and other materials from the exhaust gases and the blanket material for use in future targets. The tritium issues are very similar to those for magnetic fusion since for a given size power plant the amount of tritium burned is the same. However, one feature unique to IFE is the recirculation of other material in the targets.

For example, high atomic number materials used in the target hohlraum wall (e.g. Pb or W) should be recycled so that there is not a very large radioactive waste stream produced. However, in the case of Pb, if it is returned too quickly to the reaction chamber, there will be a build up of Po210, which is very hazardous. Neutron capture in Pb208 produces Pb209 which is radioactive with a 3.25 h half-life for beta decay. If the Pb is returned too soon to the reaction chamber, the Pb209 may capture another neutron to form Pb210, which decays by two successive beta decays to Po210. Therefore, it has been suggested that the extracted Pb be allowed to “cool” for a few days before being returned to the target factory for recycle. This allows the Pb209 to decay to the point that there will be no build up of Po210. This is an illustration of the influence that target materials will have on design of the materials cycle systems.

5.5.7 Special design issues

While the four major subsystems of an IFE power plant discussed above are separated in space to varying degrees and, therefore, can be designed somewhat independently, they must be connected and some of the interfaces pose challenges unique to IFE. The interface between the driver and the reaction chamber, for example, is not only unique to IFE but to each driver/target combination. It was pointed out above that the target illumination geometry required puts constraints on the chamber concepts that can be used. Because the specific issues for each driver/target/reaction chamber combination are unique, only the general issues of each will be discussed here.

All laser drivers must have some “final optics”, generally made of a solid material. Furthermore this final optics must directly “see” the target and will therefore be bombarded with the output of the target when it explodes. Finally, high quality optical components can be quite expensive and can be very vulnerable to damage from the emissions of the target. To avoid all damage the optical elements might have to be placed so far away that they could not achieve the desired small spot size for best target performance. To avoid these issues designers have followed two general principles: (1) Don’t make a lens the final optics (focusing optics are generally much more expensive than flat optics), (2) put some optically transmitting material between the target and final optic. One design proposed uses of a pair of fused silica wedges to displace the laser beam sufficiently that the high value optics are not in the line of sight of the target. Furthermore an X-ray absorbing gas was placed between the last wedge and the target. An examination of the damage vulnerability of this concept revealed that neutrons could change the optical characteristic of the fused silica by producing color centers that would gradually decrease the transmissivity of the fused silica. However, it was also found that the color centers would anneal out if the temperature of the wedge was elevated. Therefore, it was found that the final optics could be as close as 25 m from the target if the operating temperature were raised to about 450 °C.

An alternative final optics scheme for laser drivers is the Grazing Incidence Metal Mirror (GIMM). Pure metals can have a very high reflectivity at very small angles of incidence while at the same time this small angle reduces the flux imposed by the target explosion. Furthermore reflective optics do not suffer from the color center degradation discussed above. However, because of the small angles and large GIMM surfaces that result in each beam line the size of the containment building can get quite large for a direct drive target. In the Sombrero design discussed above (Fig. 5.21) the reaction chamber is surrounded by a building 105 m in diameter and 110 m tall.

Heavy ion drivers have the advantage that their final optical element (a magnet to focus and steer the beam) has no solid material in the line of site of the target. However for greater efficiency, cryogenic, superconducting magnets have been considered for the final "optical" element. In this case the issue becomes how to prevent scattered particles from depositing heat in the cryogenic magnet causing it to go "normal". Furthermore, since the beam line is completely open to the reaction chamber, target debris may contaminate the entire driver unless there is some kind of valve to shut it out between pulses.

The z-pinch fusion driver has different interface issues. In this case the driver must use "beams" of conducting material to transmit the high currents needed to the cylindrical plasma that is to be pinched. When the target explodes many centimeters of these transmission lines will be vaporized. These will have to be replaced before the next shot, so chamber concepts have envisioned methods of having renewable transmission lines such as sprays of liquid lithium.

As can be seen, the interface issues are challenging but are different for each driver. Therefore, further discussion will be left to the sections devoted to each type of driver.

5.6 Safety and environmental aspects of magnetic confinement systems

[J. Raeder]

5.6.1 Introduction

Nuclear fusion is a potential contributor to the future energy system. Hence assessments of its safety and environmental (S&E) aspects are an ongoing activity in the worldwide fusion programmes so that fusion is "possibly the most reviewed science and technology program in history" [95PCA].

This article largely resorts to the European Union (EU) safety studies for future fusion power reactors as well as to the safety studies for the "1998 ITER Design" [98ITF] and for the smaller device "2001 ITER Design" [02ITF] with fusion powers of 3000 MW, 1500 MW and 500 MW (for more details see [86Rae]). The devices addressed are based on deuterium-tritium (DT) fusion in toroidal, magnetically confined plasmas (see Sect. 5.4) of the tokamak type (see Chap. 6). The development of plasma parameters towards power plants is most advanced in such devices and the most detailed design work and S&E assessments have been done for this concept. It is expected that the S&E characteristics of reactors based on the stellarator concept are similar but eventually dedicated assessments will be necessary to account for specifics such as the potential for continuous operation, the absence of plasma current disruptions and the specific configuration of the magnetic field coil system.

Next generation devices aim at demonstrating in addition to fusion's feasibility also the safe operation of fusion reactors. The design work, in particular on the European NET and on the worldwide international ITER [93NET, 91ITC, 98ITF, 02ITF], has extensively addressed the S&E aspects. ITER is without precedent in safety studies with regard to technical detail [97NSR1, 01GSR1]. Some results are not yet directly applicable to future fusion power plants since next generation devices cannot yet be fully representative with regard to power densities, reactor materials, coolants and coolant parameters.

Present S&E assessments of future fusion power plants, intentionally less detailed technically but broader in scope than for next generation devices, have to accommodate the lack of fusion experience at reactor scale so that extrapolations are required. Therefore, an important element of the assessments are power plant models whose conceptual design calls for some hypotheses with regard to physics, and considers a range of material and coolant options. Design details are pursued only to the level needed for the safety assessments. This theoretical effort needs, of course, to be substantiated by future large fusion experiments.

Major European S&E assessments for future fusion power plants are the studies SEAFP, SEAL and SEIF [95SEA, 99SEA1, 99SEA2], 01SEI]. Also the fusion program reports and assessments [89EEF, 90Col, 96Bar, 00Air] elaborated for the Commission of the EU and the STOA activities of the European Parliament [91STO], [97STO] have dealt with S&E.

A classical contribution from outside the EU is the broad U.S. study ESECOM [89ESE]. The U.S. fusion S&E activities over the last decade, largely in support of ITER, have been reviewed in [00Pet], including many useful references. Specific reactor concepts from outside the EU are provided by the

ARIES study series (brief overview in [98ARI]). ARIES-RS, a recent example, deals with an advanced tokamak power reactor (1000 MW net electric power), based on a "set of top level requirements for fusion demonstration and commercial power plants" [98ARI]. The Japanese DREAM study, as another example, deals with a reactor based on very-low-activation ceramic materials and is focused at visionary S&E characteristics.

5.6.2 The safety characteristics of magnetic confinement fusion

Fusion is a nuclear energy source due to tritium usage and neutron generation. Its dominant safety characteristics are associated with the following favorable features:

- Criticality accidents cannot develop in the fusion process.
- Reaction rate excursions are limited by inherent plasma processes.
- Under off-normal conditions, plasma burn is terminated by inherent processes within seconds.
- The fuel inventory in the plasma is small (of the one gram order) and can sustain fusion for one minute at maximum. The related fusion energy content is several orders of magnitude lower than the one in fission reactor cores of comparable power rating.
- The total energy stored in a fusion plant is low (by comparison with fission equivalents) and is not sufficient to overall distort or melt the reactor.
- Fissile and fertile materials are not involved in fusion reactions.

Further characteristics with regard to S&E impact are:

- Tritium is an intermediate product inside the reactor, so that no major shipments are necessary.
- The activation of reactor materials by fusion neutrons entails nuclear decay heat and radiotoxicity which are much lower than in fission equivalents.
- Reduction of the long-term inventory of activation products can be achieved by dedicated development of materials together with a detailed control of impurities.
- The magnetic energy has the potential to locally distort reactor geometry so very careful design is needed.
- Energies are transferred across large surfaces, and big masses are available as heat sinks.
- Power densities in the reactor components during normal operation and after shutdown are moderate compared with fission equivalents.
- The low power densities combined with the high thermal inertia provide time for active measures against loss of reactor cooling.
- The low power densities together with the large heat transfer areas allow for reactors with passive removal of decay heat in the unlikely event that no cooling at all can be restored in the long term.
- Tritium if released during normal operation or accidents is not retained in body and soil, rather the concentrations decrease by several orders of magnitude within one year owing to inherent processes. Accordingly, the "biological half-life" is moderate (days to months).

5.6.3 Safety concept

5.6.3.1 Safety objectives

This article leaves aside conventional industrial hazards and concentrates on the nuclear aspects which are addressed according to internationally recognized objectives:

General safety: Individuals, society and environment shall be protected by establishing and maintaining an effective defence against hazards. This objective is the same for all nuclear installations [88IAE].

No-evacuation: A demonstration shall be provided that the safety characteristics of fusion, together with the safety approach based on them, limit the hazards from in-plant events such that there is no technical justification for public evacuation according to IAEA recommendations [96IBS].

Waste minimization: Radioactive waste masses, volumes and radiotoxicity shall be reduced to the largest extent possible.

5.6.3.2 Safety principles

The fundamental safety principles are:

– Exposures to hazards are kept as "As Low As Reasonably Achievable" (ALARA), economic and social factors taken into account.
– Passive safety features receive special emphasis. They are based on natural laws, properties of materials and internally stored energy.
– "Defence-in-depth" is applied. This general concept is described in [88IAE, p. 13] and [96IAE1] as follows: "… All safety activities, whether organizational, behavioral or equipment related, are subject to layers of overlapping provisions so that if a failure should occur it would be compensated for or corrected without causing harm to individuals or the public at large. This idea of multiple levels of safety provision is the central feature of defence-in-depth, and it is repeatedly used in the specific safety principles that follow". The most important specific principle is the establishment of three sequential levels of defence, "prevention", "protection" and "mitigation". Fusion development gives first priority to "prevention".

5.6.3.3 Criteria and guidelines

Safety criteria are necessary for regulatory approval, but detailed ones can only be set in the context of specific site countries. A framework is provided by dose limits, event categories and classification of radioactive materials for which recognized recommendations exist.

Dose categories commonly used are "chronic dose" from normal operation radioactivity releases with continuous exposure and 50-year dose commitment, "chronic dose" from accidental releases with 50-year exposure and 50-year dose commitment, and "early dose" from accidental releases with 7-day exposure and 50-year dose commitment. Both occupational (i.e. plant staff) and public exposure are addressed by ICRP and IAEA documents [90 ICR, p. 40, p. 45, Table 6], [96IBS, p. 91-93] which recommend limits as follows:

– 1 mSv/year (averaged over five years) for public exposure,
– 5 mSv/year (maximum in one year) for public exposure,
– 20 mSv/year (averaged over five years) for occupational exposure,
– 50 mSv/year (maximum in one year) for occupational exposure.

Dose criteria are also recommended with regard to evacuation which is a temporary countermeasure, possibly taken to minimize radiological effects due to early exposure at short notice but usually for a limited time. The related guidelines are expressed by early doses to the public. Values in the range 50 to 100 mSv are set with the understanding that the potential for the occurrence of such doses would trigger the consideration of evacuation but does not mandate it. Perspectives for this guideline are provided in [96IBS] by recommending "50 mSv of avertable dose in a period of no more than 1 week" as the "generic optimized intervention value for temporary evacuation" and by the footnote "In some countries a value of 100 mSv of avertable dose is considered to be the more realistic level for temporary evacuation". These values of avertable dose refer to "the average over suitably chosen samples of the population, not to the most exposed (i.e. critical groups) of individuals". "No evacuation" is a central objective of the EU Fusion Programme and is also applied to ITER.

It can be expected that the amounts of radioactive material which eventually will remain as radioactive "waste" will be determined by "clearance", a process for which criteria have been recommended by the IAEA in [96IAE2]. Clearance means that materials, in general mixtures of various isotopes, after having fallen below the "clearance levels" (specified in terms of Bq/g or Bq/m^2) should no longer be treated as radioactive. Either, the doses caused by them are "trivial" (i.e. less or equal to 10 μSv/year) according to IAEA or their specific activities lie in the domain of natural radioactivity. The isotope-by-isotope lists of clearance levels in presently emerging national regulations are equal or similar to the "derived unconditional clearance levels" recommended in [96IAE2, Table I, p. 11].

5.6.3.4 Implementation of safety

The confinement of hazardous materials is the fundamental safety function. It is provided by "barriers" which can be actual barriers or the matrix of solid materials retaining radioactive or toxic substances. Releases most significantly occur upon breach of barriers or by heating of materials to high temperatures. The design is graded to account for the differences in magnitude, radiotoxicity and toxicity of the enclosed inventories, and applies redundancy, diversity, separation, independence and testability. Typical barriers are vacuum equipment (such as plasma vessel and cryostat), coolant pipework, tritium equipment and rooms (with de-tritiation systems and low leak rates). Ancillary functions protect the confinement:

– Fusion power shutdown protects against local softening or melting of structures and cooling pipework due to heating if active cooling is lost.
– Heat removal protects against overheating, evaporation and melting.
– Control of coolant enthalpy protects against component rupture and release of coolants, in particular from the in-vessel components and from the superconducting magnets.
– Control of chemical energy protects against thermal and mechanical threats to the confinement by, in particular, minimizing hydrogen production during accidents and release of chemical energy as heat; fusion power shutdown is important in this context to limit the temperatures of plasma-facing components in the course of accidents.
– Control of magnetic energy protects against failures that can mechanically or thermally degrade adjacent confinement barriers.
– Monitoring and control provide information on operational events and accidents, and on the performance of the related safety functions.
– Active, engineered safety systems, in addition to the inherent and passive safety features, implement the safety functions required. These systems enhance safety and contribute to implementing the ALARA principle.

To protect plant staff, design and administrative measures will be such that they comply with recommendations by ICRP and IAEA. A typical "radiation protection program" with regard to "occupational safety" aims at:

– prevention of acute over-exposures;
– prevention of occupational doses over legal limits;
– maintenance of staff doses "as low as reasonably achievable" (ALARA);
– minimization of the spread of contamination.

The amount of radioactive materials is minimized by materials selection and shielding against neutrons. It is important to discriminate between the radioactive materials generated and that material fraction which eventually will remain as "waste" needing repository disposal. Material selection aims at:

– no generation of activated materials which require active cooling for decades;
– decay of the integral radiotoxicity to low levels on a "human" time scale, typically 30 to 100 years;
– technical feasibility of recycling and clearance of the dominant fraction of the radioactive materials on a "human" time scale;
– no necessity to guarantee "geological" ground water return times for the ultimately remaining waste.

Recycling of materials is very attractive and attaches a key role to the development of materials with low activation, including the minimization of those "commercial impurities" which can spoil the handling characteristics by high, long-term contact dose rates.

5.6.4 Plant models

Detailed safety assessment for future fusion power plants has been started in the EU by the Safety and Environmental Assessment of Fusion Power (SEAFP). Two plant models were set up on the basis of DT fusion in a steady state tokamak. Both models have the same basic geometry and dimensions. The materials considered are meant as typical examples for candidate materials which are presently available but need significant development to become fully suited for fusion power plants.

The models use low activation materials (the vanadium alloy V5Ti and a reduced activation martensitic ferritic steel) and minimize the overall tritium inventory to around 2 kg. In setting up the models, working hypotheses had to be introduced for still unresolved problems of plasma physics, reactor materials and component design. The hypotheses range from plasma heating by electromagnetic waves via radiative power exhaust in the divertors to breeding blankets with an endurance of typically 5 full power years [95SEA, Sect. 4].

The scope of assessments has been broadened in subsequent studies [99SEA2, 01SEI]. The latter applies a "top-down" approach to safety by starting from the key issues "accidental releases" and "long-term repository disposal of radioactivity", and concentrates on materials and design features which would allow a favorable approach to these issues.

5.6.5 Safety-relevant inventories

The hazard potential of a fusion power plant is indicated by its energy and radioactivity inventories. Energies have a potential to initiate and drive accidents. Radioactive materials are the source of doses from normal operation, accidents and waste management. The actual doses, though related to the inventories, are dominated by design provisions, failure modes, and the ultimate mobilization and dispersion of radioactivity.

The most significant energy inventories are associated with the in-vessel fusion fuel, the potential chemical reactions of cooling water or air with in-vessel armor materials (such as beryllium and tungsten), the magnetic field coil systems, the plasma thermal energy, the plasma magnetic energy, the coolant enthalpy, and the nuclear decay heat after plasma shutdown. Overall, the fusion reactor inventory is at least five orders of magnitude below the one in a fission power reactor core of similar power rating.

Tritium inventories depend very much on technical details. For future fusion power plants, the total site inventory has been estimated to range from 2 to 5 kg. The tritium inventory which may be mobilized inside the plant by most severe in-plant accidents is estimated to be of the one kg order.

Fusion neutrons activate the materials surrounding the plasma. This activation is most simply expressed in terms of "radioactivity", i.e. the total number of nuclear disintegrations per second (measured in Bequerel, Bq). The dominant part (typically around 90 %) of the activation resides in the plasma-facing components, including the blanket. By order of magnitude, the radioactivity inventories at final reactor shutdown range from 10^{19} Bq (vanadium alloy structures) to 10^{21} Bq (steel structures).

In the context of radioactivity, it is important to note that radiological consequences are actually related to "radiotoxicity" which is expressed by doses (measured in Sievert, Sv) committed to the body by the decay of incorporated "radioactivity". Doses are related to radioactivity, isotope by isotope, by "dose conversion factors" (Sv per Bq). The total dose due to the hypothetical incorporation of the activated reactor components accumulated over the whole plant life is an "inventory" indicating the radiotoxicity potential. It has been compared for different fusion reactor designs, fission reactors and ashes from coal-fired power plants (coals contain small quantities of uranium, thorium and their daughter products). These potentials, normalized so that all plants have delivered the same electrical energy, show that the fusion radiotoxicity potential at final reactor shutdown is about an order of magnitude lower than the one of fission. From there, the fusion values decay within 10 to 500 years (depending mainly on reactor materials and dose types) to values broadly in the range of coal ashes. After 100 years, fusion radiotoxicity is several orders of magnitude lower than that from fission by that time.

5.6.6 Normal operation effluents

During normal operation, radioactive substances will be released as gaseous and liquid effluents. Tritium effluents originate in particular from the first wall/blanket, divertor and plasma vessel cooling loops, and from the fuel cycle equipment. At present, input for estimates is provided by civil tritium laboratories and by commercial facilities such as tritium removal facilities and heavy water fission power plants. Volatile activation products are generated by neutron reactions with plasma-facing armors, coolant pipework, coolants, cover gases (such as nitrogen and argon), and with the impurities therein.

Owing to the many details involved, normal operation effluents will be accessible to rigorous assessment only when reactor-like devices have become operational. A scale has already been set by the numbers estimated in the course of the detailed ITER design [01GSR2] which incorporates the features necessary to ensure that the environmental impact during normal operation will be low. This includes confinement barriers, and air and water de-tritiation and filtration systems. For a "generic" site, the estimated doses are less than 1 % of the natural background radiation which ranges from 2 to 5 mSv in the European countries.

5.6.7 Personnel safety

The complex geometry of a fusion reactor together with the associated maintenance operations makes safety of the plant personnel (often named "occupational safety") a key issue. The attempts to assess occupational safety for future power plants have shown that credible analyses need as an input virtually all details of design and plant operation.

The detailed work for ITER has provided insight in occupational safety [01GSR4]. Maintenance procedures and man-power estimates have been developed together with the identification of the highest exposure areas. This information was used together with estimated dose rates due to external radiation (including deposits of activated corrosion products) and internal radiation (from tritium in air) to determine occupational exposure, and to examine the potential for reduction. As expected, the doses to personnel are dominated by maintenance operations. The current assessment of all major systems yields annual doses below 5 mSv (individual) and 0.5 person-Sv (collective).

In this context, it is particularly important to note that ITER is not fully representative of commercial power plants since the use of austenitic stainless steel instead of reduced activation steels or potentially favorable non-steel alloys together with cooling by water are not optimal with regard to occupational safety.

5.6.8 Accidents

A major part of the potential accidents are grouped around the cooling systems. The pressure inside the plasma vessel is low during normal operation and is limited by passive release systems to typically 2 to 5 bar in case of an accidental coolant ingress. Plasma vessel and cryostat have many penetrations (for plasma heating, fueling, control, diagnostics, components handling) which normally are closed or enclosed by barriers but can connect in-vessel tritium and activated dust to surrounding rooms in case of barrier failure. In broad summary, the initiators of accidents are as follows:

- *Plasma*: Transient overpower, instability, asymmetry, runaway electrons, loss of control.
- *Plasma vessel*: Loss of vacuum, i.e. loss of tightness.
- *Cooling system*: Loss of coolant flow, in-vessel loss of coolant, ex-vessel loss of coolant.
- *Fuel cycle*: Loss of component tightness, combustion of hydrogen isotopes.
- *Magnets*: Off-normal mechanical loads, loss of superconductivity ("coil quench"), electric arcs, propelled parts, water and/or air ingress into the cryostat, expansion of cryogenic helium.
- *Power supplies*: Loss of power; inability to switch off the power.
- *External events*: Earthquake, flood, tornado, aircraft, and explosion.

Many details of accidents have been identified and investigated by safety studies for fusion power plant models and in the course of the ITER work on accidents [01GSR5]. The latter is considered to be largely prototypical of future fusion power plants. To ensure to the extent possible that all aspects of plant operation have been considered, two fundamentally different approaches have been applied for identifying initiating events [01GSR7]: “Bottom-up” (starting upwards from the component level) and “Top-down” (starting downwards from the ultimate consequences of faults). The former systematically catalogued all potential faults in components and considered the conceivable consequences. In contrast, the top-down approach started at the plant level and took a global view of ultimate consequences. By considering the abnormal events which would have to occur to realize these consequences, again a catalogue of events was produced in terms of component faults. These studies have identified the:

– radioactive inventories at risk,
– confinement barriers challenged,
– mitigating systems that must fail for a hazardous plant state to occur,
– release pathways.

The overall result is a set of “reference events” (often named “design-basis accidents”), consisting of an initiating event, all consequential failures and assumed aggravating failures (additional independent failures in mitigating systems, for example). The events were analyzed by using detailed quantitative modeling and system simulation codes. The analyses for a generic site yield doses to the public that are mostly below, sometimes comparable to the average doses per year due to the natural background radiation.

The safety domain addressed by the assessment of ultimate safety margins with regard to accidents is commonly characterized by accident occurrence rates less than 10^{-6} to 10^{-7} per year.

Given the fail-safe nature of the fusion burn, the modest mobilizable radioactive inventories, the multiple layers of confinement, and passive means for decay heat removal, it is expected that fusion reactor safety will exhibit little or no dependence on active safety systems. In spite of this benign ultimate features it is good practice to include bounding considerations in safety studies. Notions used in this context are “ultimate safety margin”, “beyond-design-basis accident”, “hypothetical accident”, “residual accident”, and “cliff-edge effect”. Their assessment by reactor safety studies and ITER work have shown that “confinement bypass events” (caused by the penetrations through the first and second confinement barriers) are the most challenging ones. This fact calls for paying particular attention to the details of confinement. For ITER, ultimate safety margins were examined by analysis of hypothetical events, assuming more and more failures to occur [01GSR6]. These analyses have shown that it requires an almost inconceivable combination of failures to lead to a significant release of radioactive material. There is no single component whose failure would lead to very large consequences and there is no single event that can simultaneously damage the multiple confinement barriers.

A typical bounding consideration in [95SEA] dealt with the release of the mobilizable tritium inventory, estimated to be about 1 kg. The consequence was expressed by the early dose to the most exposed member of the public at 1 km distance from the groundlevel release point. This dose would be about 450 mSv for the most hazardous form of tritium (HTO) and a release duration of one hour. This exceedance of the no-evacuation guideline results from the assumption of worst case meteorological conditions (stable weather, wind at low speed in one direction) and pertains to a small geometrical sector. It extends a few kilometers downstream from the release point and is narrow so that an area of less than one square kilometer would be affected [97Edl]. For slightly less conservative assumptions with regard to wind direction (assuming that the wind “meanders”), the affected area would be larger but the dose would fall below the evacuation guideline.

There may exist energetic external events such as an earthquake of hitherto inexperienced magnitude. For these “residual accidents” there is no upper bound to the energy and almost all credit for the confinement may be lost owing to barrier damage. Such extreme events let expect that the increment of harm added by an associated fusion plant accident would not be very significant given the harm directly attributable to the external event. Nevertheless, such events are not excluded from consideration, rather consequences are estimated as exemplified above by the assessment of a 1 kg tritium release under adverse conditions.

5.6.9 Radioactive materials

It is important to discriminate between the arisings of "radioactive materials" (due to fusion operation) and that material which ultimately will remain as "waste" needing long-term repository disposal. It is also important that waste assessments account for the "commercial impurities" in the reactor materials. The dominant fraction of neutron-induced radioactivity is generated in the components near the plasma which will be replaced several times during plant life. Plant decommissioning will release additional radioactive masses, dominated by nuclear shields, plasma vessel and magnets.

The EU Fusion Programme highlights the importance of the issue of radioactive waste by stating that a "burden for future generations" and a "geological timespan" for isolation from the environment have to be avoided [90Col]. Present analyses suggest that each generation will leave some radioactive waste for a few generations but it also appears that significant burdens beyond this time scale can be avoided by materials development and dedicated design of fusion power plants.

The mass scale for the amounts of activated materials from future fusion power plants was set by the estimates in [95SEA] which range from about 60 000 to 90 000 tons. The higher numbers apply if the heavy metal lead is used for neutron multiplication in the blanket.

An upper-bound strategy in [95SEA] has assumed that all radioactive material would be disposed "geologically", most of it in "shallow" repositories (typically 50 m deep). Prior to final disposal, these materials would reside in interim storage for up to 50 years. The final repository volumes required would be about 40 000 m^3. The masses of radioactive materials from the three reactor models in the subsequent study [01SEI] lie in the range quoted above.

Since the upper-bound strategy may be unnecessarily conservative, also recycling and clearance were considered. In [01SEI] an extreme approach was assessed by subdividing the activated materials into "permanent disposal", "complex re-cycle", "simple re-cycle", and "non-active" (i.e. "clearable"). The material fraction which could be cleared ranges from about 25 to about 40 %, and only very few percent of the "radioactive materials" would remain as "waste" after a decay time of typically 50 years. It is prudent, though, to expect for this approach, which would need very fine subdivisions, that typically 10 % of the radioactive material will eventually remain as waste. This reservation is made with regard to the possible variance of dose rate criteria and also to account for the limited accuracy of assessing already today the complex geometry from the viewpoints of activation and waste.

On economic grounds it might be decided to not recycle, rather waste would go to a geologic repository since shallow-land disposal is not regarded as an option in Europe for unclearable material. The repository siting and design are expected to not be extremely demanding since the total radiotoxicity of the material, accumulated over the plant life is much lower than for fission equivalents.

For ITER, the issue of radioactive materials, decommissioning and waste is carefully considered but it is obvious that ITER is not fully representative of future fusion power plants in this regard. The prime reason is the use of nickel-based austenitic stainless steels for structures and shields which entail long-lived isotopes (in particular Ni-59, Ni-63, Mo-93 and Nb-94).

A plausibility check for the masses from the reactor studies is, however, provided by the 83 000 tons of radioactive material estimated for the 1998 ITER Design [97NSR2]. With its fusion power of 1500 MW, this device is at power reactor scale. The waste mass after 60 to 100 years of decay and application of clearance according to [96IAE2] is 25 000 tons, i.e. 30 % of the initial radioactive mass. This latter number has to be used with prudence since neutron flux and fluence in ITER are much lower than in a future power reactor. Waste studies were repeated for the 2001 ITER design [01GSR3]. Emphasis was put on potential waste reduction by clearance according to [96IAE2]. These studies provisionally assume that radioactive material not allowing for clearance after a decay time of up to 100 years is "waste" and show that the waste amounts to about 20 % of the radioactive materials. A reduction of the decay time to 30 years would double this percentage.

Tritium will probably reside in significant concentrations in components near the plasma. For them, clearance can anyway not be expected because of the high activation, rather they will be disposed in shallow geological repositories after de-tritiation to the extent feasible. This attaches an important role to the present development of industrial de-tritiation methods [95Boi, 00Ros] in the frame of conventional nuclear technology.

5.6.10 Proliferation

The proliferation concern is related to weapons grade materials and technological knowledge. Pure fusion reactors (reactors which do not comprise fission components) do not use or generate fissile material. They are, however, prone to proliferation by the potential diversion of tritium and fast neutrons. Weapons related technology adds in the case of inertial confinement fusion. The proliferation aspects are being considered with regard to the "Treaty on the Non-Proliferation of Nuclear Weapons" (NPT) [70NPT], the "Euratom Treaty" [57EUT] and the "Comprehensive Nuclear-Test-Ban Treaty" [96CTB].

The NPT, with the full scope of the IAEA safeguards, governs the transfer of all nuclear materials, equipment and related technology. Nevertheless, experience has shown that it is impossible to avoid with certainty the diversion of nuclear materials and technology. The aim of the technical and institutional measures is the creation of as many barriers against diversion as possible. Above all, the measures are designed for timely detection by international authorities such as the IAEA.

In principle, the fusion fuel cycle can be modified to produce tritium for nuclear weapons but this tritium can currently be generated in fission reactors by rather simple methods. The complex technology of fusion weaponry is not related to magnetic confinement but there are links to fusion by inertial confinement. It is also possible, in principle, to breed fissile material by the fusion neutrons. Both uranium or thorium ("fertile materials") could be introduced to breed Pu-239 or U-233. Uranium is the more convenient route since one ton of U-238 would allow to breed a "significant quantity" (about 10 kg according to IAEA) of Pu-239 in one year, whereas twice as much Th-232 would be required [95SEA].

The inherent absence of fertile and fissile materials in a pure fusion device offers a far more clear-cut detection criterion than is the norm in fission safeguards. There it is necessary to detect small discrepancies in large inventories. Input side monitoring would be especially effective, since it is feasible to reliably detect kilogram quantities of fertile material although only tens to hundreds of kilograms would be significant. Detection of the breeding of fissile material in the blanket, while this is in the torus, is not technically credible. Detecting on the output side the removal of fissile materials would be feasible by the use of materials-monitoring measures covering the limited number of transfer routes. Verification of the reactor design and construction is an essential early activity. Repeated verification to ensure that no significant modifications are made will also be necessary.

Inherent features of magnetic confinement fusion which are relevant in the proliferation context are:

- The plasma vessel, its extensions and the primary cooling pipework will be very tight to ensure the extreme vacuum conditions necessary for plasma operation.
- The protection of staff and public against radiological exposure from tritium and volatile activation products will be provided by at least two confinement barriers around any significant inventory of radioactivity.

The removal of tritium would imply breaking all confinement barriers around the inventories. The use of fusion neutrons to breed fissile materials would imply that the fertile materials be brought very close to the plasma by breaking all barriers, including the first high-vacuum barrier around the plasma.

After construction of a large fusion device, all design information and flow sheets will be available "as built". Compliance of device operation with the flow sheets and the related safety and quality assurance measures should be ensured by personnel not forming part of the operation staff. Typical activities in this context are:

- sampling at suitable locations and analysis of the samples to ensure that tritium is actually routed as foreseen, including possible waste streams;
- application of confinement measures (such as seals) to ensure that no tritium is routed along paths which do not comply with the flow sheets;
- wipe tests at locations where tritium removal is conceivable and analysis of the samples;
- wipe tests with regard to fertile and/or bred materials at the relevant locations and analysis of the samples.

5.6.11 Conclusions

The safety analyses used for this article can neither cover all details nor can they foresee all future technicalities. Dedicated efforts, though, have been made to remain always on the conservative side to provide confidence in the present conclusion that fusion power is attractive with regard to safety and environmental characteristics. The reasons are the inherent absence of significant power runaway, the moderate magnitude of energies, powers and power densities, the existence of passive energy removal mechanisms, the relatively small inventories of mobilizable radioactivity, and eventually the limited radiotoxicity and lifetime of most of the radioactive materials. The positive judgment does not result from just one point assessment, rather it is being based on an increasingly firm footing by the past and ongoing studies.

With regard to the implementation of safety and environmental protection, there is always the need to draw a borderline between the hazards which inevitably must be covered by the design and issues which may be allowed to remain beyond. Fusion lets expect that there do not exist any steeply increasing hazards, so called "cliff-edge effects", when certain borderlines are crossed. The perception of what can or shall be covered by engineering and what may remain beyond depends to a large extent on the public who want to consume energy but nevertheless have reservations with regard to nuclear energy sources.

To gain insight in public perceptions on fusion, socio-economic research has been initiated by the EU Fusion Programme. In this context, discussion groups were formed, basic information on fusion was provided to these groups, and eventually moderator-led group discussions took place [99Hoe]. Overall, these discussions have shown that there exists scepticism with regard to fusion, but that there is not the same strong rejection as against "atomic power" (i.e. conventional fission). Fusion is considered to be the better nuclear option.

The public is most interested in the proof that catastrophic events and the need for waste disposal on geological time scales do not exist. This supports the selection by the EU Fusion Programme of the two "central" points made in [90Col]:

– "It must be clearly shown that the worst possible fusion accident will constitute no major hazard to populations outside the plant perimeter that might result in evacuation."
– "Radioactive wastes from the operation of a fusion plant should not require isolation from the environment for a geological timespan and therefore should not constitute a burden for future generations."

5.7 Fusion resources

[T. Hamacher]

5.7.1 Introduction

Fusion is considered as a practically unlimited source of energy. This rationale was one of the main motivations from the very beginning of fusion research. The argument was mainly based on the abundance of the fusion fuels – lithium and deuterium – and the very low fuel requirements [60Gla]. Table 5.6 shows the annual deuterium and lithium consumption for a typical plant design.

Beside the fuel numerous other materials are necessary to construct and operate the plant [76Har, 94Wat]. The long-term availability of these materials will be discussed in this article. Only those materials special for fusion are considered.

Table 5.6. Annual fuel requirements of a 1 GW (el) fusion power plant.

Deuterium	110 kg
Lithium	380 kg

Currently the world electricity demand is 13 666 TWh/a (1996) [00Ene]. Most of this demand is supplied by fossil fuels, 17 % is supplied by nuclear and another 17 % by hydro power. A doubling of the world electricity demand in the course of the 21st century would result in an demand of 25 000 TWh/a in the year 2100. This assumption is rather moderate. If a thousand fusion plants of 1 GW (el) capacity and 75 % availability were installed at that time a quarter of the demand could be supplied by fusion. Therefore all the material and fuel requirements discussed below need to be multiplied by a factor 1000 to come to a realistic picture of what an intense fusion economy would mean.

The data on reserves reported below are quoted from two different sources: the Mineral Commodity Summaries 2000 [00USG] from the U.S. Geological Survey and a report of the Bundesanstalt für Geowissenschaften and Rohstoffe on materials for fusion [89BGR] published in 1989. The definitions of reserves and reserve base in the report of the U.S. Geological Survey are as follows:

– *Reserves*:
  that part of the reserve base which could be economically extracted or produced at the time of determination. The term reserves need not signify that extraction facilities are in place and operative. Reserves include only recoverable materials.
– *Reserve base*:
  that part of an identified resource that meets specific minimum physical and chemical criteria related to current mining and production practices, including those for grade, quality, thickness, and depth. The reserve base is the in-place demonstrated (measured plus indicated) resource from which reserves are estimated. It may encompass those parts of the resource that have a reasonable potential for becoming economically available within planning horizons beyond those that assume proven technology and current economies. The reserve base includes those resources that are currently economic (reserves), marginally economic (marginal reserves), and some of those that are currently subeconomic (subeconomic resources).

Both categories do still not cover the whole resource. Figure 5.24 shows the reach of numerous materials necessary to construct a fusion plant. Reach is defined as the ratio of reserve and current annual production. If the reach of a commodity exceeds several decades further exploration is uneconomic. The size of a reserve is therefore strongly coupled to the current demand.

Higher prices and advanced technology might make more resources available with time. Most of the materials discussed below are in principle much more abundant than indicated. However, ore grade or ore accessibility might make a further use of these resources practically impossible.

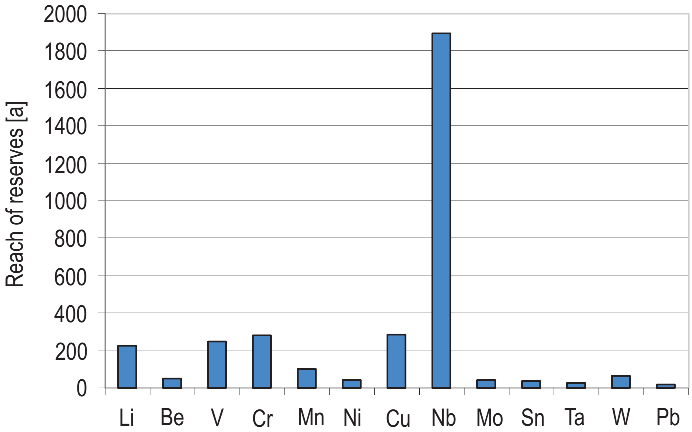

Fig. 5.24. Reach of numerous materials necessary to construct a fusion plant. The reach is the ratio of reserves and current annual production.

5.7.2 Fusion plant material requirement

The outstanding materials mass-wise necessary to construct a fusion plant are concrete, rebar and steel [98Sch]. In the order of one million tons of concrete and a hundred thousand tons of rebar and steel are necessary. These materials are common for nearly all human activities and epecially necessary to construct any kind of energy conversion plant. Therefore these materials will not be discussed further. Only those materials specific for fusion are considered.

Fusion plants do not yet exist. Information on design details like the kind and amount of materials used need to be extracted either from information on currently operating or planned experiments or on fusion plant models. The data for this analysis were extracted from the models elaborated for the European safety study Safety and Environmental Assessment of Fusion Power (SEAFP) [95Rae, 94Wat]. Two plant models were designed: one with a vanadium alloy as structural material, helium as coolant and Li_2O as breeder material (model 1), and the second with low-activation martensitic steels as structural materials, $Li_{17}Pb_{83}$ as breeder and water as coolant (model 2). Two variations of model 1 were elaborated: variant A where the beryllium armor of first wall and divertor were replaced by tungsten, and variant B where natural lithium was used in the blanket with beryllium as neutron multiplier. Table 5.7 and 5.8 show the materials for the different plant models.

Table 5.7. Materials for the plant model with vanadium alloy as structural material and helium as coolant.

Material	Quantity [t]		
	Model 1	Variant A	Variant B
W	—	658	—
Be	75	—	2978
V5Ti	10806	10806	10806
SS316	23048	23048	23048
Li_2O	—	—	1895
$^6Li_2O$	1895	1895	—
OPSTAB	17199	17199	17199
Pb	1470	1470	1470
B_4C	68	68	68
Cu	2491	2492	2491
Sn	37	37	37
Nb_3Sn	180	180	180

Table 5.8. Materials for plant model 2, with martensitic steel as structural material and a lithium-lead eutectic as breeder. Water is used as coolant.

Material	Quantity [t]
Be	75
La12	14773
SS316	23048
$Li_{17}Pb_{83}$	33194
OPSTAB	17199
Pb	1470
B_4C	68
Cu	3292
Sn	37
Nb_3Sn	180

5.7.3 Fusion fuels

Fusion fuels envisaged at least for the first phase of fusion are deuterium and tritium. At realistic plasma temperatures, the fusion cross section of these hydrogen isotopes is orders of magnitude larger than possible alternative reactions like deuterium-deuterium.

5.7.3.1 Deuterium

Deuterium is a hydrogen isotope. In terrestrial hydrogen resources, like sea water, deuterium makes up for one part in 6700. The oceans having a total mass of 1.4×10^{18} t contain 4.6×10^{13} t of deuterium. Given the above-mentioned consumption rate, fusion could go on for several million years.

The technology to extract deuterium from water is mature. One of the main applications is the production of heavy water for heavy-water moderated fission reactors. Existing plants can produce up to 250 t/a of heavy water, this means a production of 50 t/a of deuterium. This would be enough to supply deuterium for 500 fusion plants with 1 GW (el) capacity. Obviously deuterium puts no burden on the extensive use of fusion.

5.7.3.2 Lithium

In the flux of the fusion neutrons tritium is bred from lithium. Tritium is again a hydrogen isotope. Lithium is found in nature in two different isotopes, ^{6}Li (7.4 %) and ^{7}Li (92.6 %). Tritium is produced from lithium in the neutron flux by the following reactions:

$$^6\mathrm{Li} + \mathrm{n} \rightarrow \mathrm{T} + {}^4\mathrm{He} + 4.8\ \mathrm{MeV}, \tag{5.41}$$

$$^7\mathrm{Li} + \mathrm{n} \rightarrow \mathrm{T} + {}^4\mathrm{He} + \mathrm{n} - 2.5\ \mathrm{MeV}. \tag{5.42}$$

Since the second reaction is endothermic only neutrons with an energy larger than the threshold can initiate this process. In most blanket concepts the reaction with ^{6}Li dominates, but to reach a breeding ratio exceeding one the ^{7}Li content might be essential.

Lithium can be found in:

- salt brines, concentrations range from 0.015 % to 0.2 %;
- minerals: spodumene, petalite, eucrypotite, amblygonite, lepidolite. Ore grades vary between 0.6 % to 2.1 %;
- sea water, the concentration in sea water is 0.173 mg/l (Li^+).

The land-based reserves (quoted from two different sources) are shown in Table 5.9.

While the annual consumption of lithium in a fusion plant is small, as given in Table 5.6, the lithium inventories in the blankets are much larger [94Wat, 81Bue]. At least several hundred tons of lithium are necessary to build a blanket. It is expected that most lithium can be recovered and reused, although radioactive impurities like tritium will complicate the handling.

No detailed concept for recovering lithium was elaborated so far. But the following estimate should demonstrate that the lithium supply is a minor problem in contrast to the construction of the plant. Lithium can be bought today for around 17 EUR/kg. The blanket containing 146 t of lithium needs to be replaced five times in the life of a fusion plant, which would amount in a financial effort of 12 000 000 EUR which is orders of magnitude lower than the capital necessary to construct the plant.

Beside the land-based resources lithium is solved in sea water. The average Li^+ concentration in sea water is 0.173 mg/l [81Foe], leading to a total amount of 2.24×10^{11} t of lithium in sea water. Techniques to extract lithium from sea water were already elaborated [96Miy]. The energy consumption for extracting lithium from sea water is given in [97Tok].

For model 1 and model 1 A the current land-based lithium reserves would be completely depleted if a thousand plants were constructed at a time. However, the ultimate lithium resources in sea water are practically unlimited.

5.7.4 Construction materials

5.7.4.1 Neutron multipliers (beryllium and lead)

Every fusion reaction consumes one tritium particle and produces one neutron. Every neutron needs to breed one new tritium particle to keep the balance between burned and produced tritium. In the reaction with ^{6}Li, which is expected to be the dominant one, the neutron gets lost. Since other losses like geometry losses and absorption in the structural materials can not be avoided it appears to be necessary to multiply the neutrons by (n,2n) reactions. Possible materials for this process are beryllium and lead. The typical reaction for beryllium is:

$$n + {}^9\mathrm{Be} \rightarrow 2\,n + 2\,{}^4\mathrm{He}. \tag{5.43}$$

Roughly 3000 t of beryllium would be necessary in the lifetime of a fusion plant if beryllium was used as neutron multiplier. The beryllium reserves are shown in Table 5.9. Transmutation of beryllium will ke place but only in small amounts. World reserves of beryllium are not sufficient to supply the inventory even for the first thousand fusion plants. However, as described above, beryllium is hardly used today. No extensive exploration took place.

Neutron multiplication could also be done by adding lead to the blanket. The commonly followed path is the use of a $Li_{17}Pb_{83}$ eutectic. Roughly 35000 tons of lead would be necessary over the lifetime of a fusion plant. Lead reserves account for 64000000 t, the annual lead production reached 3100000 t in 1999 [00USG]. The production of lead not related to fusion will have used up the reserves of lead before fusion even comes into operation. More reserves will be made available by new exploration and recycling. The short reach of lead indicates that lead supply might fall short in the future. The reserves are shown in Table 5.9.

Both possible neutron multipliers, lead and beryllium, have only limited reserves. In case of beryllium this is mainly because beryllium is hardly used today. In case of lead it reflects a real limitation of resources.

5.7.4.2 Niobium for magnets

Super-conducting magnets are unavoidable in magnetic confinement fusion. Currently only superconductors based on niobium are available (Nb_3Sn, NbTi). Roughly a hundred tons of niobium are necessary to construct a fusion plant. The annual niobium production was up to 18500 t in 1999, the global reserves are 3500000 t [00USG] (see Table 5.9).

Even the current niobium reserves would not really be challenged by an intense fusion economy.

5.7.4.3 Vanadium as structural material

Vanadium alloys are one choice as low-activation structural materials [95Rae]. Taking into account the replacement during reactor life, 10000 tons of vanadium are necessary for one plant. Reserves accounted for 10000000 t in 1999. The world production was 40000 t in 1999.

A thousand fusion plants constructed with vanadium would consume all current reserves. Vanadium is very well suited for recycling.

5.7.4.4 Wall armors

Wall armors can be tungsten and beryllium. The plasma-facing components, first wall and divertor, need to be replaced several times in the life of a plant. Material requirements are increased by factors between five and seventeen. Roughly 60 tons of beryllium or 600 tons of tungsten would be required. Beryllium is discussed in Sect. 5.7.4.1. Tungsten reserves account for 2000000 t, the world production in 1999 was 31300 t [00USG]. The tungsten demand of an intense fusion economy could be supplied by the current reserves for a first generation of plants.

5.7.4.5 Copper

Copper will be applied in heat sinks at places of high thermal loadings and as stabilizers in the magnets. Two to three thousand tons of copper will be required to build a fusion plant. Copper is needed for numerous applications. The world copper demand is around 12600000 t/a, the reserves were estimated to be 340000000 t [00USG]. The amount of copper that will be recycled is expected to increase. The demand of an intense fusion economy would be a quarter of the current annual production. The reach even at the currently high demand exceeds 200 years. At least for the first generations of fusion plants enough copper will be available.

Table 5.9. Current annual production and worldwide reserves of various fuel and construction materials.

Material	Production [t/a]	Reserve [t] [a])	Reserve base [t] [a])	Reserve [t] [b])
Lithium	15000	3400000	9400000	1106000
Beryllium	344	18000 (Utah only)	—	369000
Lead	3100000	64000000	143000000	75000000
Niobium	18500	3500000	5500000	4124000
Vanadium	40000	10000000	27000000	7500000
Tungsten	31300	2000000	3200000	2800000
Copper	12600000	340000000	650000000	340000000

[a]) Source: [00USG].
[b]) Source: [89BGR].

5.7.5 Operation materials

Beside the fuels other materials are consumed during the operation of a fusion plant. The material which comes out to be most critical from the resource point of view is helium which is necessary as coolant for the super-conducting magnets and for some concepts as coolant in the blankets. In the cryogenic system 47 t of helium are used, and 13.7 t as coolant if helium is used. Helium is recycled but losses are unavoidable. A loss of 0.1 t/month is expected. In total 98.7 t of helium are required over the whole reactor lifetime [94Wat].

Helium is mainly obtained form natural gas fields by liquefaction of the hydrocarbon components and separation of the gas phase form the hydrocarbon liquid. In a second step helium is separated from the nitrogen content of the remaining gas. Therefore this resource is strongly coupled to the natural gas resources and these are expected to decline at the time fusion will start operation. The only way to save this resource for fusion would be to recover it today and store it until the operation of fusion as power source will start.

Another source of helium is the atmosphere, with a helium content of 5 ppm. Helium recovery from the atmosphere is possible but at a much higher cost (roughly 200 times more costly than the recovery of helium from natural gas fields).

It is not clear in as much the helium produced by fusion in the plant can be used.

5.7.6 Energy requirements

One conclusion from the above survey is that fusion fuel – the actual energy carrier – is amply available. This is not the case for all the construction materials. Recycling might be necessary to keep a fusion economy running over a long time horizon. Recycling does again need mainly one resource: energy.

The energy necessary to construct a fusion plant was estimated by different groups in the past [85Bue] and more recently by [98Sch]. Energy requirements for construction turn out to be only a small fraction of the energy released later in form of electricity. The energy necessary to construct the plant were estimated in the latter work to be 3.15 TWh.

5.7.7 Summary and conclusions

The summary of the results is given in Fig. 5.25. The figure shows the ratio of individual elements necessary to construct a fusion plant and the currently available reserves. Especially for materials like beryllium and tantalum which are hardly used today the reserve base is rather small. This is mainly due to a lack of exploration efforts.

Availability of fusion fuels will not put a constraint on the use of fusion even in the very long term.

This is not in the same way true for neutron multipliers and construction materials. Although it will in principle be possible to stretch the reserves quoted above by new technology, limits can be foreseen. Therefore recycling is necessary if an intense fusion economy should be sustained. Recycling and choice of materials should become important design criteria for future fusion plants.

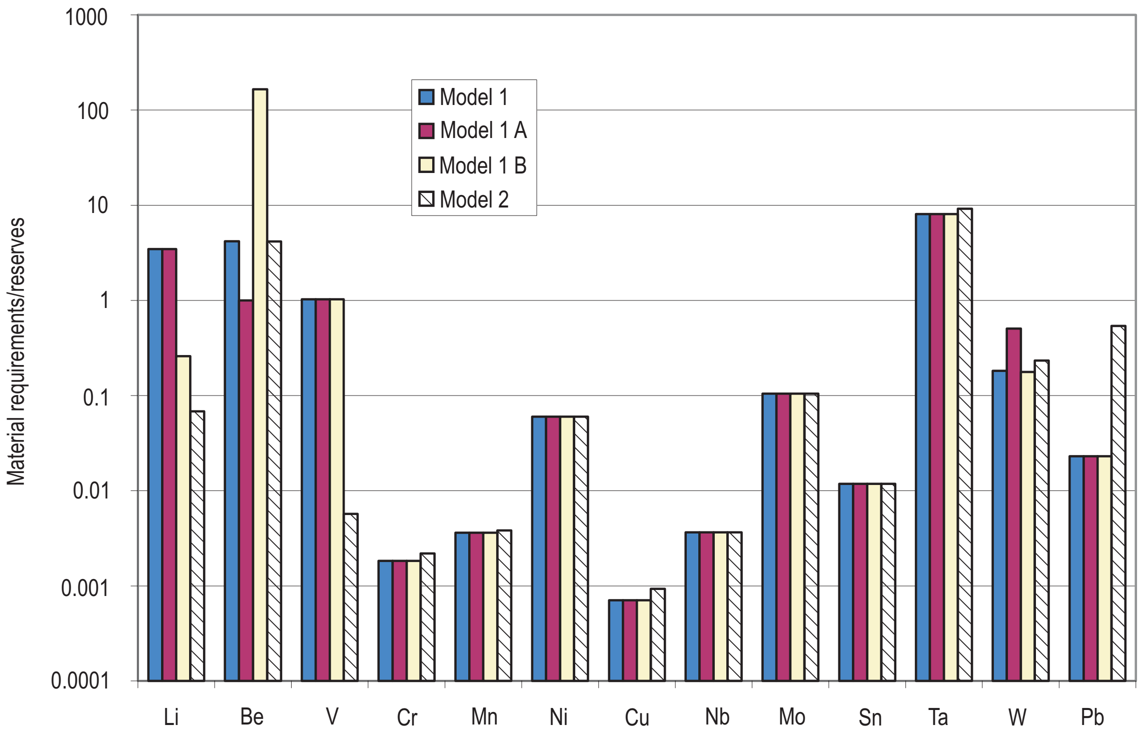

Fig. 5.25. Ratio of material requirements for the construction of a thousand 1 GW (el) fusion plants to the worldwide reserves.

5.8 References for 5

56Spi Spitzer, L.: The Physics of Fully Ionized Gases, Interscience, New York (1956).

57EUT Euratom Treaty; in 1957 Belgium, France, Germany, Italy, Luxembourg and the Netherlands entered into a treaty that established the European Atomic Energy Community (Euratom).

57Law Lawson, J.D.: Some criteria for a power producing thermonuclear reactor, Proc. Phys. Soc. **70** (1957) 6.

58Sak Sakharov, A.D.: in Plasma Physics and Problems of Controlled Fusion, Vol. 1, p. 20, Moscow, AN SSSR (1958) (in Russian).

60Gla Glasstone, S., Lovberg, R.H.: Controlled Thermonuclear Reactions, 1st edition , New York, Cincinnati, Toronto, London, Melbourne (1960).

63Sha Shafranov, V.D.: in Reviews of Plasma Physics, Vol. 2, p. 103, Consultants Bureau, New York (1963).

65Kad Kadomtsev, B.B.: Plasma Turbulence, Academic, New York (1965).

70NPT Treaty On The Non-Proliferation of Nuclear Weapons; NPT was signed at Washington, London, and Moscow, July 1, 1968, entered into force March 5, 1970.

75Kad Kadomtsev, B.B.: Sov. Physics – Journal of Pl. Physics **1** (1975) 295.

76Har Materials Availability for Fusion Power Plant Construction, BNWL-2016, UC-20 (1976).

76Miy Miyamoto, K.: Plasma Physics for Nuclear Fusion, MIT Press, Cambridge, Mass. (1976).

81Bue Bünde, R., in Raeder, J. et al.: Kontrollierte Kernfusion, Stuttgart (1981).

81Foe Förstner, U., Wittmann, G.T.W.: Metal Pollution in the Aquatic Environment, 2nd Ed., Springer-Verlag (1981).

81Sta Stacey, W.M.: Fusion Plasma Analysis, John Wiley & Sons (1981).

81Tel Teller, E. (ed.): Fusion, Vol. 1 + 2, Academic Press (1981).

82Dud Duderstadt, J.J., Moses, G.A.: Inertial Confinement Fusion, Wiley, New York (1982).

82Gho Ghoniem, N.M., Kulcinski, G.L.: A critical assessment of the effects of pulsed irradiation on the microstructure, swelling and creep of materials, Nuclear Technology/Fusion **2** (1982) 165.

83Pit Pitts, J.H.: Cascade: A Centrifugal-Action Solid Breeder Reaction Chamber, Report UCRL-88208, Lawrence Livermore National Laboratory, Livermore CA (1983); also Nucl. Techn./Fusion **4** (1983) 967.

84Che Chen, F.F.: Introduction to Plasma Physics and Controlled Fusion, Plenum Press, New York (1984).

84Gro Gross, R.A.: Fusion Energy, John Wiley & Sons, Appendix C (1984).

84Sta Stacey Jr., W.M.: Fusion: An Introduction to the Physics and Technology of Magnetic Confinement Fusion, John Wiley & Sons, New York (1984) 70.

85Bad Badger, B. et al: HIBALL-II, An Improved Conceptual Heavy Ion Beam Driven Fusion Reactor Study, Report KFK-3840, Kernforschungszentrum Karlsruhe; FPA-84-4, Fusion Power Associates; UWFDM-625, Univ. of Wisconsin, Madison (1985).

85Bue Bünde, R.: The Potential Net Energy Gain from DT Fusion Power Plants, Nuclear Engineering and Design/Fusion **3** (1985) 1-36.

85Jon Jones, P. et al.: Design and Operation of the JET Articulated Boom, Proceedings of the 11th Symposium on Fusion Engineering, Austin, USA (1985).

85Mei See, for example, Meier, W.R., Hogan, W.J.: ICF Reactor Economics: Identifying the high Leverage Design Features, 6th Topical Meeting on the Technology of Fusion Energy, San Francisco, CA, March 3-5, 1985.

87Pos Post, R.F.: Nucl. Fusion **27** (1987) 1579.

86Rae Raeder, J. et al.: Controlled Nuclear Fusion, John Wiley & Sons, Chichester, New York, Brisbane, Toronto, Singapore (1986).

88IAE Basic Safety Principles for Nuclear Power Plants, IAEA Safety Series No. 75 – INSAG-3 (1988).

88Kra Krane, K.S.: Introductory nuclear Physics, John Wiley & Sons, Chap. 14 (1988).

88Tus Tuszewski, M.: Nucl. Fusion **28** (1988) 2033.

89BGR Resources of fuel and other essential materials (including low activation materials) for fusion, Bundesanstalt für Geowissenschaften und Rohstoffe (1989).

89EEF Pease, R.S. et al.: Environmental, Safety-related and Economic Potential of Fusion Power – Main Report by the EEF Study Group, Brussels (December 1989).

89ESE Holdren, J.P. et al.: Report of the Senior Committee on Environmental, Safety, and Economic Aspects of Magnetic Fusion Energy (ESECOM), Lawrence Livermore National Laboratory, Report UCRL-53766 (Sept. 1989), Summary: UCRL-53776-Summary (1987).

89Whi White, R.B.: Theory of Tokamak Plasma, North Holland, Amsterdam (1989).

90Bod Bodin, H.A.B.: Nucl. Fusion **30** (1990) 1717.

90Col Colombo, U. (chairman) et al.: Evaluation of the Community Fusion Programme [1984-1990], Research evaluation – Report No. 45, EUR 13104 EN (July 1990).

90ICR 1990 Recommendations of the International Commission on Radiological Protection, ICRP Publication 60, Pergamon Press (1991).

90Rei Reiter, D., Wolf, G., Kever, H.: Nuclear Fusion **30** (1990) 1241.

91Aze Azechi, H. et al.: High Density Compression Experiments at ILE, Osaka, Laser Part. Beams **9** (1991) 193.

91ITC ITER Conceptual Design Report, ITER Documentation Series No. 18, International Atomic Energy Agency, Vienna (1991).

91May Mayer-Ter-Vehn, J.: Physics of Inertial Fusion **31** (1991) 395.

91STO European Parliament – Scientific and Technological Options Assessment STOA: Controlled Thermonuclear Fusion – Summary of the STOA Fusion Study, Luxembourg (February 1991).

92Bos Bosch, H.-S., Hale G.M.: Nucl. Fusion **32** (1992) 611; erratum Nucl. Fusion **33** (1993) 1919.

92Hog Hogan, W.J., Bangerter, R., Kulcinski, G.: Physics Today **45** (1992) 42.

92Kad Kadomtsev, B.B.: Tokamak Plasma: a Complex Physical System, Institute of Physics, Bristol (1992).

92Lin Lindl, J.D., McCrory, R.L., Campbell, E.M.: Physics Today **45** (1992) 32.

92Svi Sviatoslavsky, I.N. et al: A KrF laser driven inertial fusion reactor, SOMBRERO, Fusion Technology **21** (1992) 1470.

93NET NET Predesign Report, NET Team, Fusion Engineering and Design, 21 (February 1993).

94Moi Moir, R.W. et al: HYLIFE-II: A molten salt inertial fusion energy power plant design – Final report, Fusion Technology **25** (1994) 5.

94Dec Decréton, M.: Viewing Systems in the Fusion Reactor Vessel – Radiation Hardened Glasses up to 300 Mgy, Proceedings of the 17th Symposium on Fusion Technology, Karlsruhe, Germany (1994).

94Jar Jarboe, T.R.: Plasma Phys. Contr. Fusion **36** (1994) 945.

94Tab Tabak, M., Hammer, J., Glinsky, M.E., Kruer, W.L., Wilks, S.C., Woodworth, J., Campbell, E.M., Perry, M.D.: Phys. Plasmas **1** (1994) 1626.

94Wat Appraisal of Resources and Costs of Critical Chemical Elements Used in Fusion, AEA/CS/ZJ/16401091/P01 (1994).

95Boi Boisset, L., Lattaud, C.: Metallic Waste Detritiation: Performance of a Melting Process, CEA Cadarache, Note Technique 95/039 (4.8.1995).

95Hog Hogan, W.J. (ed.): Energy from Inertial Fusion, IAEA, Vienna, Austria (1995).

95Kir Kirkpatrick, R.C., Lindemuth, I.R., Ward, M.S.: Fusion Technology **27** (1995) 201.

95Lin Lindl, J.: Phys. Plasmas **2** (1995) 3933.

95Mal Malang, S., Mattas, R.: Comparison of lithium and the eutectic lead-lithium alloy, two candidate liquid metal breeder materials for self-cooled blankets, Fus. Eng. Des. **27** (1995) 399.

95PCA Holdren, J. et al.: The U.S. Program of Fusion Energy Research and Development, Report of the Fusion Review Panel, The President's Committee of Advisors on Science and Technology (PCAST), Washington (July 1995,) 41.

95Rae Raeder, J. et al.: Safety and Environmental Assessment of Fusion Power (SEAFP), European Commission DG XII, Brussels (1995).

95SEA Raeder, J., Cook, I., Morgenstern, F.H., Salpietro, E., Bünde, R., Ebert, E.: Safety and Environmental Assessment of Fusion Power (SEAFP), Report of the SEAFP Project, European Commission, EURFUBRU XII-217/95, Brussels (1995).

95Thu Thumm M.: Fusion Engineering and Design **30** (1995) 139.

96Bar Barabaschi, S. (chairman) et al.: Fusion Programme Evaluation 1996, Report of the 1996 Fusion Evaluation Board, EUR 17521, Brussels, Luxembourg (1997).

96CTB Comprehensive Nuclear-Test-Ban Treaty; the United Nations General Assembly adopted the CTBT as contained in document A/50/1027, 125th plenary meeting (Sept. 10, 1996).

96IAE1 Defence in Depth in Nuclear Safety, INSAG-10, IAEA, Vienna (1996).

96IAE2 Clearance Levels for Radionuclides in Solid Materials, IAEA-TECDOC-855, Vienna (1996).

96IBS International Basic Safety Standards for Protection against Ionizing Radiation and for the Safety of Radiation Sources, IAEA Safety Series No. 115, International Atomic Energy Agency, Vienna (1996).

96Miy Miyai, Y. et al.: Studies on Recovery of Lithium from Sea Water by Manganese Oxide Adsorbent, The Shikoku National Industrial Research Institute 2217-14 (1996).

96Sha Sharp, R.et al.: Radiation Effects on Remote Handling System Components, Proceedings of the 19th Symposium on Fusion Technology, Lisbon, Portugal (1996).

97Edl Edlund, O.: Radiation doses due to atmospheric releases of HTO, Studsvik Eco & Safety AB, Report STUDSVIK/ES-97/3 (Jan. 1997).

97Gia Giancarli, L., Dalle Donne, M., Dietz, W.: Status of the European breeding blanket development, Fus. Eng. Des. **36** (1997) 57.

97Miy Miyamoto, K.: Fundamentals of Plasma Physics and Controlled Fusion, Iwanami Book Service Center (1997).

97Naj Najmabadi, F. and the ARIES team: Fusion Engineering & Design **38** (1997) 3, see also http://aries.ucsd.edu/LIB/REPORT/ARIES-AT/final.shtml.

97NSR1 ITER Non-Site Specific Safety Report (NSSR-2), Executive Summary, Volumes I-X, Appendix A, December 1997 and Supplement Volumes, June/July 1998.

97NSR2 ITER Non-Site Specific Safety Report (NSSR-2), Vol. V – Waste Management and Decommissioning (December 18, 1997).

97Pac Pacher, H.D., Smid, I., Federici, G., Igitkhanov, Yu., Janeschitz, G., Raffray, R., Vieider, G.: Erosion lifetime of ITER divertor plates, Journal of Nuclear Materials 241-243 (1997) 255.

97STO European Parliament – Scientific and Technological Options Assessment STOA: Operational Requirements of a Commercial Fusion Reactor, Final Report, PE 166.793/Final, Luxembourg (December 1997).

97Tok Quantitative Analysis of Economy and Environmental Adaptability of Tokamak Fusion Power Reactors, The University of Tokyo (December 1997).

97Wes Wesson, J.: Tokamaks, 2nd edition, Clarendon Press, Oxford (1997).

98ARI Najmabadi, F. et al.: Overview of the ARIES-RS Reversed-Shear Tokamak Power Plant Study, Fusion Engineering and Design, Vol. 38 (1997) Nos. 1, 2, p. 3-25.

98Car Cardella, A., Lodato, A., Pacher, H.D., Parker, R.R., Ioki, K., Janeschitz, G., Lousteau, D., Raffray, R., Yamada, M., Gusic, C.: The ITER port limiter design, Fusion Engineering and Design **43** (1998) 75.

98Con Connor, J.W.: Review of models for ELMs, Plasma Phys. Contr. Fusion **40** 2 (1998) 191-213.

98Gia Giancarli, L., Benamati, G., Fütterer, M., Reimann, J.: Development of the EU water-cooled Pb-Li7Li blanket, Fus. Eng. Des. **39-40** (1998) 639.

98ITF Technical Basis for the ITER Final Design Report, Cost Review and Safety Analysis (FDR), ITER EDA Documentation Series No. 16, International Atomic Energy Agency, Vienna (1998).

98Kak Kakudate, S. et al.: Remote Handling Demonstration of ITER Blanket Module Replacement, Proceedings of the 17th IAEA Fusion Energy Conference, Yokohama, Japan (1998).

98Mal Malang, S. et al.: ARIES-RS Maintenance Approach for High Availability, Fusion Engineering and Design **41**, Elsevier (1998).

98Pat Patel, B. et al.: Operational Health Physics Experience during the JET D-T Experiment, Proceedings of the 20th Symposium on Fusion Technology, Marseille, France (1998).

98Pet Petzoldt, R.: IFE target Injection and Tracking Experiment, Fusion Technology **34** (Nov. 1998) 831.

98Rez Reznichenko, P.V., Viniar, I.V., Kuteev, B.V., Acceleration of Hydrogen Pellets in a Two-Stage Gas Gun with Cryogenic Pistons, Proc. 20th Symposium on Fusion Technology, Marseille, France (1998), Vol. 2, 975.

98Sch Schleisner, L.: Socio-Economic Research on Fusion, SERF: 1997-98. Macro Task E2: External Costs and Benefits. Sub Task: Life Cycle assessment of a fusion power plant. Report R2.1 RISØ National Laboratory (1998).

98Tec Technical Basis for the ITER Final Design Report, Cost Review and Safety Analysis (FDR) ITER EDA, Documentation Series No. 16, IAEA, Vienna (1998).

98Thu Thumm M.: State-of-the-art and recent developments of high-power gyrotron oscillators, Proc. Radio Frequency Workshop (RF 98), High Energy Density Microwaves, Pajaro Dunes, California, USA (1998), AIP Conference Proceedings 474, 146-162.

98Vin Viniar, I., Sudo, S., Umov, A., Skiblikov, S., Reznitchenko, P.: Pellet injectors for a steady state fuelling, Proc. 20th Symposium on Fusion Technology, Marseille, France (1998), Vol. 2, 917.

98Wag Wagner, F.: Transact. of Fusion Technol. **33** (1998) 67.

99Bes See, for example, Besenbruch, G.E. et al.: Design and Testing of Cryogenic Target Systems, Proceedings of the First International Conference on Inertial Fusion Sciences and Applications (IFSA'99), Elsevier Press, Paris (Sept. 1999).

99Dam Damiani, C. et al.: ITER Divertor Maintenance – L7 R&D Project, Results and Perspectives, Proceedings of the 5th Symposium on Fusion Nuclear Technology, Rome, Italy (1999).

99Hoe Hörning, G., Keck, G., Lattewitz, F.: Fusionsenergie – eine akzeptable Energiequelle der Zukunft?, Akademie für Technikfolgenabschätzung in Baden-Württemberg, Report No. 145 (Aug. 1999).

99Jaq Jaquinot, J. and the JET team: Plasma Phys. Control. Fusion **41** (1999) A13-A46.

99Nor Norajitra, P. et al.: The second advanced lead lithium blanket concept using ODA steel as structural material and SiCf/SiC flow channel inserts as electrical and thermal insulators, FZK report, FZKA 6385 (1999).

99Raf Raffray, A.R., Schlosser, J., Akiba, M., Araki, M., Chiocchio, S., Driemeyer, D., Escourbiac, F., Grigoriev, S., Merola, M., Tivey, R., Vieider, G., Youchison, D.: Critical heat flux analysis and R&D for the design of the ITER divertor, Fusion Engineering and Design **45** (1999) 377.

99Rob Robinson, D.C., Cox, M., Lloyd, B., Nightingale, M.: Fusion Engineering and Design **46** (1999) 355.

99Ros Rosen, M.: Phys. Plasmas **6** (1999) 1690.

99SEA1 Cook, I., Marbach, G., DiPace, L., Rocco, P., Girard, C., Taylor N.: Results, Conclusions and Implications of the SEAFP-2 Programme, 5th International Symposium of Fusion Nuclear Technology, Rome, September 19-24, 1999, Fus. Eng. Design **51-52** (2000) 409.

99SEA2 Gulden, W., Kajlert, E.: Safety and Environmental Assessment of Fusion Power – Long Term Programme (SEAL), Summary Report of the SEAL Project, Euratom / European Commission, EUR-19071, Brussels (December 1999).

99Spe Speth, E., Ciric, M., Feist, H.J., Frank, P., Heinemann, B., Kraus, W., Probst, F., Riedl, R., Trainham, R., Vollmer, O., Wilhelm, R.: Fusion Engineering and Design **46** (1999) 383.

99Wes Wesson, J.: The Science of JET, Abingdon, Oxon, OX14 3EA, report JET-R(99)13.

99Win Windsor, C., Keilhacker, M., Lawson, J.D., Pert, J.G., Robinson, D.C. (eds.): The approach to ignited plasma, Philosophical Transactions of the Royal Society, 357, no 1752 (1999) 371-640.

00Air Airaghi, A. (chairman) et al.: Nuclear Fusion, in Five Year Assessment Report Related to the Specific Programme Nuclear Energy, Final Report for the European Commission (June 2000).

00Boc Boccaccini, L.V. (ed.): Advanced Helium Cooled Pebble Bed Blanket, FZK report, FZKA 6402 (2000).

00Ene European Commission, Energy in Europe, 1999 – Annual Energy Review, Luxembourg (2000).

00Gia Giancarli, L., Ferrari, M., Fütterer, M.A., Malang, S.: Candidate blanket concepts for a European fusion power plant study, Fus. Eng. Des. **49-50** (2000) 445.

00Kur Kuriyama, M., Akino, N., Ebisawa, N., Grisham, L., Hikita, S., Honda, A., Itoh, T., Kawai, M., Kazawa, M., Kusaka, M., Mogaki, K., Nagase, N., Ohga, T., Oohara, H., Pengyuan, L., Satoh, F., Seki, H., Tanai, Y., Toyokawa, Y., Umeda, N., Usui, K., Yamazaki H.: Study of increasing the beam power on the negative ion based neutral beam injector for JT-60U, Paper B-10, 21st Symposium on Fusion Technology, Madrid, Spain (September 11-15, 2000).

00Moe Moeslang, A., Ehrlich, K.: Nucl. Fusion **40** 3Y (2000) 619.

00Pet Petti, D., McCarthy, K.: Progress in U.S. fusion safety and environmental activities over the last decade, Fusion Technology, vol. 37 (Jan. 2000) 1-23.

00Ros Rosanvallon, S., Courouau, J.L.: Modelling of a steel detritiation process – Influence of experimental parameters, Note Technique CEA/DRN/DER/STPI/LPCP - 2000/038.

00USG U.S. Department of the Interior, U.S. Geological Survey, Mineral Commodity Summaries 2000 (2000).

00Wu Wu, C.H.: Progress of the European R&D on plasma wall interactions, neutron effects and tritium removal in ITER plasma facing materials, Proceed. of the 21st Symp. on Fusion Technology, SOFT, Madrid, Spain (September 11-15, 2000).

01Fed Federici, G. et al.: Assessment of erosion and tritium codeposition in ITER, J. of Nucl. Matter **290-293** (2001) 260.

01GSR1 ITER Generic Site Safety Report (GSSR), Vols. I-XI (July 2001).

01GSR2 ITER Generic Site Safety Report (GSSR), Vol. IV – Normal Operation (July 2001).

01GSR3 ITER Generic Site Safety Report (GSSR), Vol. V – Radioactive Materials, Decommissioning and Waste (July 2001).

01GSR4 ITER Generic Site Safety Report (GSSR), Vol. VI – Occupational Safety (July 2001).

01GSR5 ITER Generic Site Safety Report (GSSR), Vol. VII – Analysis of Reference Events (July 2001).

01GSR6 ITER Generic Site Safety Report (GSSR), Vol. VIII – Ultimate Safety Margins (July 2001).

01GSR7 ITER Generic Site Safety Report (GSSR), Vol. X – Sequence Analysis (July 2001).

01Htt http://www.llnl.gov/nif/nif.html.

01Jan Janeschitz, G. et al.: Plasma wall interaction issues in ITER, J. of Nucl. Matter **290-293** (2001) 1.

01SEI Cook, I., Marbach, G., DiPace, L., Girard, C., Taylor, N.P.: Safety and Environmental Impact of Fusion, Report EFDA-S-RE-1, EUR (01) CCE-FU/FTC 8/5.

02ITF ITER Technical Basis, ITER EDA Documentation Series No. 24, IAEA, Vienna (2002).

02Lae Lässer, R., Dörr, L., Glugla, M., Haange, R., Hayashi, T., Kveton, O., Murdoch, D.K., Penzhorn, R.-D., Yoshida, H.: The Storage and Delivery System of the ITER Tritium Plant, Fusion Sci. Technol. **41** (2002) 854.

02Wit Wittchow, E.: Fossil-fueled power plants, in Landolt-Börnstein New Series VIII/3A, Heinloth, K. (ed.), Springer-Verlag, Berlin (2002).

03Bor Bornschein, B., Glugla, M., Günther, K., Lässer, R., Le, T.L., Simon, K.H., Welte, S.: Tritium Tests With a Technical Permcat for Final Clean-up of ITER Exhaust Gases, Fusion Eng. Design **69** (2003) 51.

03Glu Glugla, M., Lässer, R., Dörr, L., Murdoch, D., Haange, R., Yoshida, H.: The Inner Deuterium/Tritium Fuel Cycle of ITER, Fusion Eng. Design **69** (2003) 39.